

Aus der II. Medizinische Klinik  
der Medizinischen Fakultät Mannheim  
(Direktor: Prof. Dr. med. Matthias P Ebert)

EGF/STAT1-maintained ECM1 expression in hepatic homeostasis is  
disrupted by IFN $\gamma$ /NRF2 in chronic liver diseases

Inauguraldissertation  
zur Erlangung des Doctor scientiarum humanarum (Dr. sc. hum.)  
der  
Medizinischen Fakultät Mannheim  
der Ruprecht-Karls-Universität  
zu  
Heidelberg

vorgelegt von  
Yujia Li

aus  
Liaoning, China  
2023

Dekan: Prof. Dr. med. Sergij Goerd  
Referent: Prof. Dr. rer. nat. Steven Dooley

# CONTENTS

	Page
LIST OF ABBREVIATIONS .....	1
<b>1 INTRODUCTION.....</b>	<b>4</b>
1.1 Extracellular matrix protein 1 (ECM1) .....	4
1.2 Epidermal growth factor (EGF) .....	5
1.2.1 EGF structure and signaling pathway .....	5
1.2.2 EGF in liver homeostasis .....	6
1.3 Epidermal growth factor receptor (EGFR).....	6
1.3.1 EGFR family structure.....	6
1.3.2 EGFR activation.....	7
1.3.3 EGFR in disease.....	8
1.4 Signal transducer and activator of transcription 1 (STAT1) .....	8
1.5 Interferon gamma (IFN $\gamma$ ) .....	9
1.5.1 IFN $\gamma$ production .....	9
1.5.2 Cellular response to IFN $\gamma$ .....	10
1.5.3 IFN $\gamma$ signaling pathway .....	10
1.6 Nuclear factor erythroid 2-related factor 2 (NRF2).....	12
1.7 Potential distinct functions of EGF and IFN $\gamma$ .....	12
1.8 Aims of the study.....	12
<b>2 MATERIALS AND METHODS .....</b>	<b>14</b>
2.1 Materials.....	14
2.1.1 Patients and liver tissues .....	14
2.1.2 Animals .....	14
2.1.3 Primary human, mouse hepatocytes and cell lines.....	14
2.1.4 Chemicals and reagents .....	15
2.1.5 Antibodies .....	17
2.1.6 Buffer preparation .....	18

2.1.7	Kits and assays .....	20
2.1.8	Small interfering RNA .....	20
2.1.9	Experimental consumables .....	20
2.1.10	Experimental instruments .....	22
2.1.11	Software .....	23
2.2	Methods .....	24
2.2.1	Animal experiments .....	24
2.2.2	Mice genotyping .....	26
2.2.3	Primary mouse hepatocyte isolation .....	27
2.2.4	Primary human hepatocyte isolation .....	29
2.2.5	Cell culture and treatment .....	29
2.2.6	RNA isolation and qRT-PCR .....	30
2.2.7	Western blotting .....	33
2.2.8	Nuclear and cytoplasmic protein extraction .....	34
2.2.9	RNA interference .....	35
2.2.10	Immunofluorescence staining .....	36
2.2.11	Immunohistochemistry staining .....	37
2.2.12	Liver echography .....	38
2.2.13	Chromatin immunoprecipitation .....	38
2.2.14	Statistical analysis .....	40
<b>3</b>	<b>RESULTS .....</b>	<b>41</b>
3.1	Histology of liver and kidney from ECM1KO mice at ages 5, 8 and 12wks	41
3.2	Increased portal vein pressure in ECM1KO mice .....	43
3.3	Growth factors EGF and HGF induce ECM1 expression in hepatocytes....	45
3.4	EGF-EGFR keeps ECM1 expression in hepatocytes <i>in vitro</i> .....	46
3.5	EGF-EGFR keeps ECM1 expression in homeostatic liver <i>in vivo</i> .....	48
3.6	EGF-induced ECM1 expression is not dependent on MEK-ERK pathway .	50
3.7	EGF upregulates ECM1 expression through p-STAT1 S727 .....	52
3.8	EGF-induced p-STAT1 S727 binds to and positively regulates <i>Ecm1</i> gene promoter .....	54
3.9	Selection of candidate factors inhibiting ECM1 expression under chronic liver disease conditions .....	55
3.10	IFN $\gamma$ abolishes EGF-EGFR-maintained ECM1 expression <i>in vitro</i> .....	56
3.11	IFN $\gamma$ blunts p-STAT1 S727 binding to <i>Ecm1</i> gene promoter via phosphorylation of STAT1 at Y701 .....	57



3.12	IFN $\gamma$ abolishes EGF-EGFR-maintained ECM1 expression <i>in vivo</i> .....	60
3.13	Free shuttling of STAT1 total protein contributes to binding of <i>Ecm1</i> promoter .....	61
3.14	IFN $\gamma$ generates reactive oxygen species (ROS) and induces NRF2 in hepatocytes .....	63
3.15	IFN $\gamma$ administration activates NRF2 <i>in vivo</i> .....	64
3.16	NRF2 generated by H <sub>2</sub> O <sub>2</sub> reduces ECM1 expression .....	65
3.17	NRF2 agonist OPZ treatment inhibits ECM1 expression .....	66
3.18	NRF2 inhibits ECM1 expression by binding its gene promoter .....	67
3.19	EGF-maintained ECM1 is disrupted by H <sub>2</sub> O <sub>2</sub> or OPZ administration .....	68
3.20	Scheme for the regulation of ECM1 expression in healthy/diseased liver	69
4	DISCUSSION .....	71
4.1	STAT1 in ECM1 expression regulation .....	71
4.2	Excessive production of IFN $\gamma$ and liver injury .....	72
4.3	Regulation of EGFR by IFN $\gamma$ .....	73
4.4	Adverse consequences of excessive NRF2 activation .....	74
4.5	Outlook of the study .....	74
4.5.1	HGF in ECM1 expression regulation .....	74
4.5.2	Downregulation of ECM1 expression in liver regeneration and HCC ..	76
5	SUMMARY .....	79
6	REFERENCES .....	80
7	LISTS OF FIGURES AND TABLES .....	90
7.1	List of figures .....	90
7.2	List of tables .....	91
8	CURRICULUM VITAE .....	92

9 ACKNOWLEDGEMENT..... 95

## LIST OF ABBREVIATIONS

°C	Grad Celsius
μ	Micro (10 <sup>-6</sup> )
APCs	Antigen-presenting cells
AREs	Antioxidant response elements
BDL	Bile duct ligation
BSA	Bovine serum albumin
CCl <sub>4</sub>	Carbon tetrachloride
ChIP	Chromatin immunoprecipitation
ECM1	Extracellular matrix protein 1
EDTA	Ethylene Diamine Tetraacetic Acid
EGF	Epidermal growth factor
EGFR	Epidermal growth factor receptor
FBS	Fetal bovine serum
GAF	Gamma-activated factor
GAS	Gamma-activated sites
HB-EGF	Heparin-binding EGF
HBV	Hepatitis-B-virus
HCC	Hepatocellular carcinoma
H&E	Hematoxylin and eosin
HPHs	Human primary hepatocytes
HSCs	Hepatic stellate cells
IFN	Interferon
IFN <sub>γ</sub>	Interferon gamma
IFNGR	IFN <sub>γ</sub> receptor
IL	Interleukin
i.p.	Intraperitoneal
ISG	IFN-stimulated genes
ITS	Insulin-Transferrin-Selenium
i.v.	Intravenous
IVC	Inferior vena cava
KEAP1	Kelch-like ECH-associated protein 1

KO	Knock out
LPS	Lipopolysaccharide
L-TGF- $\beta$	Latent TGF- $\beta$
MPHs	Mouse primary hepatocytes
MTC	Masson Trichrome
NASH	Nonalcoholic steatohepatitis
NK	Natural killer
NRF2	Nuclear factor erythroid 2-related factor 2
NSCLC	Non-small cell lung cancer
NT	Non-tumour
OPZ	Oltipraz
PBS	Phosphate-buffered saline
PFA	Paraformaldehyde
PHx	Partial hepatectomy
PI3K	Phosphatidylinositol-3-kinase
P/S	Penicillin-streptomycin
PTB	phosphotyrosine binding
PV	Portal vein
PVP	Portal vein pressure
qRT-PCR	Quantitative real-time PCR
RNAi	RNA interference
ROS	Reactive oxygen species
RT	Room temperature
RTK	Receptor tyrosine kinase
SB	Suspension Buffer
SD	Standard deviation
SDS-PAGE	Sodium dodecyl sulfate polyacrylamide gel electrophoresis
SH2	Src homology 2
siRNA	Small interfering RNA
STAT1	Signal transducer and activator of transcription 1
S727	Serine727
TBST	Tris buffered saline with 0.05% Tween 20
TGF- $\alpha$	Transforming growth factor alpha
TGF- $\beta$	Transforming growth factor beta

## LIST OF ABBREVIATIONS

---

Th17	IL-17-producing T helper cells
TNF- $\alpha$	Tumor necrosis factor alpha
TSS	Transcription start site
WB	Western blotting
WT	Wildtype
Y701	Tyrosine701

## 1 INTRODUCTION

### 1.1 Extracellular matrix protein 1 (ECM1)

ECM1, an 85-kDa glycoprotein [1], is widely distributed in human tissues. It is found in the epidermis and the dermis [2], where it maintains the integrity and homeostasis of the skin [3]. ECM1 dysfunction may lead to two skin diseases [4], lipoid proteinosis (a rare autosomal recessive genodermatosis) and lichen sclerosus (a common acquired inflammatory skin disorder). Both share common clinicopathological features [4], for example, skin hyperkeratosis, the hyaline appearance of the papillary dermis, and disruption of basement membranes. In addition, ECM1 can also regulate the formation of endochondral bones [5] or enhance the proliferation of endothelial cells [6]. Most ECM1 functions are mediated through interactions with various extracellular and structural proteins, including perlecan [7], fibulin-1C/D [8], and MMPs (e.g., MMP9) [9]. To be specific, ECM1 interacts with the epidermal growth factor-like modules flanking the LG2 subdomain of perlecan's domain V via its C-terminal domain [7]. Disruption of this association appears to contribute to some of pathological features observed in lipoid proteinosis and lichen sclerosus [7, 10]. The second tandem repeat domain of ECM1 interacts with the major interacting domain of fibulin-1D and the C-terminal module of fibulin-1C [8]. Binding of Fibulin-1D to ECM1 has been suggested to reduce endothelial cell proliferation and angiogenesis, and thereby reducing tumour transformation and invasion [11, 12]. The C-terminal tandem repeat 2 of ECM1 interacts with MMP9, thereby inhibiting its proteolytic activity *in vitro* [9]. In addition, ECM1 also interacts with  $\alpha$ v integrin, one of the physiological regulators of latent TGF- $\beta$  (L-TGF- $\beta$ ) activation [13]. Most evidence of crosstalk between ECM1 and TGF- $\beta$  came from immunology. Su P and colleagues found that ECM1 inhibits differentiation of IL-17-producing T helper (Th17) cells and the development of experimental autoimmune encephalomyelitis by interfering with  $\alpha$ v integrin-mediated L-TGF- $\beta$  activation, suggesting clinical importance in multiple sclerosis [14]. This study was the first time to demonstrate that ECM1 has an inhibitory effect on L-TGF- $\beta$  activation. Furthermore, in several malignant epithelial tumours [15] and in tumours with metastases [12], ECM1 levels are increased, indicating ECM1 involvement during cancer development.

In the liver, ECM1 is mainly produced by hepatocytes compared with other three non-parenchymal cell types, Kupffer cells, sinusoidal endothelial cells and stellate cells

[16]. Our lab recently showed - for the first time - that ECM1 is a critical gatekeeper in the healthy liver by keeping L-TGF- $\beta$  quiescent through the interaction with  $\alpha$  integrin via RGD motif, contributing to normal architecture and physiological homeostasis of cell-cell communication [16]. Upon liver damage or injury, ECM1 expression is significantly decreased, leading to L-TGF- $\beta$  activation, thus resulting in hepatic stellate cells (HSCs) activation and the subsequent fibrosis. Several mouse models of liver disease confirmed the downregulation of ECM1 expression, e.g., carbon tetrachloride (CCl<sub>4</sub>), nonalcoholic steatohepatitis (NASH) and bile duct ligation (BDL) mouse models [16]. Moreover, ECM1KO mice developed spontaneous liver fibrosis and exhibited severe disruption of liver architecture [16]. Fan, W. et al. also found in the patients with liver fibrosis/cirrhosis caused by hepatitis-B-virus (HBV) or alcoholic hepatitis that ECM1 expression was dramatically reduced and associated with fibrosis progression stages from F1 to F4 [16]. Those observations highlight a critical role of ECM1 in maintaining liver homeostasis and controlling organ function, therefore it is important to investigate the mechanisms that regulate ECM1 expression in the context of hepatic homeostasis and/or liver damage.

## 1.2 Epidermal growth factor (EGF)

### 1.2.1 EGF structure and signaling pathway

EGF is a single-chain polypeptide consisting of 53 amino acids, which is cleaved from a large precursor, prepro-EGF, at the Arg-Asn and Arg-His bonds on its NH<sub>2</sub>- and COOH-termini, respectively [17, 18]. Precursor EGF is anchored to the plasma membrane through its prominent hydrophobic region, and mature EGF lies close to the exterior of the hydrophobic transmembrane structural domain prior to cleavage [18]. So far, EGF is widely known as the prototype of group I EGF family which comprises not only EGF but also transforming growth factor alpha (TGF- $\alpha$ ), heparin-binding EGF (HB-EGF), amphiregulin, betacellulin, epiregulin and epigen [19, 20]. The members of EGF family show structural similarities - all have EGF repeats (or EGF motifs) in their extracellular domains, a sequence of 35-40 amino acids with six conserved cysteines in between [21]. Three intramolecular disulfide bonds are formed through the pairing of the six cysteines, which are important for maintaining and exerting their biological activities [22]. Additionally, most members bind to the EGF receptor EGFR (type I transmembrane receptor tyrosine kinase, also known as HER1 or ErbB1), thereby activating downstream tyrosine kinase activity and

regulating various cellular signaling pathways, e.g., MEK/ERK, PI3K/AKT/mTOR, JAK/STAT, to affect cell proliferation, differentiation, motility, or apoptosis [21, 23, 24].

### 1.2.2 EGF in liver homeostasis

The production and distribution of EGF in the body is quite widespread. It can be produced and secreted by Brunner's glands of the duodenum, lactating breast, submaxillary gland, kidney and so on [18], and is detectable in various body fluids, such as milk [25, 26], saliva [27], urine [28], and plasma [27]. In human, the kidney is the main source of EGF production [28], although the liver does not secrete EGF, it is continuously delivered to liver from Brunner's glands of the duodenum [29, 30] via portal circulation. Together with its receptor (EGFR), the EGF signaling operates on most epithelial cells [31], including hepatocytes. Under normal conditions, there is physiological liver regeneration to restore hepatic mass, and EGF has a direct mitogenic effect on hepatocytes [32]. Sustained EGF injections lead to liver enlargement [33], besides, the ratio of EGF per hepatocyte increases threefold and EGFR is activated within 60min after partial hepatectomy (PHx) [30], all of which suggest a prominent role for EGF signaling in cell renewal and maintenance of tissue homeostasis. Based on the fundamental characteristics and clinical relevance of EGF (for instance in the healing cascade and cancer development [18]), studies have now shifted to explore its function in pathophysiology and clinical applications for human disease, which further highlights the pivotal role of EGF in biological processes and etiology.

### 1.3 Epidermal growth factor receptor (EGFR)

#### 1.3.1 EGFR family structure

EGFR, which belongs to the EGFR/ErbB superfamily, is a transmembrane receptor tyrosine kinase (RTK) that can be activated by EGF family members [34, 35]. The superfamily also includes three other RTKs, ErbB2/HER2/Neu, ErbB3/HER3 and ErbB4/HER4. In terms of molecular structure, the ErbB receptors are similar to other RTKs, consisting of an N-terminal extracellular ligand-binding domain, a transmembrane helix, and a cytoplasmic structural domain harboring a tyrosine kinase core and a following C-terminal regulatory residue [36]. Two regions located in the extracellular part are rich in cysteines and are responsible for ligand binding. It is important to note that ErbB2 does not have a direct ligand, as its extracellular domain



is already in an extended state in the absence of ligands [37]. And except for ErbB3, which has impaired kinase activity and cannot phosphorylate signaling proteins [38], all receptors contain kinase domains with catalytic capacity. Different tyrosine residues, such as Y1045, Y1068, Y1086, Y1148 and Y1173, are present at the C-terminal non-catalytic motif of EGFR and facilitate distinct biological outcomes. The single tyrosine residue of EGFR can bind multiple downstream effectors (e.g., Grb2, SHC, Src, Abl) and, in turn, the same effector can bind to multiple residues of all four receptors [37].

### 1.3.2 EGFR activation

Following ligand binding, EGFR either forms a homodimer with another EGFR or a heterodimer with other members of EGFR/ErbB family. This dimerization is a key step for the activation of intrinsic tyrosine kinases in the receptors, followed by the trans-autophosphorylation of specific tyrosine-containing residues at the C-terminus serving as docking sites for various signaling molecules that carry Src homology 2 (SH2) or phosphotyrosine binding (PTB) domains [39]. Numerous downstream signaling pathways, such as Ras/Raf/MEK/ERK, PI3K/AKT/mTOR, JAK/STAT, and PLC $\gamma$ /PKC signaling pathways, are thus activated upon receiving the transmitted signals, thereby affecting cell growth, differentiation and apoptosis and regulating many physiological functions. The EGFR signaling pathway is briefly schematized below (**Figure 1** created with BioRender.com). The different potentials of ErbB receptors to activate different downstream pathways, to some extent, depend on the type of ligand and receptor dimer, as well as the effectors recruited [37].

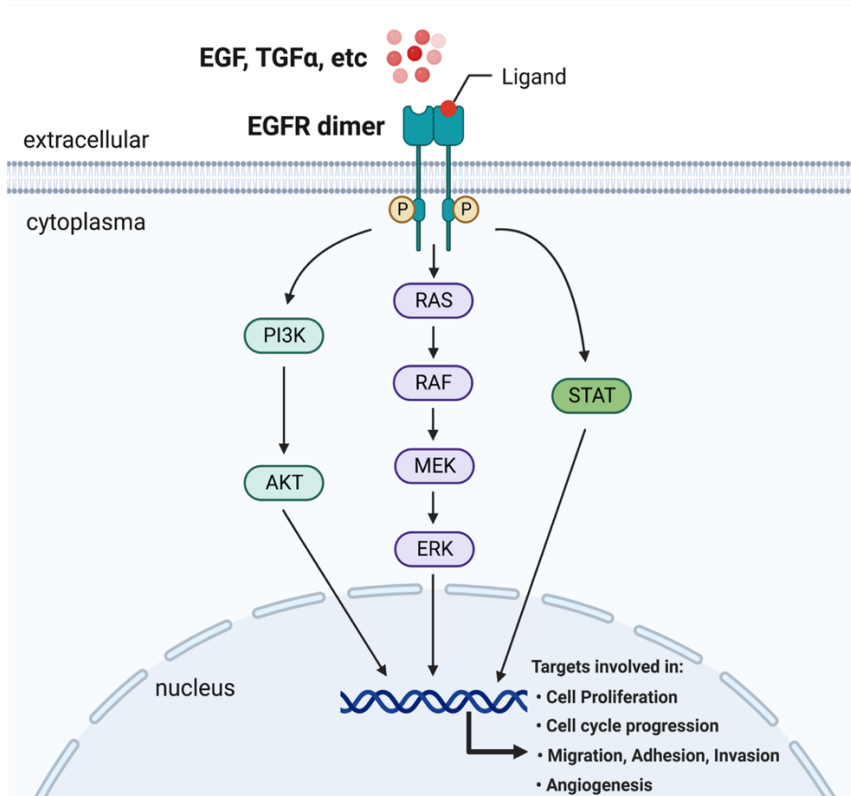


**Figure 1. EGFR signaling pathway**

### 1.3.3 EGFR in disease

Regarding the impact on body homeostasis and human disease, many studies have shown that increased EGFR expression leads to cell transformation [40], and overexpression and/or activating mutations of EGFR are associated with diverse cancers, such as breast, ovarian, and non-small cell lung cancer (NSCLC) [41-43], and with poor prognosis, drug tolerance, cancer metastasis, and reduced survivability [44-47]. Other studies revealed a novel tumor suppressive role of EGFR in HCC against TGF- $\beta$ -mediated transformation of epithelial to amoeboid, providing support for targeting the TGF- $\beta$  pathway in patients with poor EGFR expression [48]. Hence, EGFR has been one of the most crucial variables in cancer treatment.

### 1.4 Signal transducer and activator of transcription 1 (STAT1)

STAT family is a group of transcription factors, mainly activated by cytokines, that play an important role in hematopoiesis and immunology [49]. There are seven STAT family members in mammals, among which STAT1 is one of the most well-studied. It has two isoforms, STAT1 $\alpha$  (91kDa) and STAT1 $\beta$  (84kDa). Both isoforms can be phosphorylated on tyrosine 701 (Y701) site and translocate to the nucleus where they bind to the gamma-activated sites (GAS, the promoter elements for genes

rapidly activated by interferon gamma). And to maximize the transcriptional activity of STAT1, activation on serine 727 (S727) site is required [50]. As  $\beta$  isoform lacks S727 phosphorylation site and most transactivation domain at C-terminus [51], the STAT1 $\beta$  homodimer is thought to be incapable of transcriptional induction [52]. However, some studies also showed that STAT1 $\beta$  is transcriptionally active in response to interferons (IFNs), although the induction of IFN-stimulated genes (ISG) is delayed or at a lower level than STAT1 $\alpha$  [53]. STAT1 isoforms can be assembled in different ways, with type I IFN (IFN $\alpha$  and IFN $\beta$ ) mainly stimulating the formation of ISGF3 complex (STAT1, STAT2, and IRF9 heterotrimer), and type II IFN (IFN $\gamma$ ) primarily activating STAT1 homodimers. In the ISGF3 complex, both STAT1 isoforms are considered to be completely functional as the critical transactivation domain is afforded by STAT2 [54, 55].

In addition to activation by IFNs, other cytokines such as EGF also activate STAT1. Upon EGF binding, activated EGFR can activate STAT1 either directly by binding to the STAT1, where JAK is not required, or indirectly by activating c-Src, where JAK permits the maximum activation of STAT1 [37]. Once activated, the dimeric STAT1 proteins translocate to the nucleus where they regulate gene transcription and thereby modulating cell proliferation, differentiation, apoptosis and survival [43, 56]. Although interferon signaling pathway, as well as other signals, can phosphorylate STAT1 on S727, their mechanisms might be quite different and independent, yielding distinct biological consequences. For IFNs-induced STAT1 phosphorylation, the activation on Y701 is an essential prerequisite for S727 phosphorylation [57], whereas p38 MAPK only induces S727 phosphorylation in response to cellular stress [58]. Similar to p38 MAPK, in JB6 Cl 41 cells, EGF induces only S727 phosphorylation of STAT1 [59]. In addition, total STAT1 can freely shuttle between the cytoplasm and nucleus and is phosphorylated at S727 by a constitutively active nuclear kinase, also independently of Y701 phosphorylation [60, 61].

## 1.5 Interferon gamma (IFN $\gamma$ )

### 1.5.1 IFN $\gamma$ production

The interferon (IFN) family is divided into three categories, type I IFN (IFN $\alpha$  and IFN $\beta$ , et al.), type II IFN (IFN $\gamma$ ), and type III IFN (IFN $\lambda$ ) based on the receptor specificity and sequential homology [62]. Among them, IFN $\gamma$  has been well studied as an anti-viral, anti-tumour, pro-inflammatory cytokine. It can be secreted by various immune cells,

such as activated T cells, natural killer (NK) cells, NKT cells, and antigen-presenting cells (APCs) [63-65]. The production of IFN $\gamma$  is regulated by cytokines secreted from APCs in the recognition of different pathogens, with the most prominent being interleukin (IL)-12 and IL-18, which provide the connection between infection and IFN $\gamma$  production in the innate immune response [66-68]. Lymphocytes like T lymphocytes, NK cells, are attracted to the sites of inflammation by macrophages-secreted chemokines and are stimulated by IL-12 to synthesize IFN $\gamma$  [69, 70]. Co-stimulation of IL-12 and IL-18 in macrophages, NK and T cells further promotes IFN $\gamma$  synthesis [67, 71].

### 1.5.2 Cellular response to IFN $\gamma$

Many types of cells respond to IFN $\gamma$  during the inflammation to adjust growth, maturation and differentiation. Stimulation of macrophages with IFN $\gamma$  enhances antigen processing and presentation pathways and evokes direct anti-microbial and anti-tumour mechanisms [62]. Besides, the activities of NK cells [64], B cells [72, 73] and leukocytes [74] are also shown to be coordinated by IFN $\gamma$ . Although hepatocytes are not the main producers, IFN $\gamma$  can accumulate dramatically in the liver as activated T cells, NK cells and NKT cells are recruited to the liver in the presence of inflammation and damage [75]. The sensitivity of hepatocytes to IFN $\gamma$  signaling increases due to enhanced expression of the IFN $\gamma$  receptor during hepatic inflammation and injury [76, 77]. Besides immune modulation, IFN $\gamma$  exerts a significant role in the regulation of hepatocyte apoptosis and cell cycle progression during liver disease development through JAK/STAT, p53/p21/p27, NF $\kappa$ B/IRF-1, or ROS/Caspase pathways [78, 79].

### 1.5.3 IFN $\gamma$ signaling pathway

The bioactive IFN $\gamma$  dimer binds to the IFN $\gamma$  receptor (IFNGR) to initiate downstream signaling. The IFNGR is a transmembrane heterodimer consisting of two IFNGR1 chains ( $\alpha$  chain) with ligand-binding domain and two non-ligand-binding IFNGR2 chains ( $\beta$  chain) with signal transduction function [80]. The expression of IFNGR1 is usually in excess, whereas IFNGR2 is critically controlled due to cell differentiation and activation stage, and is a rate-limiting component for the activation of IFN $\gamma$  signaling [81, 82]. Upon interaction with IFNGR1, IFN $\gamma$  triggers the association of the IFN $\gamma$ -IFNGR1 complex with IFNGR2, which brings inactive receptor-associated JAK1

and JAK2 tyrosine protein kinases into close proximity to each other, leading to their trans-autophosphorylation [83]. As both receptor chains lack intrinsic kinase activity, the activated JAKs are responsible for the phosphorylation of the C-terminal tyrosine tail (Y440 in human) in the IFNGR1 chain [84, 85], offering docking sites for the SH2 domain of STAT1 [86]. The two receptor-recruited STAT1 proteins are then phosphorylated at Y701, probably by JAK2 [87], and form a STAT1 homodimer that acts as gamma-activated factor (GAF). For maximum transcriptional activity of STAT1, an additional phosphorylation at S727 is required [50]. The activated STAT1 dimer dissociates from the receptors and translocates into the nucleus, where it binds to the GAS binding site located in the DNA sequence, thereby acting as a transcription factor to mediate target gene expression. The following scheme (**Figure 2**) briefly describes the IFN $\gamma$ -JAK-STAT1 signaling pathway [88]. In addition to signaling downstream mediators JAK-STAT1, IFN $\gamma$  may also operate independently of this pathway, e.g. through c-Myc [89], or NF $\kappa$ B/IRF-1 [90].

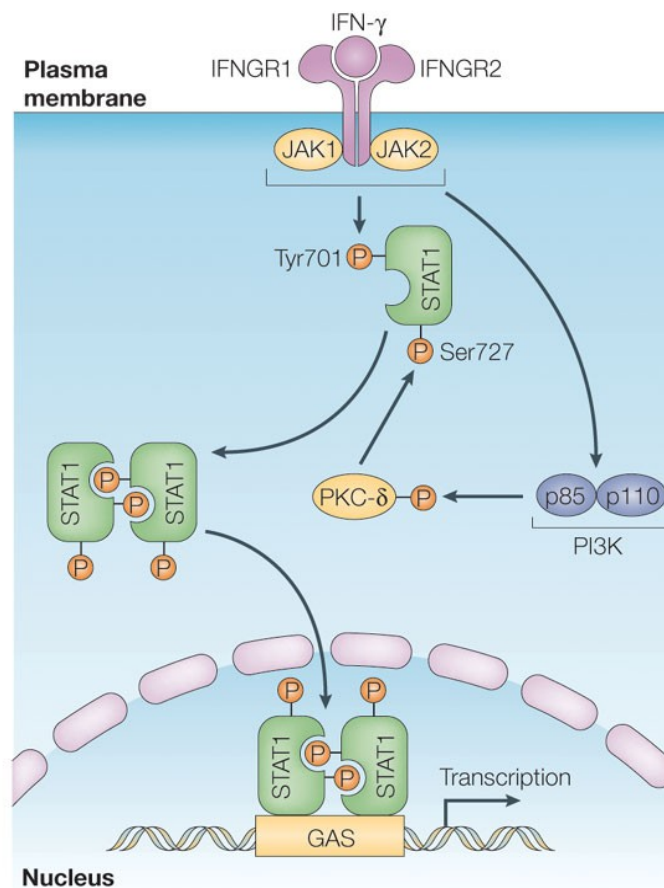


**Figure 2. IFN $\gamma$ -JAK-STAT1 signaling pathway [88]**

### 1.6 Nuclear factor erythroid 2-related factor 2 (NRF2)

NRF2 is a transcription factor, which can be activated in the presence of an imbalance in the redox system of hepatocytes [91]. It is a key regulator of the antioxidant response, defending cells from damage triggered by oxidative stress. Under regular conditions, NRF2 binds to another protein called Kelch-like ECH-associated protein 1 (KEAP1) in the cytoplasm. However, when cells are exposed to oxidative stress or other cellular stimuli, NRF2 is released from KEAP1 and translocates to the nucleus, where it binds to antioxidant response elements (AREs) in the target genes' promoter regions, leading to their activation or inhibition. NRF2 is also involved in the regulation of many other cellular processes, such as cell growth, inflammation, and metabolism. Dysfunction of the NRF2 signaling pathway is implicated in the pathogenesis of many diseases, including cancer, nervous degenerative diseases and metabolic disorders. Therefore, NRF2 has emerged as a prospective therapeutic target for many illnesses.

### 1.7 Potential distinct functions of EGF and IFN $\gamma$

During the hepatic inflammation and injury, although EGF signaling is further activated, IFN $\gamma$  produced mainly by activated immune cells, also accumulates in the liver [75]. The two cytokines probably have opposing modulatory effects on cells. In one study, the authors announced that IFN $\gamma$ -induced HLA class II expression in human thyrocytes could be partly decreased by exposing thyrocytes to EGF, which happened when the cells were treated with two cytokines together or when EGF was added earlier or later than IFN $\gamma$  [92]. Similar contrary regulatory role was also observed in hepatocyte apoptosis modulation [93]. The researchers found that EGF exerted a cytoprotective effect against IFN $\gamma$ -induced apoptotic response in the liver. Such intriguing findings imply that EGF and IFN $\gamma$  may have opposing functions in the regulation of liver homeostasis, e.g. through affecting the gatekeeper of hepatic homeostasis ECM1 expression.

### 1.8 Aims of the study

Based on previous studies, ECM1 is a gatekeeper for maintaining L-TGF- $\beta$  quiescent in the healthy liver, and is significantly decreased during progression of chronic liver diseases. However, signaling pathways that maintain steady state ECM1 expression in hepatic homeostasis and those leading to a reduction in ECM1 expression under

liver damage conditions remains unknown. In this study, I aimed to uncover the underlying mechanisms of hepatic ECM1 regulation in both physiological and pathological situations with the following work packages:

- 1) Predict transcription factor candidates in the promoter region of the human and mouse *ECM1* genes using *in silico* analyses.
- 2) Directed by *in silico* analysis, functionally prove which cytokines regulate ECM1 expression in hepatocytes under normal conditions *in vitro* and *in vivo* in mouse liver.
- 3) Simulate chronic injury and inflammation conditions to identify cytokines/signals that downregulate ECM1 expression in damage situations, and experimentally confirm predictions *in vitro* and *in vivo*.
- 4) Delineate downstream signals/transcription factors that directly contribute to ECM1 expression repression in hepatocytes and approve the findings *in vivo*.

Elucidating the regulation of hepatic ECM1 expression may provide key information for modulating and improving the prognosis of chronic liver diseases and provide evidence for the development of ECM1 as a clinical anti-fibrotic agent.

## 2 MATERIALS AND METHODS

### 2.1 Materials

#### 2.1.1 Patients and liver tissues

The liver tissues of HCC patients were received and collected from Chirurgische Klinik, Universitätsmedizin Mannheim for biobanking. The research protocol complied with national laws and has been approved by the local Ethics Committee (approval 2012-293N-MA).

#### 2.1.2 Animals

8 to 10 weeks old male C57BL/6J mice were purchased from Janvier Lab and generally weighed 22-25g at the beginning of the corresponding experiments. All animals were allowed to acclimatize to controlled conditions of temperature ( $23 \pm 2^\circ\text{C}$ ), humidity ( $35 \pm 5\%$ ) and a 12hrs light–dark cycle in the animal house at Universitätsmedizin Mannheim for at least 1 week. They were provided with standard laboratory chow and water ad libitum and housed in laboratory cages.

The generation of ECM1 knockout (KO) mice has been described previously [94], in which the exons 2-11 of *Ecm1* gene were knocked out. All mice were of C57BL/6J background. The ECM1 wildtype (WT) and ECM1KO mice used in this study were generated from ECM1 heterozygous mice. Use genotyping to screen mice for different genotypes. The mice were bred under the same conditions as above.

All animal protocols were carried out in full accordance with animal care guidelines and were approved by the local Animal Care Committee.

#### 2.1.3 Primary human, mouse hepatocytes and cell lines

Table 1. Cells and culture medium

Cells	Culture medium
HPHs	Williams E, 10% FBS, 1% L-Glutamine, 1% P/S, 0.5% ITS, 0.1% Dexamethasone
MPHs	Williams E, 10% FBS, 1% L-Glutamine, 1% P/S, 0.5% ITS, 0.1% Dexamethasone
AML12	DMEM/F-12, 10% FBS, 1% L-Glutamine, 1% P/S, 0.5% ITS, 0.1% Dexamethasone
HCC cell lines	DMEM with high glucose, 10% FBS, 1% L-Glutamine, 1% P/S



## 2.1.4 Chemicals and reagents

Table 2. Chemicals and reagents

Chemical and reagents	Company	Cat. No.
Acetic acid	Sigma-Aldrich	338826
Acrylamide/Bis solution 37,5:1	Serva	10688.01
Ampicillin Natriumsalz	Carl Roth	K029.4
APS	Sigma-Aldrich	A3678
Bovine Serum Albumin	Serva	11930
Chloroform	Sigma-Aldrich	C2432
Collagen, Rat Tail	Roche	11179179001
Deoxyribonucleic acid sodium salt from salmon testes	Sigma-Aldrich	D1626
DEPC treated water	Thermo Fisher	4387937
Dexamethasone	Sigma-Aldrich	D4902
DMEM	Gibco	11965092
DMEM/F-12	Gibco	21331-020
DMSO	Sigma-Aldrich	41639
dNTP Mix	Thermo Fisher	R0191
DPBS	Thermo Fisher	14190169
ECL buffer (WB)	Perkin Elmer	NEL103001EA
EDTA	Sigma-Aldrich	E9884
EGF (m)	Corning	354001
EGF (h)	PeproTech	AF-100-15
Erlotinib	Cell signaling	5083S
Ethanol 96%	Carl Roth	T171.4
Ethanol 99.8%	Carl Roth	K928.4
Ethanol absolut zur Analyse	Neolab	LC-4045.1
FBS	Lifetechnologies	10270-106
Fluoromount-G mounting medium	Invitrogen	00-4958-02
Formaldehyde	Sigma-Aldrich	f1635
GelRed	GeneOn	S420
GeneRuler 100bp DNA Ladder	Thermo Fischer	SM0323
GeneRuler 1kb DNA Ladder	Thermo Fischer	SM0314
Glycine	Carl Roth	3790.2

HGF (m)	R&D	2207-HG-025
HGF (h)	R&D	294-HG-005
Hydrogen Peroxide 30%	Sigma-Aldrich	1072102500
IFN $\gamma$ (m)	PeptoTech	315-05
Insulin-Transferrin-Selenium (100x)	Lifetechnologies	41400-045
Isopropanol	VWR	1096342511
L-Glutamine 200mM	Sigma-Aldrich	G7513
Lithium chloride	Sigma-Aldrich	L-4408
LPS	Sigma-Aldrich	L3012
Methanol	Carl Roth	4627.6
NaHCO <sub>3</sub>	Biochrom	L1713
Nonidet P40 Substitute	Sigma-Aldrich	11754599001
NuPAGE™ LDS Sample Buffer (4X)	Lifetechnologies	NP0007
O.C.T compound	Hartenstein	TTEK
Oltipraz	Santa Cruz	sc-205777
Opti-MEM	Gibco	31985-070
Pageruler protein ladder	Thermo Fisher	26619
PBS	Biochrom	L182-50
Penicillin Streptomycin	Sigma-Aldrich	P0781
Phosphatase inhibitor cocktail 2	Sigma-Aldrich	P5726
Protease inhibitor cocktail	Roche	04693132001
PowerUp SYBR Green Master Mix	Thermo Fisher	A25918
Protein A/G Plus Agarose	Santa Cruz	SC-2003
Protein Assay Reagent A	Bio Rad	5000113
Protein Assay Reagent B	Bio Rad	5000114
Protein Assay Reagent S	Bio Rad	5000115
Proteinase K	Thermo Fisher	EO0491
Random Hexamer	Thermo Fisher	SO142
REDTaq ReadyMix	Sigma	R2523-100RXN
RevertAid H Minus Reverse Transcriptase	Thermo Fisher	EP0452
RiboLock RNase Inhibitor	Thermo Fisher	EO0382
RNAlater Stabilization Solution	Thermo Fisher	AM7020
RNase A	Thermo Fisher	EN0531

Sample Reducing Agent (10X)	Lifetechnologies	NP0009
SDS	Carl Roth	2326.2
Sodium chloride (NaCl)	Carl Roth	3957.2
Stripping buffer	Thermo Fisher	21059
TAE buffer (50X)	Jena Bioscience	BU-119-50
TEMED	Sigma-Aldrich	T9281
TNF- $\alpha$	PeproTech	300-01A
Tris	Carl Roth	5429.5
Triton™ X-100	Sigma-Aldrich	X100
Trizol reagent	Thermo Fisher	15596018
Trypsin-EDTA Solution (10X)	Sigma-Aldrich	T4174
Tween20	Neolab	1247ML500
Williams E medium ohne Phenolrot	ThermoFisher	A1217601

### 2.1.5 Antibodies

Table 3.1 Antibodies for immunoblotting

Antibody	Species	Dilution	Company	Cat.No.
ECM1 (m)	Rabbit	1:1000	Abcam	ab253185
ECM1 (h)	Mouse	1:500	Provided by Prof. Bing Sun [16]	
p-EGFR Y1068	Rabbit	1:1000	Cell Signaling	3777T
EGFR	Rabbit	1:1000	Cell Signaling	2232S
p-STAT1 S727	Rabbit	1:1000	Cell Signaling	8826S
p-STAT1 Y701	Rabbit	1:1000	Cell Signaling	9167S
STAT1	Rabbit	1:1000	Cell Signaling	9172T
p-ERK T202/Y204	Rabbit	1:1000	Cell Signaling	4370S
ERK 1/2	Mouse	1:1000	Santa Cruz	sc-135900
NRF2	Rabbit	1:500	Proteintech	16396-1-AP
p-STAT3 Y705	Rabbit	1:1000	Cell Signaling	9145S
STAT3	Mouse	1:1000	Santa Cruz	sc-8019
$\alpha$ -TUBULIN	Rabbit	1:2000	Abcam	ab4074
$\beta$ -ACTIN	Mouse	1:2000	Santa Cruz	sc-47778
GAPDH	Mouse	1:2000	Santa Cruz	sc-32233
Histone H3	Mouse	1:500	Santa Cruz	sc-517576

Anti-Rabbit IgG	Mouse	1:5000	Santa Cruz	sc-2357
Anti-Mouse IgG	Goat	1:5000	Santa Cruz	sc-2005

Table 3.2 Antibodies for immunofluorescence

Antibody	Species	Dilution	Company	Cat.No.
ECM1 (m)	Rabbit	1:100	Provided by Prof. Bing Sun [16]	
NRF2	Rabbit	1:100	Invitrogen	PA5-27882
DRAQ5		1:1000	Cell Signaling	4084L
Alexa Fluor 555 Goat anti-Rabbit	Goat	1:200	Invitrogen	A-21429
Alexa Fluor 488 Goat anti-Rabbit	Goat	1:200	Invitrogen	A-11008

Table 3.3 Antibodies for ChIP assay

Antibody	Species	Dilution	Company	Cat.No.
p-STAT1 S727	Rabbit	1:50	Cell Signaling	8826S
p-STAT1 Y701	Rabbit	1:50	Cell Signaling	9167S
NRF2	Rabbit	1:50	Invitrogen	PA5-27882
IgG Control	Rabbit	2.5µg/ml	Cell Signaling	3900S

### 2.1.6 Buffer preparation

Table 4 Buffer

Buffer	Compounds
Antibody dilution buffer (IF)	PBS 1x FBS 5% Triton X-100 0.3%
Blocking buffer (IF)	PBS 1x BSA 1% Triton X-100 0.3%
RIPA (Western blotting) pH 7.2	Tris 50mM NaCl 250mM Nonident P40 2% EDTA-Na 2.5mM SDS 0.1%

	Deoxycholic acid Na-salt 1.6g
Running buffer (WB) (10x) pH 8.3	Glycin 144g
	Tris 30.34g
	SDS 10g
Transfer buffer (WB) (10x)	Glycin 144g
	Tris 30.2g
	Methanol (before use, add 200ml/L)
TBST (WB) (10x) pH 7.5	Tris 12.1g
	NaCl 87.66g
	Tween-20 10ml
Lysis buffer (ChIP)	SDS 1%
	EDTA 10mM
	Tris-Cl (pH 8.0) 50mM
Dilution buffer (ChIP)	SDS 0.01%
	Triton X-100 1.1%
	EDTA 1.2mM
	Tris-Cl (pH 8.0) 16.7mM
	NaCl 167mM
TSE I (ChIP)	SDS 0.1%
	Triton X-100 1%
	EDTA 2mM
	Tris-Cl (pH 8.0) 20mM
	NaCl 150mM
TSE II (ChIP)	SDS 0.1%
	Triton X-100 1%
	EDTA 2mM
	Tris-Cl (pH 8.0) 20mM
	NaCl 500mM
Buffer III (ChIP)	LiCl 0.25M
	NP-40 1%
	Deoxycholic acid 1%
	EDTA 1 mM
	Tris-Cl (pH 8.0) 10mM
TE buffer (ChIP)	Tris-Cl (pH 8.0) 10mM

Elution buffer (ChIP)	EDTA 1mM
	SDS 1%
	NaHCO <sub>3</sub> 0.1M

### 2.1.7 Kits and assays

Table 5 Kits and assays

Product	Company	Cat.No.
Lipofectamine® RNAiMAX kit	Thermo Fischer	13778-075
Phusion® High-Fidelity DNA Polymerase	New England Biolabs	M0530S
Bio-Rad protein assay kit	Bio Rad	5000113-115
SYBR Green Master Kit	Thermo Fisher	A25918
MinElute PCR Purification Kit	Qiagen	28006
NE-PER™ Nuclear and cytoplasmic extraction reagents	Thermo Fisher	78835

### 2.1.8 Small interfering RNA

Table 6 Small interfering RNA

RNAi	Species	Company	Cat.No.
siEgfr	Mouse	Santa Cruz	sc-29302
siStat1	Mouse	Santa Cruz	sc-44124
siErk1	Mouse	Santa Cruz	sc-29308
siErk2	Mouse	Santa Cruz	sc-35336
Control siRNA		Qiagen	SI03650318

### 2.1.9 Experimental consumables

Table 7 Experimental consumables

Material	Company	Cat.No.
10ul Tip	StarLab	S1111-3000
200ul Tip	StarLab	S1111-0006
1000ul Tip	StarLab	S1111-6001
Safe lock tubes 0.5ml	Eppendorf	30121023
Safe lock tubes 1,5ml	Eppendorf	30120086
Safe lock tubes 2.0ml	Eppendorf	30123344

PCR tubes 0.2 mL	Eppendorf	30124359
Cryotubes, 2 ml	Greiner	126280
50 ml Falcons	Greiner	227261
15 ml Falcons	Greiner	188271
Serol. Pipette 50ml, single packed	Greiner	768180
Serol. Pipette 25ml, single packed	Greiner	760180
Serol. Pipette 10ml, single packed	Greiner	607180
Serol. Pipette 5ml, single packed	Greiner	606180
Aspiration pipette 2mL	Greiner	710183
6-well plate	Greiner	657160
12-well plate	Greiner	665180
24-well plate	Greiner	662160
96-well plate	Greiner	655180
Petri Dish 100 x 20, sterile	Greiner	P5737-360EA
Cell Culture Flask 25cm <sup>2</sup> , 50ml	Greiner	690175
Cell Culture Flask 75cm <sup>2</sup> , 250ml	Greiner	658175
Cell Culture Flask 175cm <sup>2</sup> , 550ml	Greiner	660175
Cryomold Standard 25x20x5mm	Labor Weckert	4557
Cryomold Standard 15x15x5mm	Labor Weckert	4566
Zirconium Beads 2.0mm	Carl Roth	N039.1
Filtropur S 0.45	Sarstedt	831826
Filtropur S 0.2	Sarstedt	831826001
MicroAmp Fast Optical 96-Well Reaction Plate	Lifetechnologies	4346907
Adhesive seals 100 sheets	Thermo Fisher	AB-0558
96 MicroWell™ Platten, Nunc™	Thermo Fisher	732-2717
0.2µm Nitrocellulose membranes	GE Healthcare Life Sciences	10600001
Sponge Pad	Invitrogen	E19052
Blotting Paper, 100/PAK	Whatman	WH3030-917
Mini-protean Spacer Plates 1.5mm Integrated Spacers	Bio-Rad	1653312
Mini-PROTEAN® Short Plates	Bio-Rad	1653308
Mini-PROTEAN® comb, 15well, 1.5mm	Bio-Rad	1653366

Mini-PROTEAN® comb, 10-well, 1.5 mm	Bio-Rad	1653365
Mini-PROTEAN® Casting Frame	Bio-Rad	1653304
Microscope cover glasses, No 1, 18 mm	Paul Marienfeld	0111580
Microscope cover glasses, No 1, 12 mm	Paul Marienfeld	0111520
Microscope slides	Carl Roth	ET081
Microtom Klengen R35	Hartenstein	0207500005
DAKO PEN	DAKO	S2002
XCEED Nitrile Gloves, Powder Free, Blue	Star Lab	XC-INT-S
Parafilm 10cm x 38m	Häberle	743311

### 2.1.10 Experimental instruments

Table 8 Experimental instruments

Instruments	Company	Cat.No.
Ultra-clean workbench	Kendro	KS 9
Autotechnikon	Leica	TP1020
CO <sub>2</sub> incubator	Thermo Scientific	HERACELL
Benchtop Centrifuge	Heraeus	30023354
BioRuptor water bath sonicator	Diagenode	B01020001
Microscope for cell culture	Leica	521665
Microscope Confocal, TCS SP8	Leica	N.A.
Water Bath	VWR	10128
Counting Chamber	BRAND	N.A.
Cryo 1°C Freezing Container	NALGENE	5100-0001
Liquid nitrogen tank	Cryotherm	78204183
4°C refrigerator	LIEBHERR	22336
-20°C refrigerator	Premium NoFrost	3366
-80°C refrigerator	Thermo Scientific	HFU T SERIES
Incubator	BINDER	9010-0080
Centrifuge for 96-well plate	Heraeus Christ	00097349
Multimode microplate reader	TECAN	Spark 10M
Precellys Evolution	Bertin Technologies	FAK-0704
PCR analyzer	VWR	732-2548
StepOnePlus Real-Time PCR System	Thermo Fisher	4376600



Thermomixer compact	Eppendorf	5382000015
Vortex Mixers	VWR	444-1372
Duomax 1030 Shakers & Mixers	Heidolph	543-32210-00
RM5	CAT	60207-0110
Sprout Mini-Centrifuge	Heathrow Scientific	120611
Electrophoresis Chambers	Bio-Rad	1658004
Trans-Blot Cell	Bio-Rad	1703939
Power Supplies	Bio-Rad	1645070
Imaging system	PEQLAB	Fusion SL4
Cryotome	Leica	CM3050S
Microwave oven	MDA	44577
Autoclave	Systec	VX-150
Ice Machine	Manitowoc	UD0310A
1ml Pipette	Eppendorf	2897987
200ul Pipette	Eppendorf	293339
100ul Pipette	Eppendorf	1007324
20ul Pipette	Eppendorf	1969964
10ul Pipette	Eppendorf	1984124
2.5ul Pipette	Eppendorf	1966584
DualRange Balance	Sartorius	BP211D
Digital Balance	Sartorius	LP6200
Gel Electrophoresis Device	CLP	75.1214
Gel iX 20 Imager	INTAS	N.A.
Rotator	Stuart	SB3
Hot plate magnetic stirrers	IKA-Werke	RCT basic
Pipette filler pipetus	Hirschmann	13014
pH/mV/°C meters	inoLab	pH7110

---

### 2.1.11 Software

Table 9 Software

---

Software	Source	Link
GraphPad Prism 8.0	Graphpad	<a href="https://www.graphpad.com/scientificsoftware/prism/">https://www.graphpad.com/scientificsoftware/prism/</a>

---

BioRender	Crunchbase	<a href="https://biorender.com/">https://biorender.com/</a>
ImageJ	NIH	<a href="https://imagej.nih.gov">https://imagej.nih.gov</a>
Primer bank	harvard.edu	<a href="https://pga.mgh.harvard.edu/primerbank/">https://pga.mgh.harvard.edu/primerbank/</a>
Primer blast	NIH	<a href="https://www.ncbi.nlm.nih.gov/tools/primer-blast/">https://www.ncbi.nlm.nih.gov/tools/primer-blast/</a>
GeneCards	the Weizmann Institute of Science	<a href="https://www.genecards.org/">https://www.genecards.org/</a>
ENCODE	NHGRI	<a href="https://www.encodeproject.org/">https://www.encodeproject.org/</a>

---

## 2.2 Methods

### 2.2.1 Animal experiments

The male C57BL/6J mice (8 to 10 weeks old) purchased from Janvier Lab were divided into groups randomly (n=3) and were used for the injection of EGF/PBS, or erlotinib/DMSO, or IFN $\gamma$ /PBS.

#### (1) EGF injection

EGF was dissolved in PBS (14190169, ThermoFisher) to make a stock of 100ug/ml. Mice were administered intravenously with PBS (control group) or 1.2mg/kg EGF. Samples were collected 24/48hrs after the administration of PBS or EGF. Body weights were recorded. Blood samples were obtained from the retro-orbital plexus. The animals were killed by cervical dislocation, and livers were quickly removed and weighed.

#### (2) Erlotinib injection

Erlotinib was dissolved in DMSO (41639-500ML, Sigma-Aldrich) to make a stock of 10mg/ml. Mice were administered intraperitoneally with DMSO (control group) or 40mg/kg/day erlotinib for 2 days (once per day). Samples were collected 48hrs after the first dose of DMSO or erlotinib was injected. Body weights were recorded. Blood samples were obtained from the retro-orbital plexus. The animals were killed by cervical dislocation, and livers were quickly removed and weighed.

#### (3) IFN $\gamma$ injection

IFN $\gamma$  was dissolved in PBS (14190169, ThermoFisher) to make a stock of 100ug/ml. Mice received a series of 4 intraperitoneal injections (once per day) of PBS (control group) or 400 $\mu$ g/kg/day IFN $\gamma$ .

Samples were collected 96hrs after the first dose of PBS or IFN $\gamma$  was treated. Body weights were recorded. Blood samples were obtained from the retro-orbital plexus. The animals were killed by cervical dislocation, and livers were quickly removed and weighed.

#### (4) Liver/blood sampling from the mouse

a) Preparation before starting: mark the cryotubes for each RNA (put 1ml RNAlater in cryotubes for RNA), protein, blood sample; mark the embedding cassettes for each immunohistochemistry sample; mark the cryomolds for each immunofluorescence sample. Have all other needed supplies ready on the bench, for example, autoclaved sterilized forceps and scissors, cotton tips, 70% ethanol, 100mm petri dishes, liquid nitrogen, dry ice, ice, 4% PFA et al.

b) Anesthetize mouse with an intraperitoneal injection of 10% ketamine hydrochloride (5mg/100mg body weight) and 2% xylazine hydrochloride (1mg/100mg body weight). After cervical dislocation, place the mouse on the dissection tray and fix the limbs with needles.

c) Disinfect the abdomen thoroughly with 70% ethanol. Cut through skin and abdominal muscles using scissors. Expose the liver using the cotton tip.

d) Carefully remove the liver from the mouse, place the liver on the surface of 100mm petri dish filled with ice.

e) Divide the median lobe for RNA and protein collection, put the tissue for RNA in the cryotubes with RNAlater, keep on ice/4°C storing room. The second day remove RNAlater and transfer to -80°C. The tissue for protein can be fast frozen in liquid nitrogen and transferred to -80°C for storing.

f) The cassettes with the left lobes are placed in 4% PFA, 4°C overnight. The second day change to 2% PFA for long-term storage. Prior to paraffin embedding, the tissue cassettes are dehydrated in Autotechnikon. Embed the tissues in paraffin, after solidification, store at RT.

g) Right and caudate lobes can be fast frozen on the dry ice in the cryomolds with O.C.T compound (TTEK, Hartenstein), transfer them to -80°C for long-term storage.

h) Centrifuge blood samples at 3000rpm, 4°C for 5min, aspirate the supernatant to a new 1.5ml Eppendorf tube, store at -80°C.

(5) Organs sampling for mouse clinics

ECM1WT and ECM1KO mice at 5 and 8wks were used to collect different organs, e.g. liver, kidney, spleen, pancreas, colon, lung, heart, brain, muscle and bone. The tissues were placed in the cassettes and kept in 4% PFA, 4°C overnight. After two days of fixation, the tissues were dehydrated prior to paraffin embedding. The embedded tissues were sent to the mouse clinics department for further analysis.

2.2.2 Mice genotyping

To select the ECM1KO mice, genotyping was performed after earmarking. Neo cassette is inside the ECM1KO construct (indicates either hetero- or homo-zygosity).

(1) DNA extraction from cut ears

- a) Briefly centrifuge the cut ears to the bottom of tubes
- b) Add 50µl 50mM NaOH
- c) Boil at 99°C for 20min while shaking
- d) Briefly centrifuge
- e) Add 12.5µl 1M Tris pH6.0
- f) Centrifuge at 13,000rpm for 10min
- g) The supernatant can be directly used for next PCR step or stored at -20°C

(2) PCR analysis

a) Prepare the following mixture in each tube:

ReadyMix RedTaq	5µl
DEPC water	3.6µl
Primer Forward	0.2µl
Primer Reverse	0.2µl
Extracted DNA	1µl

b) Run PCR program as follows:

Initial denaturation	95°C	5min	
Denaturation	95°C	30s	
Annealing	58°C	40s	35 cycles
Extension	72°C	1min	

Final extension	72°C	5min
	4°C	Hold

c) Add 6x DNA loading, run PCR products on a 2% gel, 130V for 50min

d) Confirm the genotypes according to the imaging under UV lamp:

Genotype	ECM1	NEO
WT	+	-
ECM1KO hetero	+	+
ECM1KO homo	-	+

Table 10 Primers used for Genotyping

Gene	Forward primers (5'-3')	Reverse primers (5'-3')
<i>Ecm1</i>	GCAGACTGGCTACTCTCACC	AGTCTAGGCGGTTTGTGTCG
<i>Neo</i>	CATTCGACCACCAAGCGAAACATC	ATATCACGGGTAGCCAACGCTATG

### 2.2.3 Primary mouse hepatocyte isolation

8 to 10 weeks old male C57BL/6J mice were purchased from Janvier Lab and generally weighed 22-25g for the hepatocyte isolation.

(1) Preparation before starting: Heat water bath to 37°C, pre-cool centrifuge to 4°C. Assemble the perfusion pump and the autoclaved tubing, connect the 27G needle to the outlet end of the tubing. Have all other needed supplies ready on the bench, for example, 50ml falcon with 10ml pre-cooled suspension buffer (SB), autoclaved sterilized forceps and scissors, cotton tips, 70% ethanol et al.

(2) Prepare the buffers (EGTA buffer, Collagenase buffer, and SB) for perfusion as shown in Table 11.

Table 11 Buffer for perfusion

Buffer (ml)	EGTA Buffer	Collagenase Buffer	Suspension Buffer (SB)
enough for mice	2x	2x	2x
Glucose	124	77,5	310
KH -Buffer	20	12,5	50
Hepes pH 8,5	20	12,5	
Amino. Acid Solu.	30	19	75
Glutamin	2	1,25	5
EGTA	0,8		
CaCl <sub>2</sub>		5	4
Hepes pH 7,6			50
MgSO <sub>4</sub>			2

BSA		1g
total volume	127,75	
ratio from Vol. to CaCl <sub>2</sub>	25,55	
	in 65ml final	
	coll.buffer add	
	2,54ml CaCl <sub>2</sub>	

---

(3) Pre-warm EGTA buffer, Collagenase buffer to 37°C in the water bath, pre-cool SB in 4°C refrigerator. Aspirate 10ml SB to 50ml falcon and keep on ice for later use.

(4) Insert the needleless end of the tubing into EGTA buffer, turn on the perfusion pump, drive out air in the tubing, let the warm EGTA buffer reach the end. Stop the pump.

(5) Primary mouse hepatocyte isolation was performed as previous description [95] with minor modifications.

a) Anesthetize mouse with an intraperitoneal injection of 10% ketamine hydrochloride (5mg/100mg body weight) and 2% xylazine hydrochloride (1mg/100mg body weight). Place the mouse on the dissection tray and fix the limbs with needles.

b) Disinfect the abdomen thoroughly with 70% ethanol. Cut through skin and abdominal muscles using scissors. Expose the liver, portal vein, and inferior vena cava using the cotton tip.

c) Insert the needle (disconnection from the tubing) to the inferior vena cava, ensure that the needle is in the vein and is flat against the vessel, and stays stable.

d) Turn on the pump and keep its speed at 3ml/min, connect the tubing to the needle in the vena cava, then stop the pump and adjust the speed to 6ml/min.

e) Cut the portal vein and in the meantime turn on the pump, the mouse liver is sequentially perfused with 50ml EGTA buffer through vena cava to portal vein. After approximately 5min, stop the pump, change the tubing to the bottle containing Collagenase buffer, turn on the pump, the liver is now digested, causing the disruption of supporting extracellular matrix. Digestion time is based on collagenase activity and the observation of liver condition, if the liver turns pale in colour and appears swollen and relaxed, digestion can be terminated.

f) Remove the perfused liver, put it in the pre-cooled 10ml SB on ice, transfer the liver with SB into 100mm petri dish. Place a 100µm cell strainer on a 50ml falcon.

- g) Mince liver using two forceps under the hood to release hepatocytes in SB. After pipetting cells into 100µm cell strainer, wash the petri dish with 12ml pre-cooled SB and then transfer this washed SB into cell strainer.
- h) Centrifuge the cell suspension at 50g, 4°C for 5min, discard the supernatant, and fill with 30ml SB.
- i) Centrifuge the cell suspension at 28g, 4°C for 2min, discard the supernatant.
- j) To remove dead cells, add 19ml Percoll solution and then centrifuged at 270g, 4°C for 10min. Discard the upper cell layer and the percoll solution.
- k) Add 10ml SB to the bottom pellet, transfer to a new 50ml falcon, add another 25ml SB.
- l) Centrifuge the cell suspension at 28g, 4°C for 5min, discard the supernatant, add 10ml Williams-medium to the pellet.
- m) Count the cell number and start seeding and plating as usual.

#### 2.2.4 Primary human hepatocyte isolation

Primary human hepatocytes were isolated by the Department of General, Visceral, Vascular, and Pediatric Surgery, University of Saarland Medical Center, Homburg, using a two-step collagenase perfusion technique with modifications [96].

The study protocol complied with national laws and was approved by the local Ethics Committee (approval Nr. 143/21).

#### 2.2.5 Cell culture and treatment

##### (1) Cell culture

Cells and culture medium used in this study are listed in the Table 1. AML12 cells were grown in DMEM/F-12 medium (21331-020, Gibco) supplemented with 10% Fetal bovine serum (FBS), 2mM L-glutamine, penicillin (100U/mL)-streptomycin (100µg/mL) (P/S), 0.5% Insulin-Transferrin-Selenium (ITS) and 40ng/ml dexamethasone. The isolated mouse primary hepatocytes and human primary hepatocytes were seeded on Rat Tail Collagen I (11179179001, Roche, 250µg/mL in 0.2% acetic acid)-precoated plates in William's E medium (A1217601, ThermoFisher) supplemented with 10% FBS, 2mM L-glutamine, 1% P/S, 40ng/ml dexamethasone and 0.5% ITS. HCC cell lines, HuH7, HLF, Hep3B, HLE and PLC/PRF/5 were grown in DMEM with high glucose (11965092, Gibco) supplemented with 10% FBS, 2mM L-

glutamine, 1% P/S. All cells were cultured in the 37°C incubator with a humidified atmosphere containing 5% CO<sub>2</sub>.

(2) Growth factor/cytokine treatment

After seeding, cells were cultured in complete medium for 24hrs. Before the treatment with 100ng/ml epidermal growth factor (EGF), 100ng/ml hepatocyte growth factor (HGF) or 100ng/ml interferon gamma (IFN $\gamma$ ), 4ng/ml tumor necrosis factor alpha (TNF- $\alpha$ ) or 5 $\mu$ g/ml Lipopolysaccharide (LPS), cells underwent a 4-to-6-hour starvation in FBS-free medium. Cells were collected at indicated time points.

In the experiments where EGF and IFN $\gamma$  were co-treated, cells were collected after 24hrs of co-treatment.

(3) Inhibitor treatment

For inhibitor experiment, cells were pretreated with erlotinib (1 $\mu$ M) for 2hrs prior to incubation with EGF (100ng/ml) for 24hrs.

(4) siRNA transient transfection

For transient transfection of siRNA, cells were seeded with completed medium for 24hrs. Before knockdown, cells underwent a 4-to-6-hour starvation in FBS-free medium, followed by the addition of siRNA for 24hrs (30nM each for siEgfr, siErk1, siErk2 and siStat1), and then the growth factor/cytokine were added. Cells were collected after 24hrs of growth factor/cytokine treatment. Details are provided in 2.2.9 RNA interference.

## 2.2.6 RNA isolation and qRT-PCR

All reagents and containers used for RNA processing were either RNase-free grade or treated with 0.1% DEPC to eliminate RNase contaminants.

(1) RNA isolation from cells

Total RNA was extracted with TRIzol according to the manufacturer's instructions.

a) Add 100 $\mu$ l TRIzol per well to a 12-well plate, scrape the cells, collect the lysate and transfer to a 1.5ml Eppendorf tube.

b) Lyse on ice for 10min.

c) Add 20 $\mu$ l chloroform, vigorously shake for 15s, incubate at RT for 3min.

d) Centrifuge at 13,000rpm for 15min at 4°C.



- e) Collect transparent extracts from the upper layer into a new 1.5ml Eppendorf tube. Aspirate carefully, do not touch other layers.
- f) Add 100ul isopropanol, gently shake for 15s, incubate at RT for 10min.
- g) Centrifuge at 13,000 rpm at 4°C for 10min, discard the supernatant.
- h) Add 150ul 75% ethanol (750ul Absolute ethanol plus 250ul DEPC water) to rinse the precipitation, centrifuge at 13,000rpm for 10min at 4°C, discard the supernatant.
- i) Dry at RT for 10min. Add 20~50ul DEPC to dissolve the precipitated RNA.
- j) The concentration of RNA was measured by absorbance at 260nm and 280nm using a multimode microplate reader TECAN.

(2) RNA isolation from liver tissues

- a) Cut a small amount of tissue on ice, place in a 1.5ml Eppendorf tube, add 1ml Trizol. After adding a few beads, grind with a homogeniser until no big pieces of tissue remain.
- b) Lyse on ice for 10min.
- c) The rest of the procedure is the same as cell RNA isolation, with appropriate adjustments to the amount of all reagents added.

(3) cDNA synthesis

- a) Prepare the following RNA/primer mixture in each tube:

- Total RNA 500ng
- Random primer 0.5µl
- DEPC water (nuclease-free) to 6.5µl

- b) Prepare reaction master mixture. For each reaction:

- 5x Reaction Buffer 2µl
- 10mM dNTP mix 1µl
- RevertAid H Minus Reverse Transcriptase 0.25µl
- RiboLock Rnase Inhibitor 0.25µl

- c) Perform PCR program of cDNA synthesis

- Heat lid to 110°C

- Temp. 65°C for 5min

- Pause at 4°C (while pausing, add the reaction mixture to the RNA/primer mixture, mix briefly)

- Temp. 25°C for 5min

Temp. 42°C for 1hr

Temp. 70°C for 5min

Temp. 4°C

Store cDNA at -20°C until using for qRT-PCR.

#### (4) qRT-PCR

Dissolve the forward and reverse primers according to the instructions to make a stock of 100pmol/ml. All primers were synthesized by Eurofins. Before use, dilute the primers in Aqua dest at a ratio of 1:10. The synthetic cDNA was also diluted in Aqua dest according to 1:10. Mix the reaction system as follows:

Reagent	Volume
SYBR Green	5µl
Primer-F	0.5µl
Primer-R	0.5µl
H <sub>2</sub> O	9µl
cDNA	5µl

qRT-PCR assays were performed on a StepOnePlus system (Applied Biosystem) using SYBR Green Master Kit. Each sample ran in triplicate. Perform qRT-PCR program as follows:

Polymerase activation	95°C	15min	
Denaturation	95°C	15s	
Annealing	60°C	20s	40 cycles
Extension	72°C	20s	
	95°C	15s	
Melt curve stage	60°C	1min	
	95°C	15s	

The relative quantification of target genes was normalized to the house keeping gene PPIA. Three biological replicates of each condition were measured. The relative fold change in abundance of each target gene compared to a set of internal controls was determined by the  $-2^{\Delta\Delta CT}$  formula [97]. Primers for qRT-PCR chosen from Primerbank (<https://pga.mgh.harvard.edu/primerbank/>) were listed in Table 12. All primers were compared with BLAST to avoid non-specific annealing and cross-amplification (<https://www.ncbi.nlm.nih.gov/tools/primer-blast/>).

Table 12 Primers used for qRT-PCR in the study

Gene	Forward primers (5'-3')	Reverse primers (5'-3')
<i>Ppia</i>	GAGCTGTTTGCAGACAAAGTT	CCCTGGCACATGAATCCTGG
<i>Ecm1</i>	GCCAGCTCTGTGGAAGTGGA	CCGGAATCTGTTTATGCTTGC
<i>Egfr</i>	GCCATCTGGGCCAAAGATAACC	GTCTTCGCATGAATAGGCCAAT
<i>Stat1</i>	TCACAGTGGTTCGAGCTTCAG	GCAAACGAGACATCATAGGCA
<i>Erk1</i>	TCCGCCATGAGAATGTTATAGGC	GGTGGTGTGATAAGCAGATTGG
<i>Erk2</i>	GGTTGTTCCCAAATGCTGACT	CAACTTCAATCCTCTTGTGAGGG
<i>Nrf2</i>	CTGAACTCCTGGACGGGACTA	CGGTGGGTCTCCGTAAATGG
<i>Nox4</i>	AAAGCAAGACTCTACACATCACAT	AGTTGAGGGCATTACCAAG
<i>PPIA</i>	AGCATGTGGTGTGGCAA	TCGAGTTGTCCACAGTCAGC
<i>ECM1</i>	TGAACCAAATCTGCCTTCCTAAC	GCTGGACTGTGGTAGGTTCCA

### 2.2.7 Western blotting

#### (1) Whole protein extraction

a) For cultured cells: Cells were washed twice with ice-cold PBS, RIPA buffer (80µl per well of a 6-well plate) supplemented with protease inhibitor and phosphatase inhibitor was immediately added.

For liver tissue: Cut a small amount of tissue on ice, place in a 1.5ml Eppendorf tube, add 500µl RIPA buffer. After adding a few beads, grind with a homogeniser until no big pieces of tissue remain.

b) Lyse on ice for 10min.

c) The cultured cells were scraped to collect the lysate and transferred to 1.5ml Eppendorf tubes. The liver tissue went directly to the next step.

d) Centrifuge at 13,000rpm for 10min at 4°C. The supernatant was collected in a new 1.5ml Eppendorf tube.

#### (2) Protein concentration measurement

##### a) Measurement standard curve

Add 20µl of Reagent A diluted with Reagent S (50:1) to a 96-well plate, then add 2µl of each standard sample and mix with 200µl Reagent B. The standard samples albumin (0.125, 0.25, 0.5, 1, 1.5, 2mg/ml) used were provided from Bio-Rad Protein Assay Kit. Incubate at RT while shaking for 10min, the plate was then applied to multimode microplate reader TECAN and absorbance was measured at 565nm. Standard curve was generated based on absorbance values and sample concentrations.

b) The absorbance at 565nm of the supernatant from the samples was determined in the same way. The sample concentration was calculated from the standard curve. After addition of LDS sample buffer (4x) and Sample reducing agent (10x), samples were all standardised to the same concentration and boiled at 99°C for 10min. Store at -20°C until use.

### (3) Western blotting

30µg protein were separated by 8-12% sodium dodecyl sulfate polyacrylamide gel electrophoresis (SDS-PAGE) and transferred to 0.2µm Nitrocellulose membranes (10600001, GE Healthcare Life Sciences). After blocking with 5% BSA in TBST (Tris-buffered saline with 0.05% Tween 20) for 1hr at RT, the membranes were incubated with primary antibodies overnight at 4°C. The next day, following the TBST washing steps, the membranes were incubated with secondary antibodies for 1hr at RT. After washing with TBST three times, signals were visualized by the Western Lightning Plus-ECL (NEL103001EA, Perkin Elmer) and recorded by the imaging system Fusion SL4 (PEQLAB, Germany). Antibodies used were listed in Table 3.1. Beta-ACTIN, GAPDH, and Alpha-TUBULIN were used as loading controls. Each Western blotting experiment was repeated at least three times.

### 2.2.8 Nuclear and cytoplasmic protein extraction

The extraction was performed using NE-PER Nuclear and Cytoplasmic Extraction Reagents according to the manufacturer's instructions.

#### (1) Cell culture preparation

- a) Harvest with trypsin-EDTA and then centrifuge at 500g for 5min.
- b) Wash the cells by suspending the cell pellet in DPBS.
- c) Transfer 1-10 x 10<sup>6</sup> cells to a 1.5ml Eppendorf tube and centrifuge at 500g for 2-3min to pellet the cells.
- d) Carefully remove and discard the supernatant with a pipette, allowing the cell pellet to dry as much as possible.
- e) 200µl ice-cold CER I was added to the cell pellet.

#### (2) Extraction of cytoplasm and nuclear proteins

- a) Vortex the tube vigorously for 15s on the highest setting to completely suspend the cell pellet. Incubate the tubes on ice for 10min.

- b) Add 11µl ice-cold CER II to the tube.
- c) Vortex the tube on the highest speed for 5s. Incubate on ice for 1min.
- d) Vortex for 5s at maximum speed. Centrifuge the tube at maximum speed for 5min (~16,000g).
- e) Immediately transfer the supernatant (cytoplasmic extract) to a clean pre-cooled tube. Place the tube on ice until use or store at -80°C.
- f) Suspend the insoluble (pellet) fraction containing the nuclei produced in step d) in 100µl ice-cold NER.
- g) Vortex for 15s at the highest setting. Place the sample on ice and continue vortexing for 15s every 10min, for a total of 40min.
- h) Centrifuge the tube at the highest speed (~16,000 g) for 10min.
- i) Immediately transfer the supernatant (nuclear extract) fraction to a clean pre-cooled tube. Place on ice.
- j) Store the extract at -80°C until use.

(3) Protein concentration measurement and Western blotting were performed as described in 2.2.7.

### 2.2.9 RNA interference

Small interfering RNAs (siRNAs) were transfected into cells using Lipofectamine RNAiMAX reagent according to the manufacturer's instruction.

(1) Cells were seeded 24hrs before transfection and expected to be 60-80% confluent when transfection started. Before knockdown, cells underwent a 4-to-6-hour starvation in FBS-free medium.

(2) Prepare siRNA-lipid complexes

- a) Dilute Lipofectamine RNAiMAX reagent in Opti-MEM medium by adding 3µl RNAiMAX into 75µl Opti-MEM medium in tube A, mix well;
- b) Dilute siRNA in Opti-MEM medium by adding 3µl siRNA (10µM) into 75µl Opti-MEM medium in tube B, mix well;
- c) Add diluted siRNA to diluted Lipofectamine RNAiMAX Reagent with a ratio of 1:1, mix well, then incubate the mixture for 5min at RT.

(3) Carefully add siRNA-lipid complexes to cells. The transfected cells were incubated at 37°C and subjected to different treatments after 24hrs of transfection. RNA and whole cell protein were collected 48hrs after transfection.

siRNAs used in the study were listed in Table 6. The AllStars Negative Control siRNA (SI03650318, Qiagen) was used as a negative control.

#### 2.2.10 Immunofluorescence staining

##### (1) Liver tissue staining

Fresh liver blocks were frozen under dry ice in O.C.T compound (TTEK, Hartenstein) and stored at -80°C. 6µm thick sections were cut by cryotome.

a) Tissue slides were fixed with 4% PFA at RT for 15min.

b) Rinse with PBS three times, then permeabilize and block slides with 0.5% Triton X-100 and 1% BSA in PBS for 1hr at RT.

c) Incubate the slides subsequently with primary antibodies (1:100) diluted in PBS with 1% BSA at 4°C overnight.

d) Next day, wash the slides in PBS three times, then incubate with fluorochrome-conjugated secondary antibodies (1:200) and DRAQ5 (1:1000) diluted in PBS for 1hr. Protect from light during this and the next steps.

e) Wash with PBS three times, mount slides with a drop of Fluoromount-G mounting medium (00-4958-02, Invitrogen).

f) Dry at RT overnight. Store at 4°C until use.

g) Images were scanned under the Leica Microscope Confocal TCS SP8.

##### (2) Cultured cell staining

Cultured cells were seeded onto 12-well plates with microscope cover glasses (0111580, MARIENFELD) for corresponding experiments. After the experiments, wash cells with PBS three times. Fix cells with 4% PFA for 15min at RT. Wash with PBS three times, and block and permeabilize cells with 0.5% Triton X-100 and 1% BSA in PBS for 1hr at RT. Other steps were as described above. Antibodies used were listed in Table 3.2.

### 2.2.11 Immunohistochemistry staining

All organs collected from ECM1WT and ECM1KO mice were fixed in 4% formalin and paraffin embedded. For histology 3-5 $\mu$ m-thick sections were cut and stained with hematoxylin and eosin (H&E) and Masson Trichrome (MTC).

#### (1) HE staining

- a) Baking: tissue sections were baked in an oven at 60°C for 1-2hrs.
- b) Deparaffinization: deparaffinize in xylene 2 times for 5min each.
- c) Hydration: rinse in 100% ethanol, 95% ethanol, 90% ethanol, 80% ethanol, 70% ethanol for 3min and in distilled water for 2min respectively.
- d) Hematoxylin staining: hematoxylin dye on sections, incubation at room temperature for 10min, rinse with tap water; fractionation with 1% hydrochloric acid in 75% ethanol for 30s, wash with tap water.
- e) Eosin staining: 5% eosin dye on sections, incubation for 3min at room temperature, rinse in distilled water for 1min.
- f) Dehydration: rinse in 95% ethanol, 95% ethanol, 100% ethanol and 100% ethanol for 1min each; rinse in xylene twice for 5min each time; mount the sections with mounting medium.
- g) Scanning and image acquisition of HE-stained sections using a section scanner.

#### (2) MTC staining

- a) Deparaffinization of paraffin sections.
- b) Wash with distilled water.
- c) Stain of nucleus with hematoxylin dye for 5-10min.
- d) Fractionation with 1% hydrochloric acid in 75% ethanol for 5-15s, wash with distilled water.
- e) Add 0.1-1% lithium carbonate dropwise for 5min to increase the degree of anti-blue, wash with distilled water.
- f) Stain with Masson Lichon Red for 5-10min.
- g) Wash with 2% glacial acetic acid aqueous solution for 1min.
- h) Fractionation with 1% aqueous phosphomolybdic acid for 3-5min, wash with 2% aqueous glacial acetic acid for 1min.
- i) Directly stain with aniline blue aqueous solution for 1-2min without water washing; wash with 0.2% glacial acetic acid aqueous solution for 1min.

j) Dehydration in 95% ethanol for 2-3s, 100% ethanol 3 times for 5s each time, xylene 3 times for 1min each time, mount the sections with mounting medium.

k) Scanning and image acquisition of MTC-stained sections using a section scanner.

#### 2.2.12 Liver echography

Echography of the liver was utilized to non-invasively estimate portal vein diameter and portal blood flow in ECM1WT and KO mice as a reflection of portal pressure magnitude. B-mode images were acquired in a modified short-axis view depicting the lobes of the liver. In addition, the portal vein was recorded in both B-mode and M-mode long-axis views.

#### 2.2.13 Chromatin immunoprecipitation

Chromatin immunoprecipitation was performed as previously described with minor modifications [98]. For each ChIP, approximately  $1 \times 10^7$  cells were seeded on a 10cm cell culture dish (95% confluence) and treated accordingly.

(1) Incubate cells with 1% PFA for 10min at 37°C to crosslink chromatin and protein.

(2) Remove PFA, wash cells with cold PBS twice and scrape in cold PBS following centrifugation at 1000g, 4°C for 5min.

(3) Discard the supernatant, resuspend the cell pellet in 500µl lysis buffer containing 1% protease inhibitor cocktail and lyse on ice for 10min.

(4) The chromatin was sonicated using a BioRuptor water bath sonicator (Diagenode), 30sec on/30sec off for 35-40 cycles, to obtain DNA fragments averaging 300-500bp in length.

(5) Centrifuge at 8000g, 4°C for 10min. Collect the supernatant.

(6) Remove 50µl from each sonicated sample to serve as input. Dilute the remaining chromatin 1:10 with dilution buffer.

(7) Preparation of protein A/G beads: Wash Protein A/G beads three times in dilution Buffer. Aspirate dilution buffer and add single-stranded herring sperm DNA to a final concentration of 75ng/µl beads and BSA to a final concentration of 0.1µg/µl beads. Add dilution buffer to twice the bead volume and incubate for 30min with rotation at RT. Wash once with dilution buffer and add dilution buffer to twice the bead volume.

(8) Pre-wash samples with 60µl protein A/G beads (Santa Cruz) on a rotating device for 1h at 4°C.



(9) Centrifuge at 2000g, 4°C for 5min, transfer the supernatant to a new 1.5ml Eppendorf tube. Incubate with 5µg primary antibody or IgG for at least 8hrs at 4°C.

(10) Add 60µl protein A/G beads to samples, and incubate on a rotating device overnight at 4°C.

(11) Centrifuge at 2000rpm for 5min, discard the supernatant, wash the bottom beads in several buffers with rotation sequentially: TSEI, TSEII, Buffer III and TE buffer for 10min each at 4°C.

(12) Centrifuge at 2000g for 1min, elute the beads with 120µl elution buffer for 15min at 30°C.

(13) Add 4.8µl of 5M NaCl and 2µl RNase A (EN0531, Thermo Fisher), reverse crosslink the immunoprecipitated complexes together with the inputs at 65°C overnight.

(14) Next day, add 2µl proteinase K (EO0491, Thermo Fisher) to samples and incubate while shaking at 60°C for 1hr, and then the samples were purified with a MinElute PCR Purification Kit.

(15) The DNA obtained was used for subsequent PCR analysis and for qRT-PCR analysis.

a) ChIP PCR analysis using Phusion High-Fidelity DNA Polymerase

Mix the reaction system as follows:

Reagent	Volume
5x High-fidelity	2µl
dNTP	0.2µl
Primer-F	0.5µl
Primer-R	0.5µl
Polymerase	0.1µl
H <sub>2</sub> O	5.7µl
DNA	1µl

Perform ChIP PCR program as follows:

Initial denaturation	98°C	30s
	98°C	10s
35 cycles	60°C	30s
	72°C	30s
Final extension	72°C	7min

The PCR amplified products were shown on 2% agarose gel electrophoresis.

## b) ChIP qRT-PCR analysis using SYBR Green Master Kit

ChIP qRT-PCR were performed on a StepOnePlus system (Applied Biosystem). The reaction system and the program were as described in 2.2.6. Each sample ran in triplicate. The qRT-PCR result was normalized to input fragments, relative fold change of immunoprecipitated genomic fragments in the treatment group was compared to untreated control group.

Primers for ChIP were listed in Table 13.

Table 13 ChIP-Primer used in the study

Gene	Forward primers (5'-3')	Reverse primers (5'-3')
<i>Ecm1</i> (-157 ~ +118bp)	GTGCTCCCTTCCATCACCTC	GGCAAGAAGCTGGTCACTGGT
<i>Ecm1</i> (-867 ~ -588bp)	GCTCTGCTCCTACCTTTCCTAA	TCACCAATGGACATGACTCAGA
<i>Ppia</i>	GAGCTGTTTGCAGACAAAGTT	CCCTGGCACATGAATCCTGG

## 2.2.14 Statistical analysis

Statistical analyses were performed using GraphPad Prism version 6.0 software. Unpaired two tailed Student's t test was used to compare the means between two different groups. One-Way ANOVA was used to determine statistical significance among three or more groups. Variables were described as means and standard deviations (SD). *P* values less than 0.05 were considered statistically significant and indicated as follows: \*, *P*<0.05; \*\*, *P*<0.01; and \*\*\*, *P*<0.001.

### 3 RESULTS

#### 3.1 Histology of liver and kidney from ECM1KO mice at ages 5, 8 and 12wks

To compare the histopathological changes in ECM1KO mice, I collected different organs from ECM1KO and ECM1WT mice at 5 and 8wks, e.g. liver, kidney, spleen, pancreas, colon, lung, heart, brain, muscle and bone. All the samples were stained with hematoxylin and eosin (H&E) and Masson Trichrome (MTC). According to the results from mouse clinics (**Figure 3A, 3C**), pathological changes were mainly observed in the liver and kidney from KO mice, and none of the other organs from both ages of KO animals showed histopathological alterations; the organs of WT mice showed normal histology, without pathological alterations.

In the KO mice at 5 and 8wks, perisinusoidal fibrosis was observed in the liver (**Figure 3A**). Importantly, the pathological phenotypes of the liver were more severe in the KO mice at 12wks, with areas of basement membrane disruption and fibrosis indicated by arrows (**Figure 3B**). In the KO mice at 5 and 8wks, in addition to the observed perisinusoidal fibrosis in the liver, I also identified histopathological changes in the kidney (**Figure 3C**). For example, in 5-week-old KO mice some glomeruli were enlarged with mesangial proliferation and sclerosis (indicated by arrows). The tubule showed normal histology. And in 8-week-old KO mice, there were as well severe abnormalities in the kidney. Most of the glomeruli were enlarged with edema, mesangial sclerosis and fibrinoid necrosis of the mesangium, pointing to a glomerulonephritis (indicated by arrows). The tubule also showed normal histology. In conclusion, ECM1 depletion in mice caused damage to different organs. The KO mice showed fibrosis in the liver and histopathological changes in the kidney with enlarged glomeruli, mesangial sclerosis, and fibrinoid deposits, the phenotype being stronger with aging.

These results imply that ECM1 is a critical factor in keeping organs homeostasis, and it is worth investigating the mechanisms that regulate ECM1 expression under normal and diseased conditions.

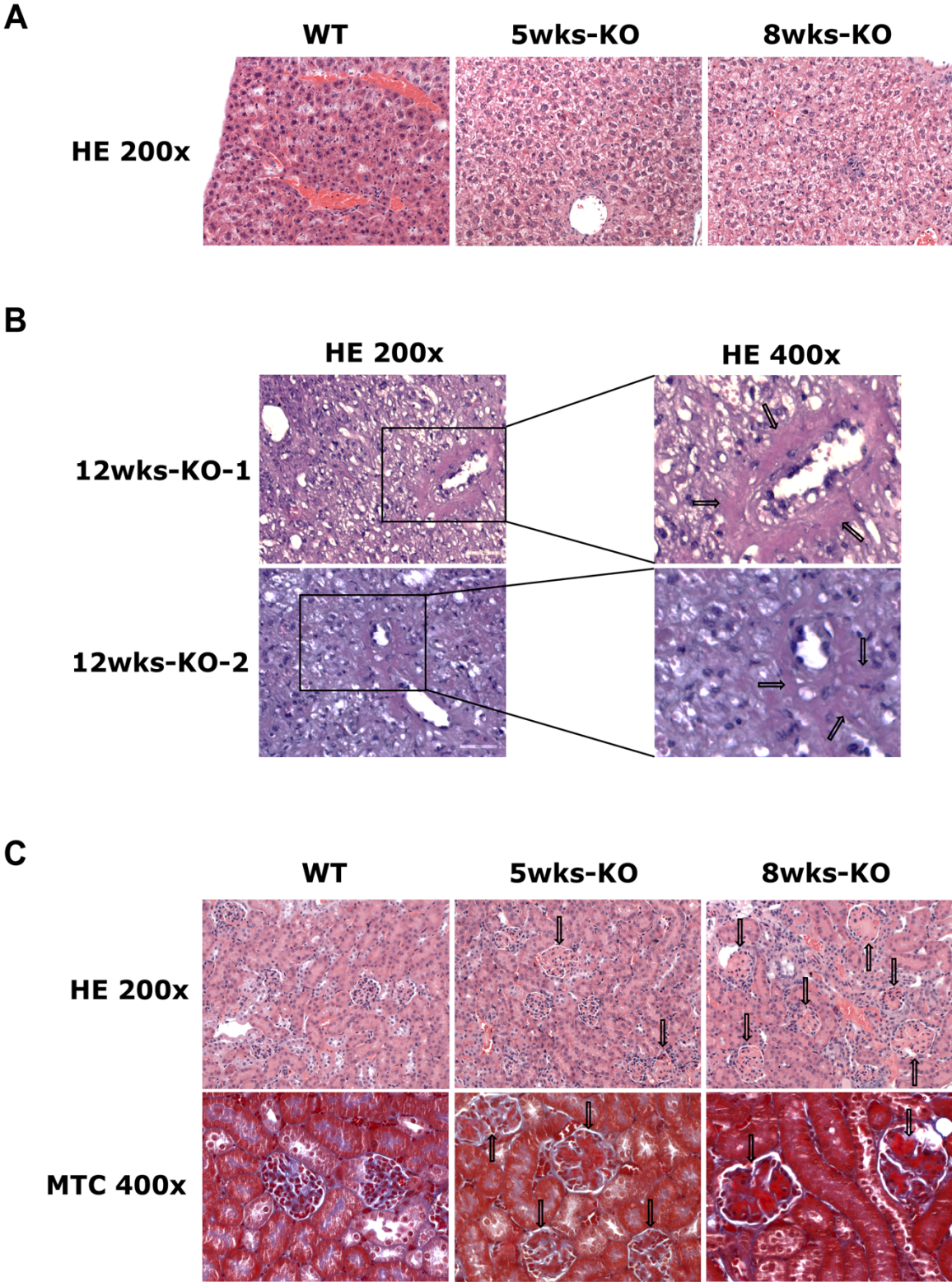


**Figure 3. Histology of liver and kidney from ECM1WT and ECM1KO mice**  
**(A)** H&E staining for liver tissues from ECM1WT and ECM1KO mice at 5 and 8wks; Original magnification: 200x. **(B)** H&E-stained liver tissues of ECM1KO mice at

12wks and representative images (200× and 400× magnification). Arrows indicated basement membranes disruption and fibrotic areas in liver tissues. **(C)** H&E and MTC staining for kidney tissues from ECM1WT and ECM1KO mice at 5 and 8wks; Original magnification: 200x, 400x, respectively. Arrows indicated histopathological changes in the kidney.

### 3.2 Increased portal vein pressure in ECM1KO mice

Mice lacking ECM1 develop liver fibrosis spontaneously, with scar tissue replacing healthy tissue and obstructing blood flow to the liver. As the disease progresses, it causes vascular obstruction, resulting in an increase in portal vein pressure (PVP), which further damages hepatocytes and exacerbates the progression of fibrosis, creating a vicious cycle. Therefore, I measured the portal vein diameter and peak flow of ECM1WT and KO mice using liver echography, which can be used as indicators of portal vein pressure; typically, the greater the vein pressure, the smaller the diameter and the lower the peak flow.

The transverse/axial B-mode images clearly depicted the size and location of the portal vein (PV), inferior vena cava (IVC), and the artery in the livers of ECM1WT and ECM1KO mice (**Figure 4A**). And color Doppler images of the livers from ECM1WT and ECM1KO mice revealed intrahepatic blood flow (**Figure 4B**). Using M-mode and pulse wave Doppler to measure portal vein diameter and portal vein peak flow, I discovered that ECM1KO mice exhibited a smaller portal vein diameter at 8wks, although they showed a decline at 5wks, but no significant difference; and both age groups of KO animals had lower portal vein peak flow (**Figure 4C-D**, at 8wks, there were only five KO mice at the time of measurement as one KO mouse died), demonstrating that ECM1KO mice manifest a strong portal hypertension phenotype. Taken together, ECM1KO mice spontaneously develop liver fibrosis and display symptoms of portal hypertension, demanding further investigation into the regulatory mechanisms of ECM1.

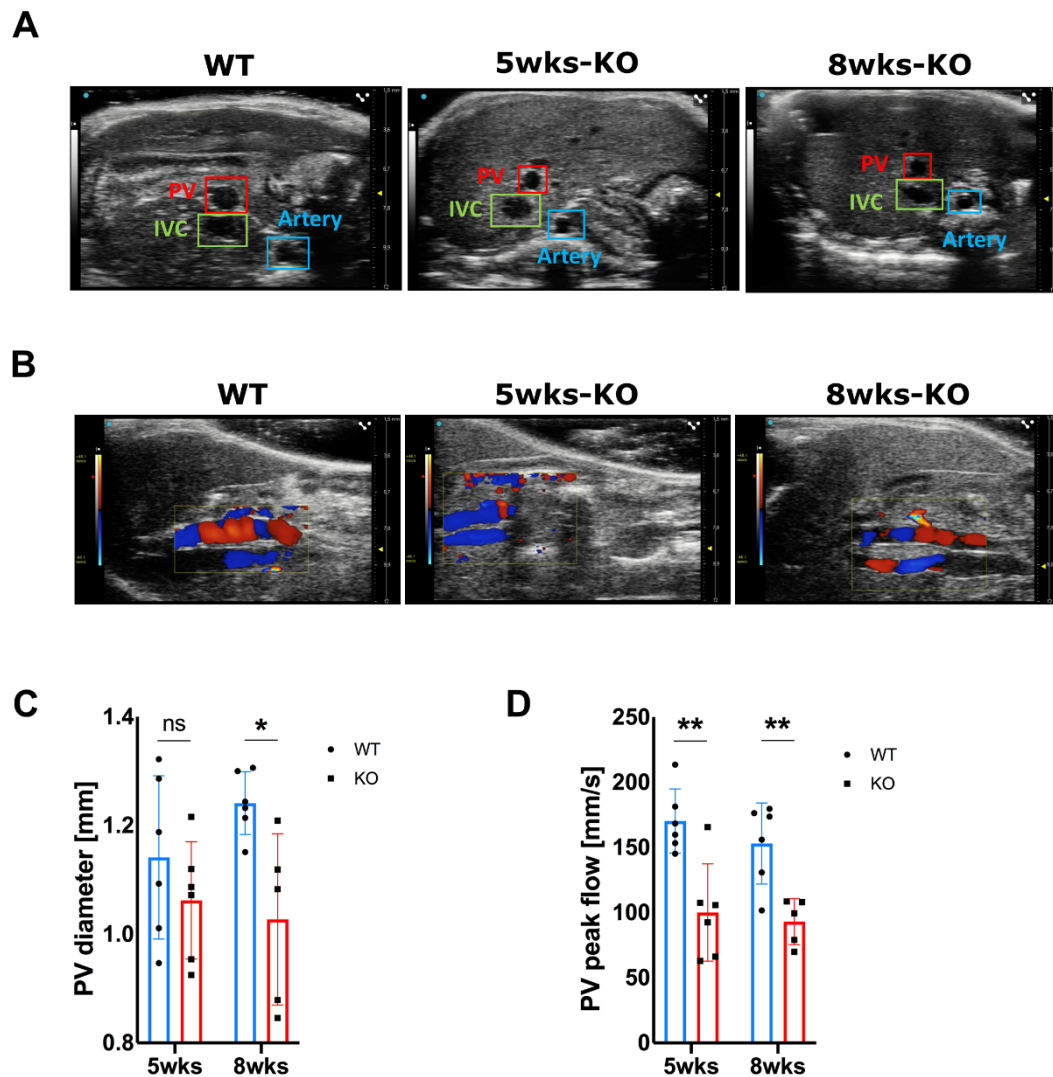


#### Figure 4. Increased portal vein pressure in ECM1KO mice

(A) Transverse/axial B-mode images of the livers from ECM1WT and ECM1KO mice. Imaging with a 30MHz probe. (B) Color Doppler images of the livers from ECM1WT and ECM1KO mice showing hepatic blood flow within the liver. (C) Portal vein diameter (mm) and (D) portal vein peak flow (mm/s) of ECM1WT and ECM1KO mice (n=6) were measured by M-mode and pulse wave Doppler, respectively; five measurements were performed on each mouse and the data were presented as mean and SD. *P*-values were calculated by unpaired Student's t test. Bars represent the mean ± SD. \*, *P*<0.05; \*\*, *P*<0.01; \*\*\*, *P*<0.001.



### 3.3 Growth factors EGF and HGF induce ECM1 expression in hepatocytes

To identify putative transcription factors in the promoter region of *Ecm1* gene (-2000bp ~ +200bp relative to TSS), a GeneCards-based *in silico* analysis ([ECM1 Gene - GeneCards | ECM1 Protein | ECM1 Antibody](#)) was conducted. JUND, JUNB, FOS, MYC, and STAT1 were frequently observed in all predicted outcomes; they can all be regulated by growth factors such as EGF and HGF. AML12, mouse primary hepatocytes (MPHs), and human primary hepatocytes (HPHs) treated with EGF or HGF demonstrated a significant upregulation of *ECM1* mRNA expression (**Figure 5A**). Western blotting analyses also confirmed the increased protein expression of ECM1 in AML12 and MPHs treated with EGF (**Figure 5B**).

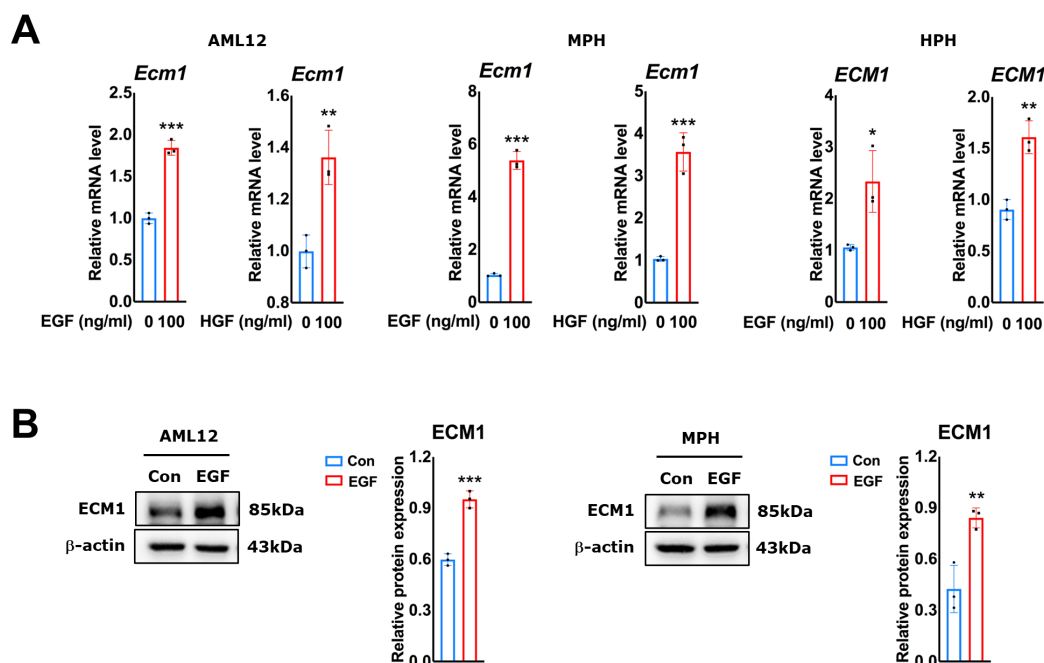


**Figure 5. Growth factors EGF and HGF induce ECM1 expression in hepatocytes**

**(A)** qRT-PCR for *ECM1* mRNA expression in AML12, MPHs and HPHs with or without EGF or HGF treatment for 24hrs. Results were normalized to *PPIA*. **(B)** Western blotting of ECM1 protein expression in AML12 and MPHs treated with 24hrs EGF.  $\beta$ -actin was a loading control. Quantification of protein expression was measured by ImageJ (National Institutes of Health, Bethesda, Maryland, USA). *P*-values were calculated by unpaired Student's *t* test. Bars represent the mean  $\pm$  SD. \*,  $P < 0.05$ ; \*\*,  $P < 0.01$ ; \*\*\*,  $P < 0.001$ .

### 3.4 EGF-EGFR keeps ECM1 expression in hepatocytes *in vitro*

Given the crucial role of EGFR in the EGF signaling pathway, I applied erlotinib, a selective EGFR inhibitor, to investigate its function in maintaining ECM1 expression. qRT-PCR and Western blotting analyses demonstrated that erlotinib substantially inhibited EGF-induced EGFR phosphorylation and ECM1 expression in AML12 (**Figure 6A**) and MPHs (**Figure 6B**). Furthermore, *Egfr* knockdown with siRNA transfection severely suppressed EGF-induced EGFR phosphorylation and ECM1 expression in MPHs (**Figure 6C**). As STAT1 is also an EGF-EGFR downstream target, its total expression and phosphorylation at S727 were measured in MPHs. Western blotting showed EGF-induced total expression and phosphorylation of STAT1 were dependent on EGFR (**Figure 6C**).

These findings demonstrate that EGF-EGFR maintains the expression of ECM1 in hepatocytes *in vitro*.



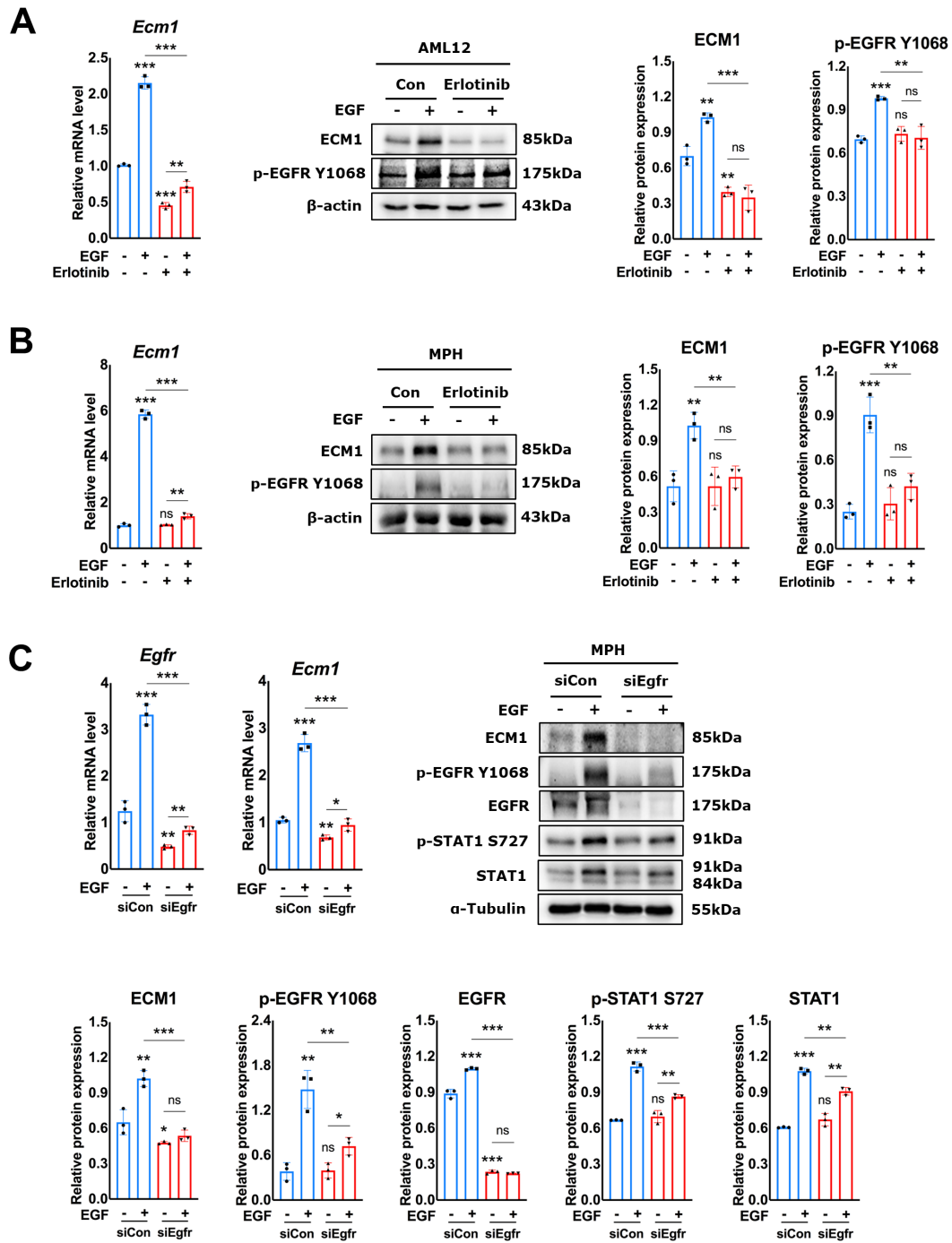


**Figure 6. EGF-EGFR keeps ECM1 expression in hepatocytes *in vitro***

(A-B) qRT-PCR and Western blotting showing the effect of erlotinib on ECM1 and p-EGFR Y1068 expression in AML12 and MPHs with or without EGF treatment. (C) Effects of *Egfr* knockdown on mRNA and protein expression of ECM1 and EGFR in EGF-treated MPHs by qRT-PCR and Western blotting. p-EGFR Y1068, p-STAT1

S727 and STAT1 were also measured using Western blotting. The results of qRT-PCR were normalized to *Ppia*.  $\beta$ -actin,  $\alpha$ -tubulin were loading controls. Quantification of protein expression was measured by ImageJ (National Institutes of Health, Bethesda, Maryland, USA). *P*-values were calculated by unpaired Student's *t* test. Bars represent the mean  $\pm$  SD. \*, *P*<0.05; \*\*, *P*<0.01; \*\*\*, *P*<0.001.

### 3.5 EGF-EGFR keeps ECM1 expression in homeostatic liver *in vivo*

Next, to determine whether EGF induces ECM1 *in vivo*, I intravenously (i.v.) administered EGF to WT mice. Animals treated with EGF for 24 and 48hrs exhibited no change in *Ecm1* mRNA expression levels and no effect on ECM1 protein expression (**Figure 7A**). This may be because physiological levels of EGF are sufficient to maintain ECM1 expression in healthy conditions, and additional EGF does not further increase ECM1 levels. Therefore, I also injected the receptor inhibitor erlotinib intraperitoneally (i.p.) into WT animals. qRT-PCR, Western blotting, and immunofluorescence analyses demonstrated a significant decrease in ECM1 expression in the erlotinib-treated group compared to the control group (**Figure 7B-C**). Notably, EGFR inactivation also inhibited the phosphorylation of STAT1 at S727 site *in vivo* (**Figure 7B**).

These findings suggest that EGF-EGFR maintains ECM1 expression in physiological conditions to keep hepatic homeostasis.

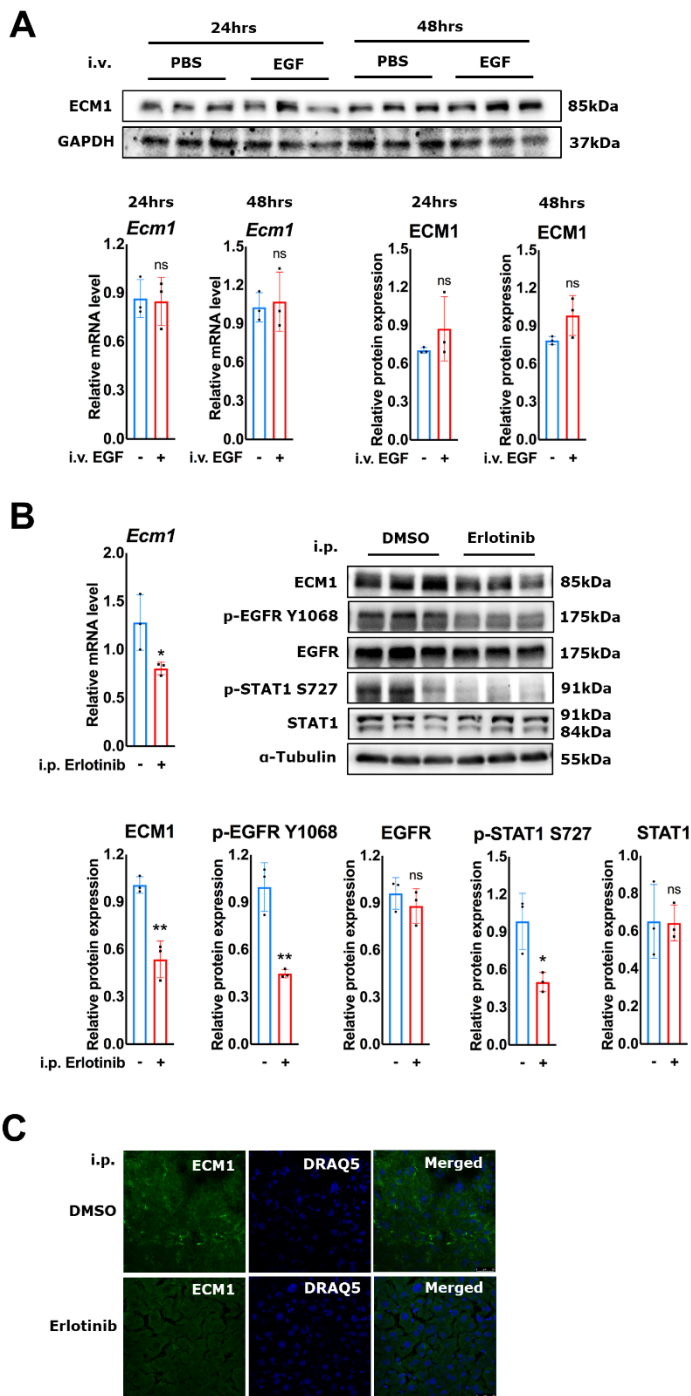


**Figure 7. EGF-EGFR keeps ECM1 expression in homeostatic liver *in vivo***

(A) qRT-PCR and Western blotting for ECM1 expression in the liver tissues from mice treated with PBS or EGF (1.2mg/kg, i.v., collected after 24 and 48hrs). Mice were divided into four groups (n=3), PBS was administered as a placebo. (B) qRT-PCR and Western blotting for ECM1 expression in the liver tissues from mice treated with DMSO or erlotinib (40mg/kg/day, i.p., for 2 days). p-EGFR Y1068, EGFR, p-

STAT1 S727 and STAT1 were measured using Western blotting. Mice were divided into two groups (n=3), DMSO was administered as a placebo. **(C)** Immunofluorescence staining for ECM1 expression in the liver tissues from DMSO- or erlotinib-treated mice. The results of qRT-PCR were normalized to *Ppia*. GAPDH,  $\alpha$ -tubulin were loading controls. Quantification of protein expression was measured by ImageJ (National Institutes of Health, Bethesda, Maryland, USA). *P*-values were calculated by unpaired Student's t test. Bars represent the mean  $\pm$  SD. \*, *P*<0.05; \*\*, *P*<0.01; \*\*\*, *P*<0.001.

### 3.6 EGF-induced ECM1 expression is not dependent on MEK-ERK pathway

As MEK-ERK is one of the most frequently employed downstream pathways of EGF-EGFR signaling, it is thought to be implicated in the mechanism by which EGF-EGFR upregulates ECM1 expression in hepatocytes. However, when both *Erk1* and *Erk2* genes were silenced down in AML12, EGF-induced mRNA and protein expression of ECM1 was not suppressed (**Figure 8A**). Besides, *Erk1* and *Erk2* genes knockdown in MPHs also demonstrated that ERK inhibition did not prevent EGF-induced ECM1 expression (**Figure 8B**).

These findings suggest that the MEK-ERK pathway is not responsible for the EGF-induced upregulation of ECM1 expression in hepatocytes, and that other downstream pathways must play an important role in this process.

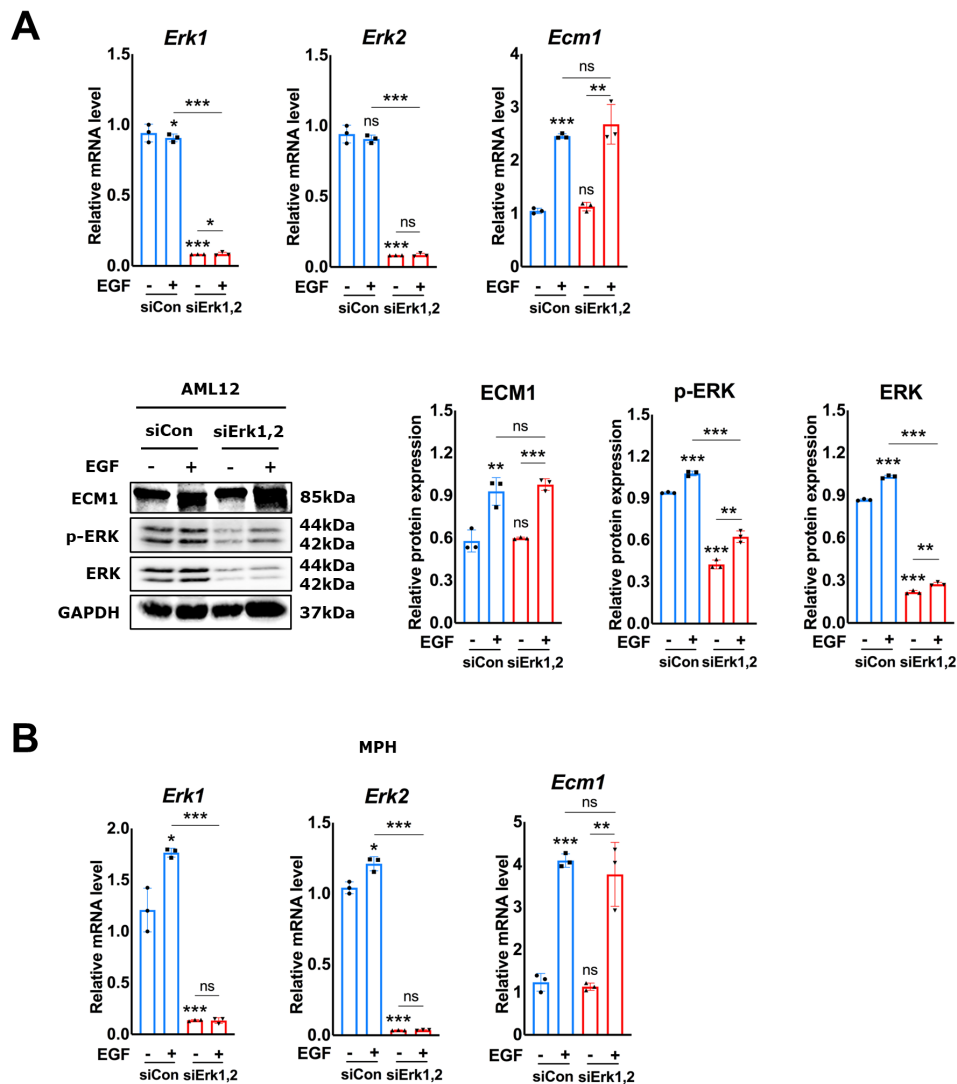


**Figure 8. MEK-ERK pathway is not responsible for EGF-induced ECM1 expression in hepatocytes**

(A) qRT-PCR and Western blotting showing the impact of *Erk1* and *Erk2* knockdown on mRNA and protein expression of ECM1, ERK1 and ERK2 in EGF-treated AML12. p-ERK T202/Y204 was also measured using Western blotting. (B) qRT-PCR for the impact of *Erk1* and *Erk2* knockdown on mRNA expression of *Ecm1*, *Erk1* and *Erk2* in EGF-treated MPHs. The results of qRT-PCR were normalized to *Ppia*. GAPDH was a loading control. Quantification of protein expression was measured by ImageJ (National Institutes of Health, Bethesda, Maryland, USA). *P*-values were calculated by unpaired Student's *t* test. Bars represent the mean  $\pm$  SD. \*,  $P < 0.05$ ; \*\*,  $P < 0.01$ ; \*\*\*,  $P < 0.001$ .

### 3.7 EGF upregulates ECM1 expression through p-STAT1 S727

To elucidate potential downstream pathways of EGF-EGFR signaling that regulate ECM1 expression, a number of predicted transcription factors, such as Fos/Jun and c-Myc, were screened using *in silico* analyses and tested via siRNA interference experiments (data not shown). Among these, there was evidence that STAT1 is a promising candidate. Western blotting analyses indicated that EGF phosphorylated STAT1 on S727 within 1hr, which was still detectable 24hrs after treatment in MPHs (**Figure 9A**). In addition, qRT-PCR and Western blotting further revealed that *Stat1* silencing by siRNA markedly suppressed EGF-induced ECM1, p-STAT1 S727, and total STAT1 expression in both AML12 (**Figure 9B**) and MPHs (**Figure 9C**).

These findings show that STAT1 is activated by EGF-EGFR signaling and is involved in the regulation of ECM1.

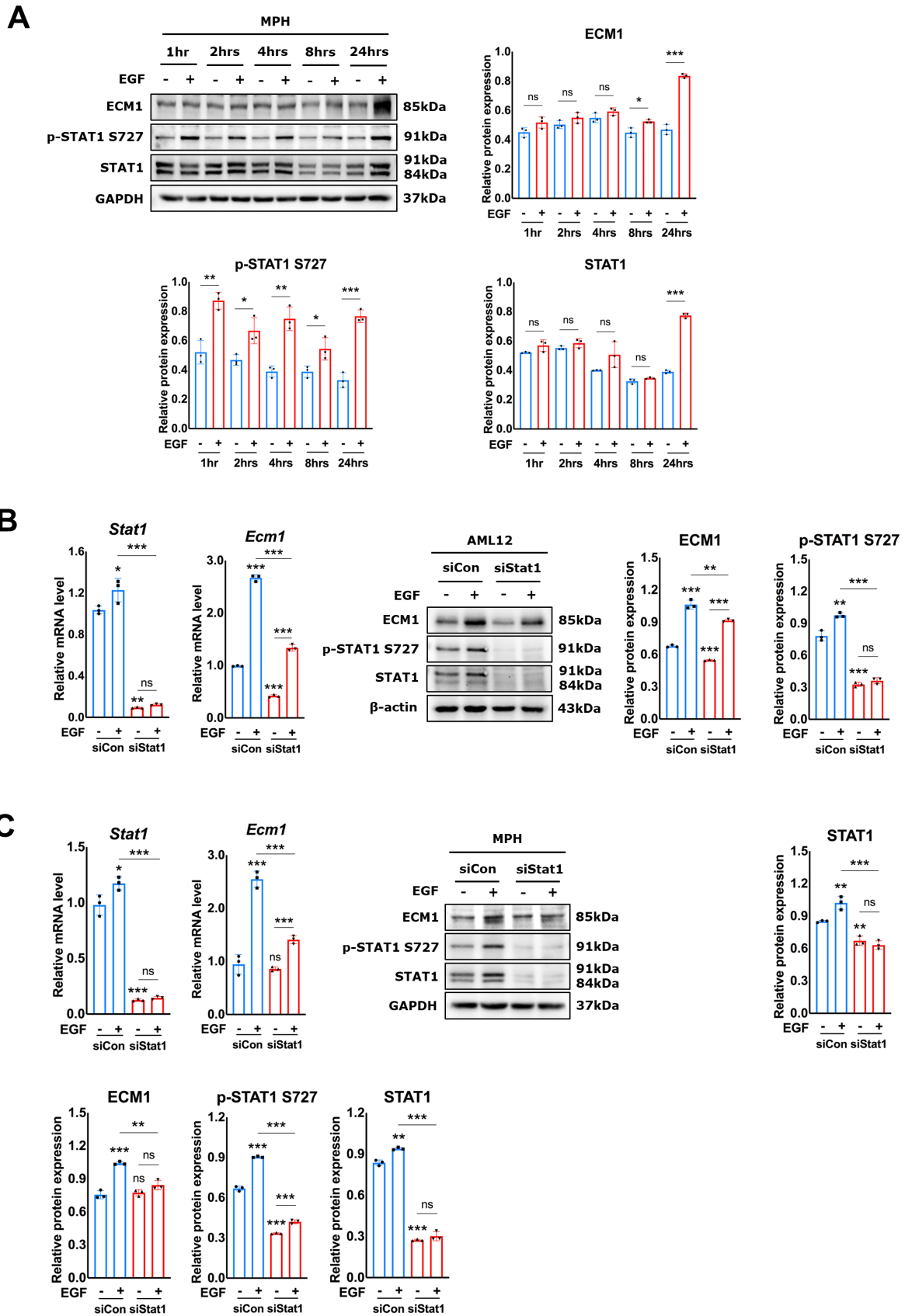


Figure 9. EGF upregulates ECM1 expression through p-STAT1 S727

**(A)** Western blotting showing the effect of EGF on ECM1, p-STAT1 S727 and STAT1 expression in MPHs at 1, 2, 4, 8, 24hrs. **(B-C)** qRT-PCR and Western blotting for mRNA and protein expression of ECM1 and STAT1 in EGF-treated AML12 and MPHs with or without *Stat1* knockdown by RNAi. p-STAT1 S727 was also measured using Western blotting. The results of qRT-PCR were normalized to *Ppia*. GAPDH,  $\beta$ -actin were loading controls. Quantification of protein expression was measured by ImageJ (National Institutes of Health, Bethesda, Maryland, USA). *P*-values were calculated by unpaired Student's t test. Bars represent the mean  $\pm$  SD. \*, *P*<0.05; \*\*, *P*<0.01; \*\*\*, *P*<0.001.

### 3.8 EGF-induced p-STAT1 S727 binds to and positively regulates *Ecm1* gene promoter

To further investigate the regulatory role of STAT1 in the *ECM1* gene, its binding peak was identified in the promoter region of *ECM1* gene using publicly accessible STAT1 ChIP-seq data from the ENCODE website (GM12878, accession number: ENCFF011BMN) **(Figure 10A)**. Chromatin immunoprecipitation (ChIP) qRT-PCR confirmed the binding of STAT1 to the *Ecm1* gene promoter in AML12 and MPHs **(Figure 10B, control group)**. Additionally, EGF treatment significantly increased STAT1 binding to the *Ecm1* promoter region fragment "-157bp +118bp" **(Figure 10B, EGF group)**, leading to a rise in ECM1 expression in AML12 and MPHs. The ChIP assay results were also shown on a 2% agarose gel using the PCR-amplified products **(Figure 10C)**.

These findings suggest that STAT1 critically regulates *Ecm1* gene transcription, particularly in the upstream proximal promoter region (typically within 250bp upstream of the transcription start site), and that STAT1 as a transcription factor for the *Ecm1* gene is required for EGF-mediated ECM1 expression in hepatocytes.



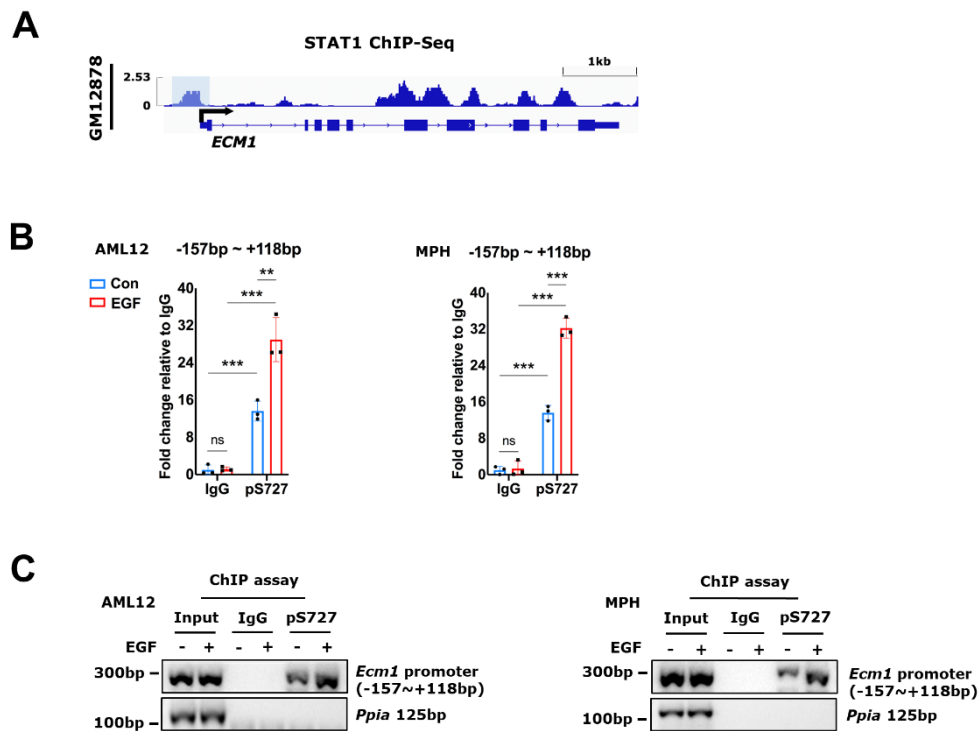


### Figure 10. EGF-induced p-STAT1 S727 binds to and positively regulates *Ecm1* gene promoter

(A) Representative readouts of peaks (signal *P*-value) from STAT1 ChIP-seq at *ECM1* gene locus of GM12878. Data is retrieved from ENCODE (ENCFF011BMN). (B) ChIP qRT-PCR showing the binding of p-STAT1 S727 to the *Ecm1* gene promoter in AML12 and MPHs treated with or without EGF for 24hrs. Relative fold change of immunoprecipitated genomic fragments in EGF-treated cells was compared to untreated control group. Fragment “-157bp ~ +118bp” was relative to the transcription start site of *Ecm1* gene. Rabbit IgG-bound chromatin served as a negative control. *Ppia* represents non-specific binding. (C) The PCR amplified products of “-157bp ~ +118bp” fragments were shown on a 2% agarose gel. *P*-values were calculated by unpaired Student's *t* test. Bars represent the mean  $\pm$  SD. \*,  $P < 0.05$ ; \*\*,  $P < 0.01$ ; \*\*\*,  $P < 0.001$ .

### 3.9 Selection of candidate factors inhibiting ECM1 expression under chronic liver disease conditions

When inflammation and injury occur in the liver, ECM1 expression decreases significantly, while inflammatory cytokines such as tumor necrosis factor alpha (TNF- $\alpha$ ), lipopolysaccharide (LPS), and interferon gamma (IFN $\gamma$ ) accumulate in the liver in

large amounts; therefore, I investigated whether these factors are responsible for the decrease in ECM1 expression. TNF- $\alpha$  and LPS did not affect the expression of ECM1 in MPHs, indicating that they are not regulators of ECM1 expression (**Figure 11A-B**). However, when MPHs were treated with IFN $\gamma$ , *Ecm1* mRNA expression decreased significantly (**Figure 11C**).

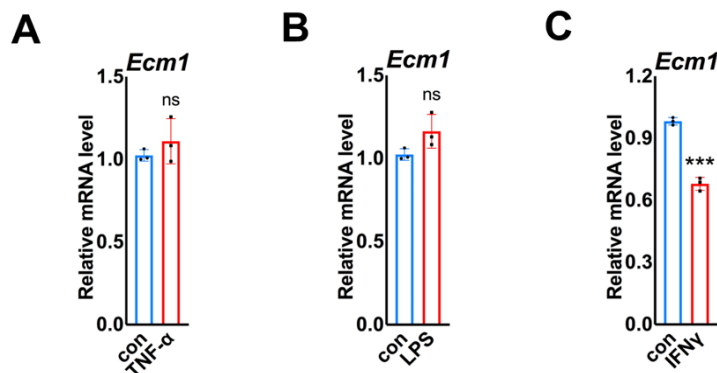


**Figure 11. Selection of candidate factors inhibiting ECM1 expression under chronic liver disease conditions**

qRT-PCR for *Ecm1* mRNA expression in MPHs incubated with (**A**) TNF- $\alpha$  (4ng/ml), or (**B**) LPS (5 $\mu$ g/ml), or (**C**) IFN $\gamma$  (100ng/ml) for 24hrs. The results were normalized to *Ppia*. *P*-values were calculated by unpaired Student's t test. Bars represent the mean  $\pm$  SD. \*, *P*<0.05; \*\*, *P*<0.01; \*\*\*, *P*<0.001.

### 3.10 IFN $\gamma$ abolishes EGF-EGFR-maintained ECM1 expression *in vitro*

Next, in MPHs co-incubated with EGF and IFN $\gamma$ , the results showed that IFN $\gamma$  treatment not only dramatically decreased ECM1 expression on mRNA and protein levels, but also abolished EGF-induced ECM1 expression and EGFR expression as measured by qRT-PCR and Western blotting (**Figure 12A-B**).

These findings imply that IFN $\gamma$  inhibits EGFR expression *in vitro*, thereby abrogating EGF-maintained ECM1 expression.

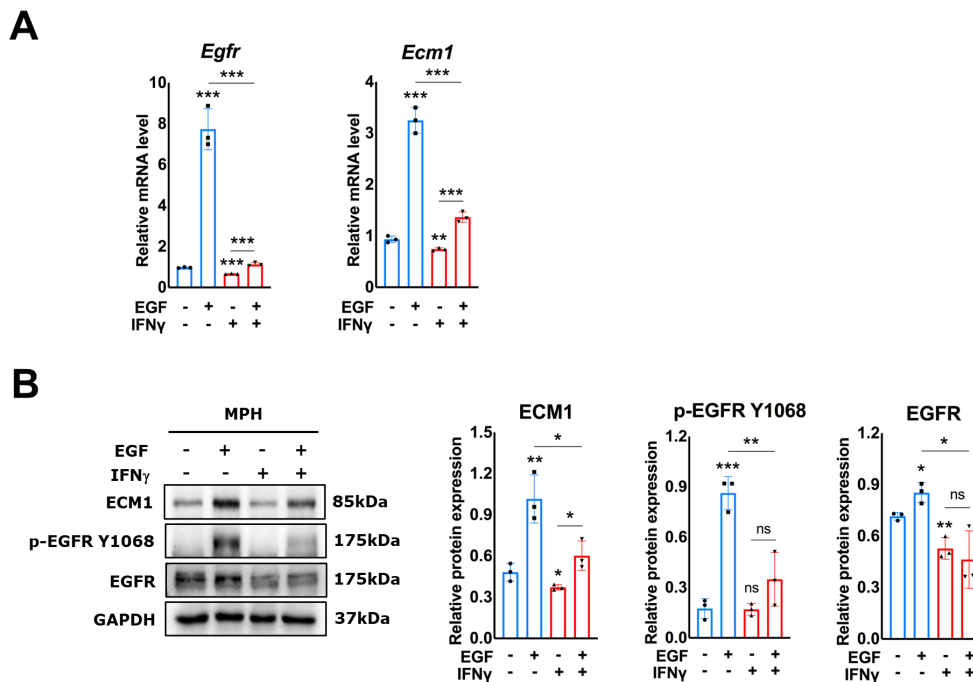


**Figure 12. IFN $\gamma$  abolishes EGF-EGFR-maintained ECM1 expression *in vitro***

(A) qRT-PCR and (B) Western blotting showing the impact of IFN $\gamma$  on ECM1 and EGFR expression in EGF-treated MPHs. The results of qRT-PCR were normalized to *Ppia*. GAPDH was a loading control. Quantification of protein expression was measured by ImageJ (National Institutes of Health, Bethesda, Maryland, USA). *P*-values were calculated by unpaired Student's *t* test. Bars represent the mean  $\pm$  SD. \*, *P*<0.05; \*\*, *P*<0.01; \*\*\*, *P*<0.001.

### 3.11 IFN $\gamma$ blunts p-STAT1 S727 binding to *Ecm1* gene promoter via phosphorylation of STAT1 at Y701

It is well known that IFN $\gamma$  is the most potent modulator of STAT1 signaling, which has sparked interest in studying the differences between EGF and IFN $\gamma$  signaling pathways in the regulation of ECM1 expression. Although both EGF and IFN $\gamma$  occupy the STAT1 pathway, their signaling regulatory mechanisms are distinct. EGF and IFN $\gamma$  both phosphorylate STAT1 on S727, however IFN $\gamma$  must first phosphorylate the Y701 site before it can phosphorylate S727, whereas EGF phosphorylates STAT1 on S727 directly, which are independent and have diverse consequences [60]. Western blotting analyses, in which MPHs were treated with EGF or IFN $\gamma$  at different time

points, confirmed this by showing that IFN $\gamma$  phosphorylated STAT1 on Y701 within 5min, with activation of S727 occurring at around 10~30min, whereas EGF-induced phosphorylation of STAT1 on S727 arose rapidly, no activation of Y701 was observed (**Figure 13A**). Furthermore, in response to EGF stimulation, p-EGFR Y1068 appeared at 5min and then gradually declined; IFN $\gamma$  failed to phosphorylate EGFR and tended to inhibit total EGFR expression (**Figure 13A**). In addition, the ChIP assay demonstrated that IFN $\gamma$  treatment did not increase STAT1 binding to the *Ecm1* gene promoter in MPHs (**Figure 13B**). This may suggest that, unlike STAT1 with S727 phosphorylation alone, STAT1 with both p-Y701 and p-S727 cannot bind to the *Ecm1* gene promoter to induce its transcription.

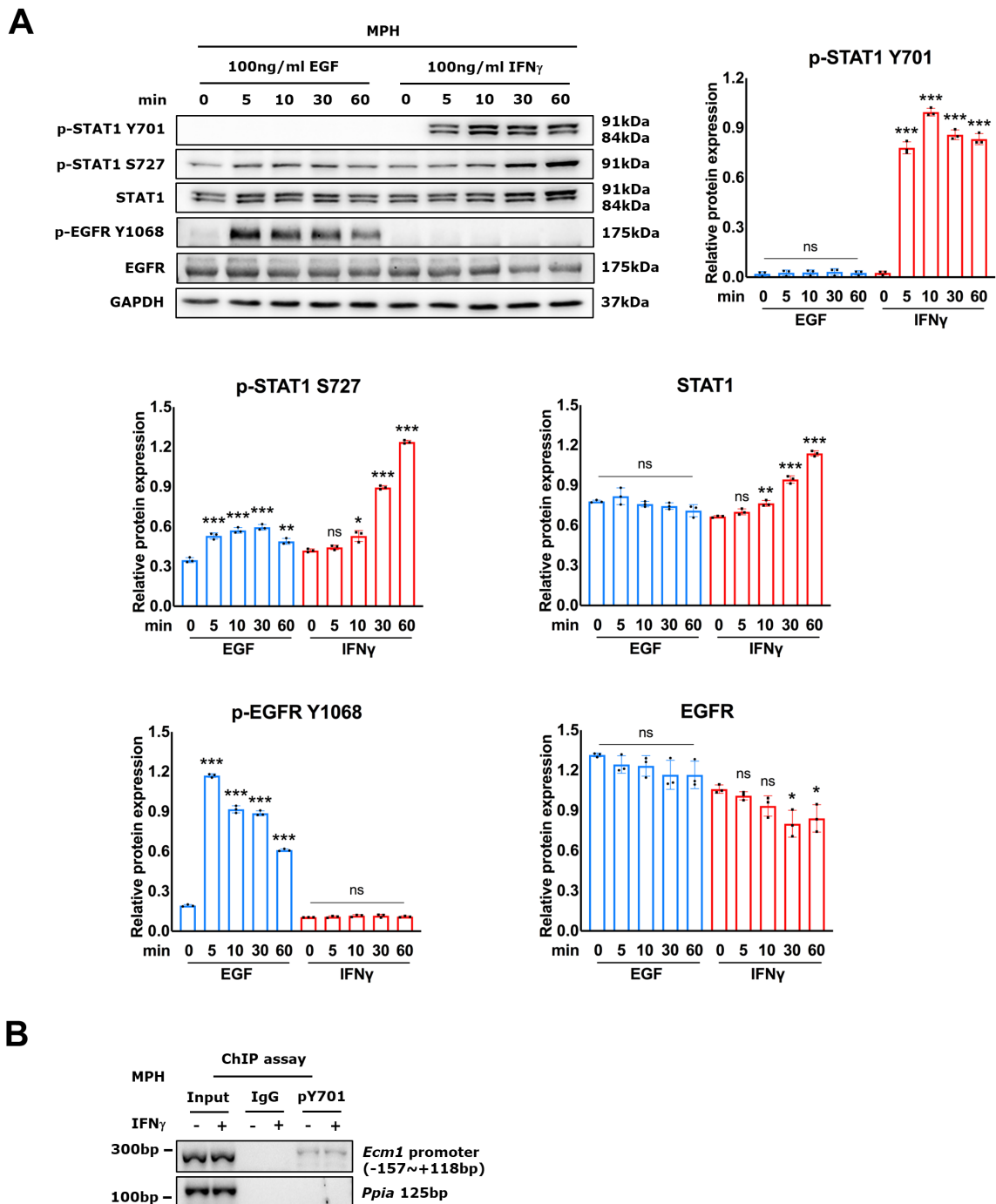


**Figure 13. IFN $\gamma$  blunts p-STAT1 S727 binding to *Ecm1* gene promoter via phosphorylation of STAT1 at Y701**

**(A)** Western blotting showing the effect of EGF or IFN $\gamma$  on p-STAT1 S727, p-STAT1 Y701, STAT1 expression and p-EGFR Y1068, EGFR expression in MPHs at 5, 10, 30, 60min. GAPDH was a loading control. Quantification of protein expression was

measured by ImageJ (National Institutes of Health, Bethesda, Maryland, USA). **(B)** ChIP assay displaying the effect of 24hrs IFN $\gamma$  on the binding of p-STAT1 Y701 to the *Ecm1* gene promoter in MPHs. Fragment “-157bp ~ +118bp” was relative to the transcription start site of *Ecm1* gene. Rabbit IgG-bound chromatin served as a negative control. *Ppia* represents non-specific binding. *P*-values were calculated by unpaired Student's t test. Bars represent the mean  $\pm$  SD. \*, *P*<0.05; \*\*, *P*<0.01; \*\*\*, *P*<0.001.

### 3.12 IFN $\gamma$ abolishes EGF-EGFR-maintained ECM1 expression *in vivo*

Next, IFN $\gamma$  was administered to mice by i.p. injection. The expression of ECM1 and EGFR was significantly reduced in the IFN $\gamma$ -treated group compared to the control group, as determined by Western blotting (**Figure 14A**). The decrease in ECM1 expression was further confirmed by immunofluorescence analyses (**Figure 14B**).

These findings suggest that in addition to its prominent anti-viral activity, IFN $\gamma$  antagonizes the EGF-EGFR signaling pathway, suppresses ECM1 expression, and, to some extent, affects hepatic homeostasis, thereby potentially influencing the recovery from chronic liver injuries.

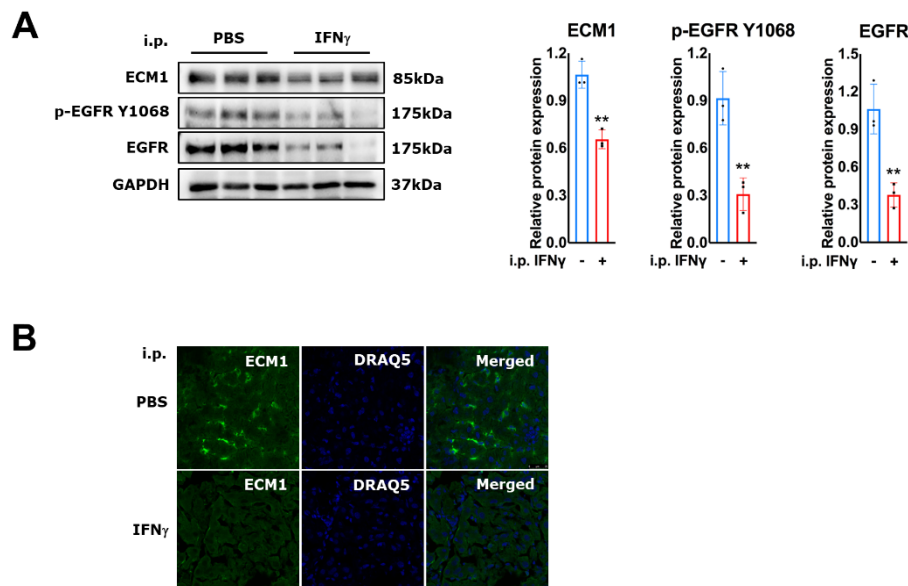


**Figure 14. IFN $\gamma$  abolishes EGF-EGFR-maintained ECM1 expression *in vivo***

**(A)** Western blotting for ECM1, p-EGFR Y1068 and EGFR expression in the liver tissues from mice treated with PBS or IFN $\gamma$  (400 $\mu$ g/kg/day, i.p., for 4 days). Mice

were divided into two groups (n=3), PBS was administered as a placebo. **(B)** Immunofluorescence staining for ECM1 expression in the liver tissues from PBS- or IFN $\gamma$ -treated mice. GAPDH was a loading control. Quantification of protein expression was measured by ImageJ (National Institutes of Health, Bethesda, Maryland, USA). *P*-values were calculated by unpaired Student's *t* test. Bars represent the mean  $\pm$  SD. \*, *P*<0.05; \*\*, *P*<0.01; \*\*\*, *P*<0.001.

### 3.13 Free shuttling of STAT1 total protein contributes to binding of *Ecm1* promoter

Using an antibody that detects STAT1 phosphorylation at S727 site, the STAT1-*Ecm1* ChIP assay was performed on IFN $\gamma$ -treated MPHs. **Figure 15A** revealed a surprising increase in STAT1 binding to the *Ecm1* gene promoter. To our knowledge, IFN $\gamma$  treatment not only promoted STAT1 phosphorylation, but also significantly increased total STAT1 protein expression (**Figure 15B**), and STAT1 protein can freely shuttle between the cytoplasm and nucleus and can be phosphorylated at S727 site by a constitutively active nuclear kinase [60, 61]. Thus, the increase in binding could be explained by a rise in the expression of total STAT1 protein. As this is not the primary mechanism by which IFN $\gamma$  regulates STAT1 signaling, the ultimate regulatory effect of IFN $\gamma$  on ECM1 expression should still be largely attributed to the phosphorylation of STAT1 at Y701, which means that most STAT1 is unable to bind to the *Ecm1* gene promoter upon IFN $\gamma$  stimulation (**Figure 13B**). This part will be explained in more detail in the discussion.

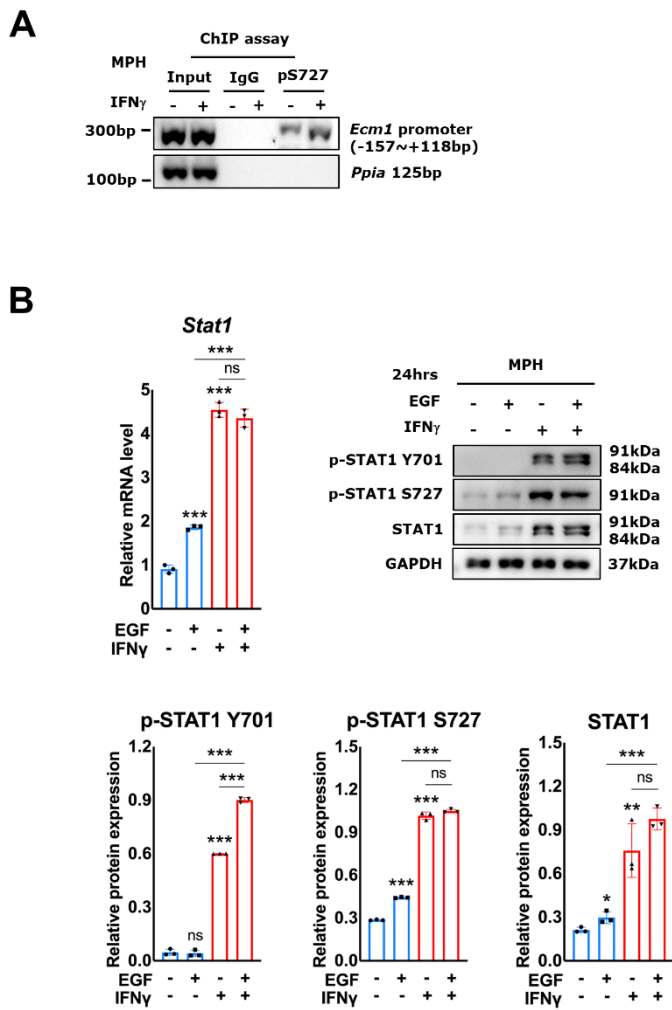


**Figure 15. Free shuttling of STAT1 total protein contributes to binding of *Ecm1* promoter**

**(A)** ChIP assay showing the effect of 24hrs IFN $\gamma$  on the binding of p-STAT1 S727 to the *Ecm1* gene promoter in MPHs. Fragment “-157bp ~ +118bp” was relative to the transcription start site of *Ecm1* gene. Rabbit IgG-bound chromatin served as a negative control. *Ppia* represents non-specific binding. **(B)** qRT-PCR and Western blotting displaying the impact of IFN $\gamma$  on STAT1 and p-STAT1 Y701, S727 expression in EGF-treated MPHs. The results of qRT-PCR were normalized to *Ppia*. GAPDH was a loading control. Quantification of protein expression was measured by ImageJ (National Institutes of Health, Bethesda, Maryland, USA). *P*-values were calculated by unpaired Student's t test. Bars represent the mean  $\pm$  SD. \*, *P*<0.05; \*\*, *P*<0.01; \*\*\*, *P*<0.001.



### 3.14 IFN $\gamma$ generates reactive oxygen species (ROS) and induces NRF2 in hepatocytes

Next, I further analyzed whether there is a transcription factor induced by IFN $\gamma$  that binds directly to the *Ecm1* gene promoter, leading to *Ecm1*'s transcriptional downregulation. In the context of disease, IFN $\gamma$  promotes inflammation and induces ROS [99, 100], thereby triggering various downstream regulators including anti-oxidative signaling, for example NRF2, which is activated in response to oxidative stress and is predicted to have binding sites on the promoter region of *Ecm1* gene. Given that NRF2 translocates to the nucleus upon activation, I performed cytoplasmic and nuclear protein separation. Western blotting analyses confirmed that IFN $\gamma$  stimulated nuclear translocation of NRF2 in MPHs (**Figure 16A**). This was further supported by immunofluorescence showing that NRF2 was activated and located in the nucleus of MPHs under IFN $\gamma$  treatment (**Figure 16B**).

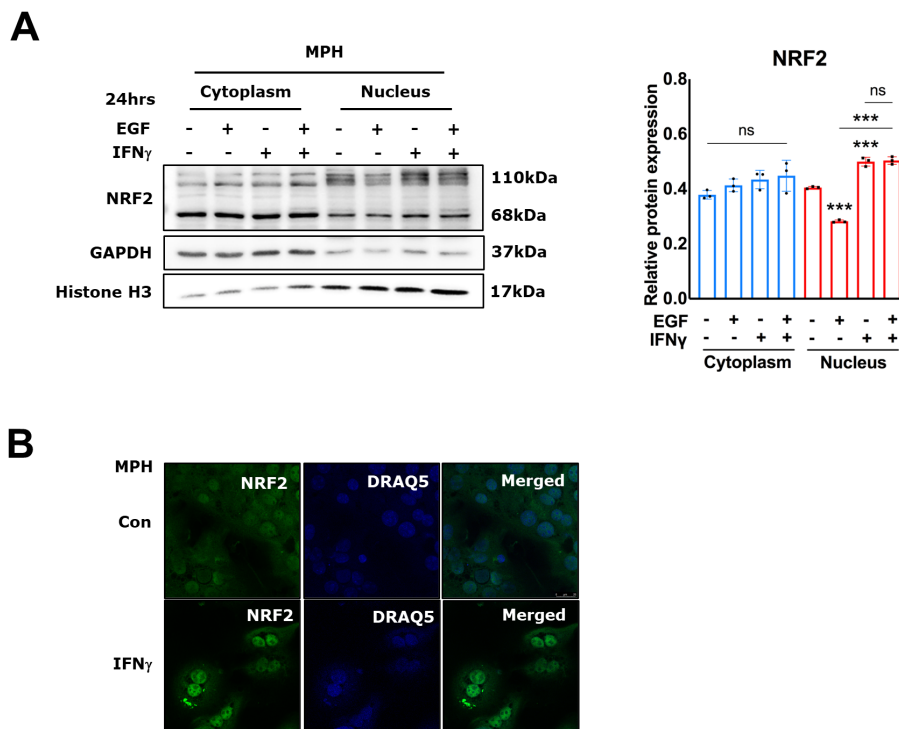


**Figure 16. IFN $\gamma$  generates reactive oxygen species (ROS) and induces NRF2 in hepatocytes**

**(A)** Western blotting for cytoplasmic and nuclear expression of NRF2 in MPHs treated with EGF and/or IFN $\gamma$  for 24hrs. GAPDH and Histone H3 were loading controls for cytoplasmic and nuclear proteins, respectively. Quantification of protein expression was measured by ImageJ (National Institutes of Health, Bethesda, Maryland, USA). **(B)** Immunofluorescence staining showing the expression and localization of NRF2 in MPHs treated with IFN $\gamma$  for 24hrs. *P*-values were calculated by unpaired Student's *t* test. Bars represent the mean  $\pm$  SD. \*, *P*<0.05; \*\*, *P*<0.01; \*\*\*, *P*<0.001.

### 3.15 IFN $\gamma$ administration activates NRF2 *in vivo*

Using liver tissues from mice injected with IFN $\gamma$ , I found that the mRNA expression levels of *Nox4* (NADPH oxidase) and *Nrf2* were significantly elevated (**Figure 17A**), however, there was no upregulation of NRF2 protein expression (**Figure 17B**). Immunofluorescence further demonstrated hepatic nuclear translocation of NRF2 in IFN $\gamma$ -treated mice (**Figure 17C**), indicating that the NRF2 pathway was activated *in vivo* by IFN $\gamma$  through nuclear translocation instead of enhanced protein expression.

These results suggest that IFN $\gamma$  activates NRF2 *in vivo*, which might contribute to the IFN $\gamma$ -mediated reduction in ECM1 expression.

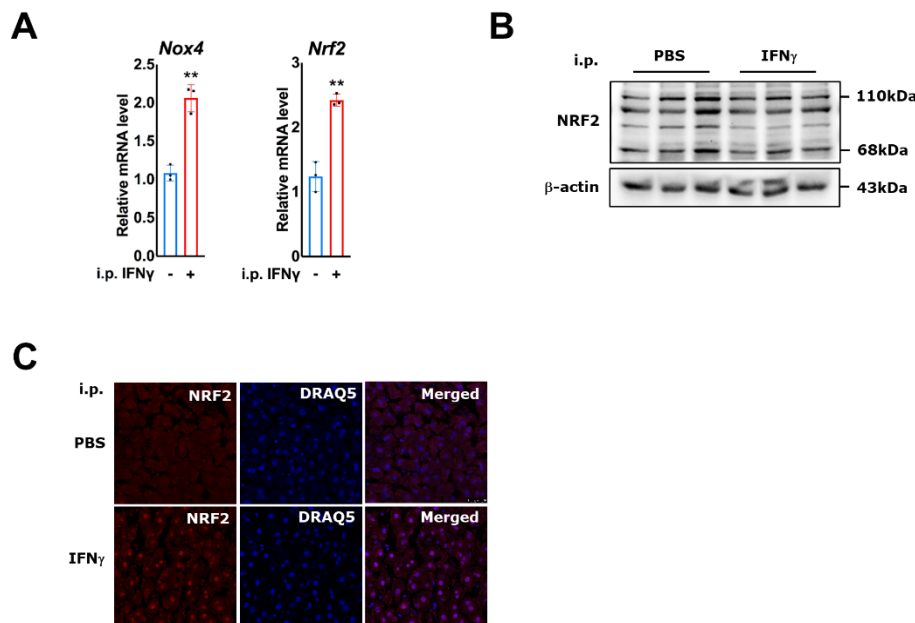


**Figure 17. IFN $\gamma$  administration activates NRF2 *in vivo***

**(A)** qRT-PCR for mRNA expression levels of *Nox4* and *Nrf2* in the liver tissues from mice treated with PBS or IFN $\gamma$  (400 $\mu$ g/kg/day, i.p., for 4 days). The results were normalized to *Ppia*. **(B)** Western blotting showing no change in NRF2 protein level.  $\beta$ -actin was a loading control. **(C)** Immunofluorescence staining for NRF2 expression in the liver tissues from PBS- or IFN $\gamma$ -treated mice. *P*-values were calculated by unpaired Student's t test. Bars represent the mean  $\pm$  SD. \*, *P*<0.05; \*\*, *P*<0.01; \*\*\*, *P*<0.001.

### 3.16 NRF2 generated by H<sub>2</sub>O<sub>2</sub> reduces ECM1 expression

Given that NRF2 is activated by ROS, I treated MPHs with hydrogen peroxide (H<sub>2</sub>O<sub>2</sub>) and observed a significant decrease in *Ecm1* mRNA expression (**Figure 18A**). Using Western blotting I also found an increase in NRF2 with a concomitant decrease in ECM1 protein expression (**Figure 18B**), demonstrating that NRF2 leads to the downregulation of ECM1 following reactive oxygen stimulation.

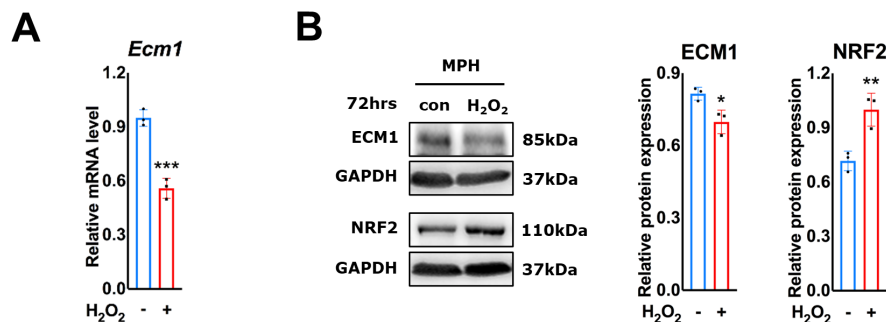


### Figure 18. NRF2 generated by H<sub>2</sub>O<sub>2</sub> reduces ECM1 expression

**(A)** qRT-PCR showing the impact of 72hrs H<sub>2</sub>O<sub>2</sub> (200 $\mu$ M) on mRNA expression of *Ecm1* in MPHs. The results were normalized to *Ppia*. **(B)** Western blotting for the impact of 72hrs H<sub>2</sub>O<sub>2</sub> (200 $\mu$ M) on protein expression of ECM1 and NRF2 in MPHs. GAPDH was a loading control. Quantification of protein expression was measured by ImageJ (National Institutes of Health, Bethesda, Maryland, USA). *P*-values were calculated by unpaired Student's t test. Bars represent the mean  $\pm$  SD. \*, *P*<0.05; \*\*, *P*<0.01; \*\*\*, *P*<0.001.

### 3.17 NRF2 agonist OPZ treatment inhibits ECM1 expression

To investigate further the effect of NRF2 on ECM1 expression, I induced NRF2 nuclear translocation with its agonist Oltipraz (abbreviated as OPZ) and analyzed the alterations in ECM1 expression. **Figure 19A** depicted the mRNA and protein levels of the OPZ-induced NRF2 expression. Immunofluorescence additionally revealed nuclear translocation of NRF2 in OPZ-treated MPHs (**Figure 19B**). Importantly, the expression of ECM1 was significantly downregulated in MPHs treated with OPZ (**Figure 19C**).

These findings indicate that OPZ, as a specific agonist of NRF2, is able to decrease the expression of ECM1.

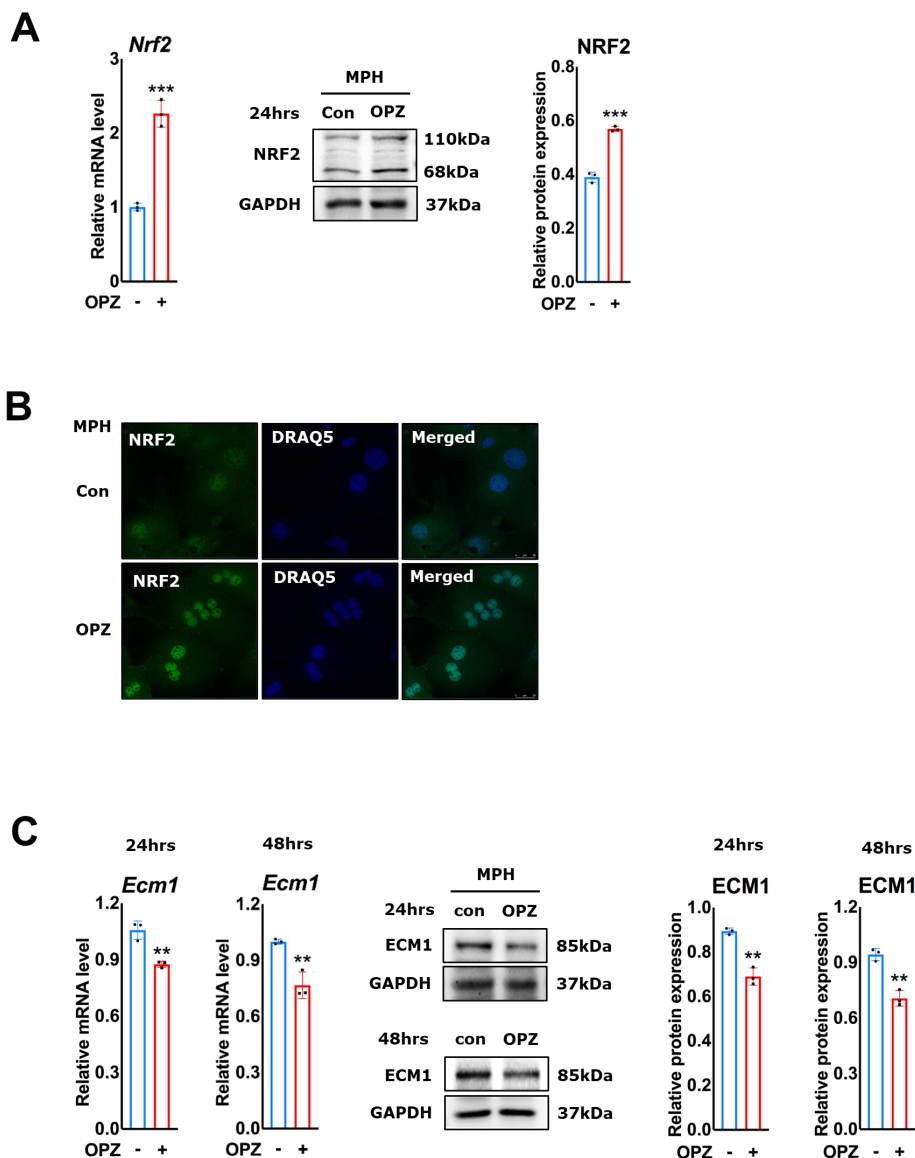


### Figure 19. NRF2 agonist OPZ treatment inhibits ECM1 expression

(A) qRT-PCR and Western blotting showing the effect of 24hrs OPZ (50 $\mu$ M) on NRF2 expression in MPHs. (B) Immunofluorescence staining for NRF2 expression in MPHs treated with OPZ (50 $\mu$ M) for 24hrs. (C) qRT-PCR and Western blotting displaying the effect of OPZ (50 $\mu$ M) on ECM1 expression in MPHs at the indicated time. The results of qRT-PCR were normalized to *Ppia*. GAPDH was a loading control. Quantification of protein expression was measured by ImageJ (National Institutes of Health, Bethesda, Maryland, USA). *P*-values were calculated by unpaired Student's *t* test. Bars represent the mean  $\pm$  SD. \*, *P*<0.05; \*\*, *P*<0.01; \*\*\*, *P*<0.001.

### 3.18 NRF2 inhibits ECM1 expression by binding its gene promoter

Considering that NRF2 is predicted to bind to the *Ecm1* gene promoter, NRF2-*Ecm1* ChIP qRT-PCR was performed. The result showed that NRF2 indeed bound to the promoter region (-867bp ~ -588bp) of *Ecm1* gene upon OPZ treatment in MPHs (Figure 20A). PCR data analysis in a 2% agarose gel further confirmed the increased binding (Figure 20B).

These findings suggest that NRF2 binds directly to the *Ecm1* gene promoter and negatively regulates its transcription, thereby suppressing ECM1 expression in response to oxidative stress.

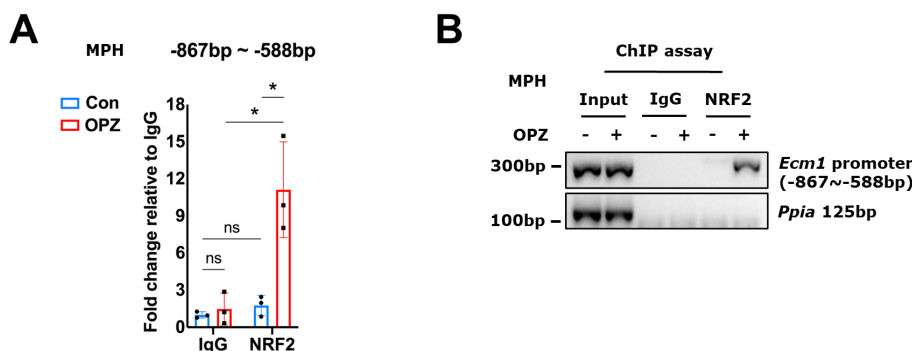


### Figure 20. NRF2 inhibits ECM1 expression by binding its gene promoter

(A) ChIP qRT-PCR showing the effect of OPZ (50 $\mu$ M) on the binding of NRF2 to the *Ecm1* gene promoter in MPHs. Relative fold change of immunoprecipitated genomic fragments in OPZ-treated cells was compared to untreated control group. Fragment “-867bp ~ -588bp” was relative to the transcription start site of *Ecm1* gene. Rabbit

IgG-bound chromatin served as a negative control. *Ppia* represents non-specific binding. **(B)** The PCR amplified products of “-867bp ~ -588bp” fragments were shown on a 2% agarose gel. *P*-values were calculated by unpaired Student's t test. Bars represent the mean  $\pm$  SD. \*,  $P < 0.05$ ; \*\*,  $P < 0.01$ ; \*\*\*,  $P < 0.001$ .

### 3.19 EGF-maintained ECM1 is disrupted by H<sub>2</sub>O<sub>2</sub> or OPZ administration

To mimic hepatic fibrosis or cirrhosis, which are characterized by increased levels of EGF, IFN $\gamma$ , and oxidative stress, I subsequently treated MPHs with EGF and H<sub>2</sub>O<sub>2</sub> (or OPZ) together. qRT-PCR and Western blotting analyses showed that H<sub>2</sub>O<sub>2</sub> inhibited EGF-induced expression of ECM1 and p-EGFR Y1068 (**Figure 21A**). The same modulation was also found in MPHs co-incubated with EGF and OPZ, where EGF-induced ECM1 protein expression and p-EGFR Y1068 were markedly decreased by OPZ treatment (**Figure 21B**).

These results point to the predominance of NRF2 in regulating ECM1 expression compared with EGF, which explains why ECM1 is reduced in the microenvironment of chronic liver diseases despite the presence of elevated EGF levels due to liver injuries.

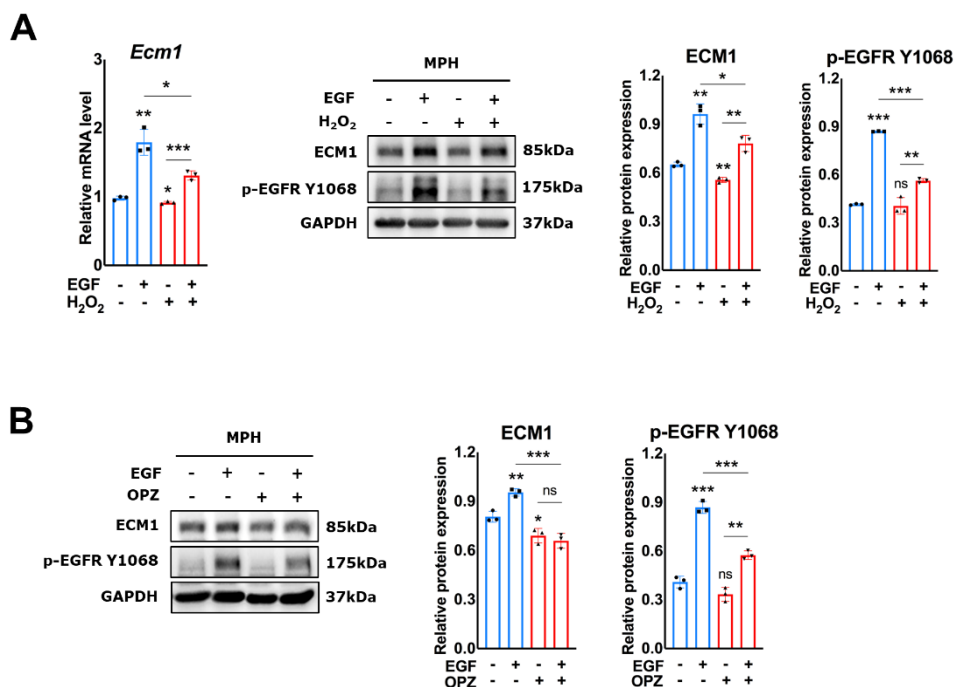


**Figure 21. EGF-maintained ECM1 is disrupted by H<sub>2</sub>O<sub>2</sub> or OPZ administration**

**(A)** qRT-PCR and Western blotting showing the effect of H<sub>2</sub>O<sub>2</sub> on ECM1 and p-EGFR Y1068 expression in EGF-treated MPHs. Cells were treated with H<sub>2</sub>O<sub>2</sub> (200μM) and EGF (100ng/ml) for 72hrs. **(B)** Western blotting displaying the effect of OPZ on ECM1 and p-EGFR Y1068 expression in EGF-treated MPHs. Cells were treated with OPZ (50μM) and EGF (100ng/ml) for 48hrs. The results of qRT-PCR were normalized to *Ppia*. GAPDH was a loading control. Quantification of protein expression was measured by ImageJ (National Institutes of Health, Bethesda, Maryland, USA). *P*-values were calculated by unpaired Student's *t* test. Bars represent the mean ± SD. \*, *P*<0.05; \*\*, *P*<0.01; \*\*\*, *P*<0.001.

### 3.20 Scheme for the regulation of ECM1 expression in healthy/diseased liver

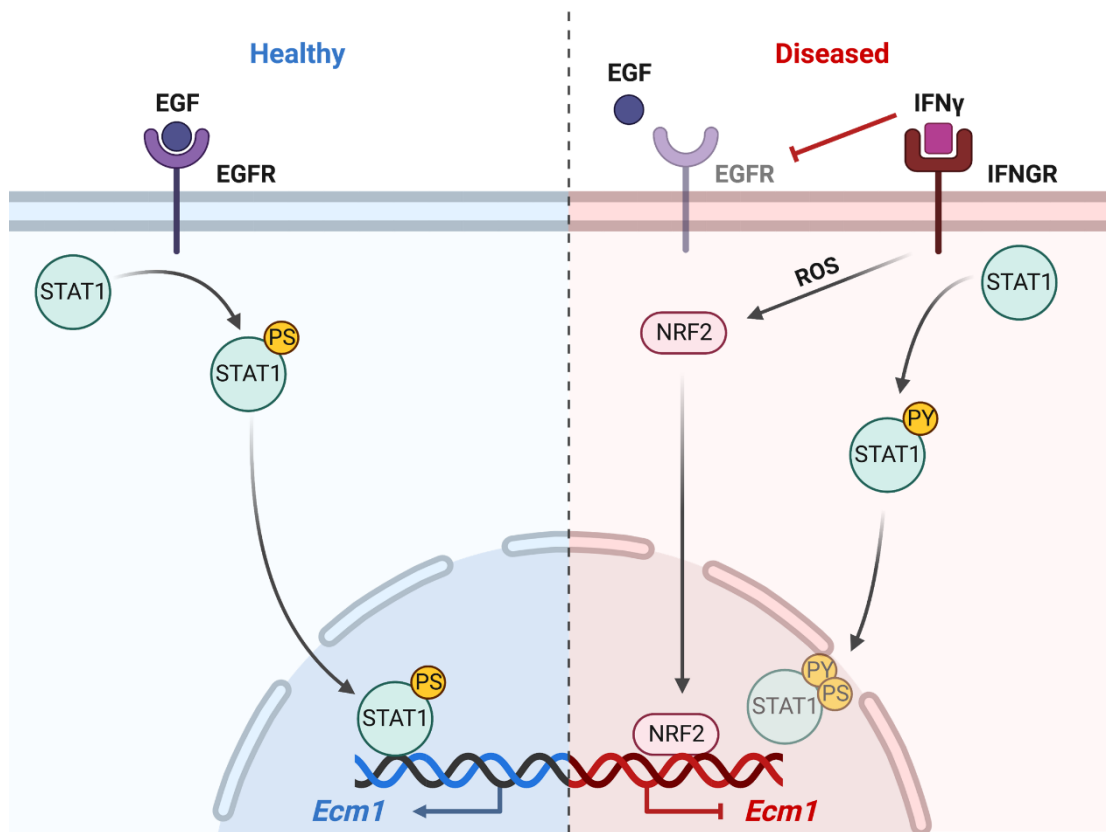


**Figure 22. Regulation of ECM1 expression in different contexts in the liver**

In the physiological state (**left panel**), ECM1 expression in hepatocytes is maintained by the EGF/EGFR/p-STAT1 S727 pathway. Signal-phosphorylated STAT1 S727 translocates to the nucleus and binds to the *Ecm1* gene promoter to maintain its expression. In the pathological situation (**right panel**), inflammation-accumulated high levels of IFN $\gamma$  intercepts EGF signaling through downregulating EGFR, leading

to the loss of ECM1 expression. Importantly, IFN $\gamma$ -induced STAT1 Y701 phosphorylation further impairs the ability of S727-phosphorylated STAT1 to bind the *Ecm1* gene promoter. Additionally, IFN $\gamma$  induces NRF2 nuclear translocation, which directly binds to and negatively regulates the *Ecm1* gene promoter, further reducing ECM1 expression, and therewith facilitating L-TGF- $\beta$  activation and fibrogenesis (Figure created with BioRender.com).



## 4 DISCUSSION

This study investigated how ECM1 expression is regulated under various pathophysiological challenges in the liver. Based on the previous research [16], our group confirmed that ECM1 plays a role as a gatekeeper of liver homeostasis and is critically downregulated upon liver damage and injuries, thus leading to massive spontaneous activation of L-TGF- $\beta$ , and subsequently inducing the activation of HSCs, onset and progression of liver fibrosis. However, the regulatory mechanism of ECM1 expression in the homeostatic and/or diseased liver remained largely unknown. My study illustrated that (1) in normal hepatocytes, EGF/EGFR/STAT1 signaling pathway maintains ECM1 expression; (2) upon external insults, hepatic accumulated IFN $\gamma$  abrogates homeostatic expression of ECM1 through blocking EGFR expression and (3) promotes NRF2 nuclear translocation to bind to and negatively regulate the *Ecm1* gene promoter. I summarize these findings in **Figure 22**.

### 4.1 STAT1 in ECM1 expression regulation

The non-MEK-ERK dependent induction of ECM1 expression by growth factor EGF (**Figure 8A-B**) prompted the exploration on the possibility of other transcription factors. It was proposed that a plethora of transcription factors may contribute to the *Ecm1* transcription. Among these candidates, this study focused on the transcription factor STAT1, as (1) loss-of-function experiments confirmed STAT1 was required for *Ecm1* transcription in normal hepatocytes; and (2) *in vitro*, ChIP assay demonstrated that STAT1 possessed binding sites on the promoter of *Ecm1* gene. Given the importance of STAT1 in the network of signaling pathways regulated by EGF and IFN $\gamma$ , I assumed that they would share a similar mechanism for regulating ECM1 expression. Interestingly, EGF and IFN $\gamma$  play opposing roles in regulating ECM1 in MPHs: EGF promotes, whereas IFN $\gamma$  inhibits ECM1 expression. Why is the regulation of ECM1 expression so different despite the fact they both exploit STAT1 signaling? Based on three lines of evidence, it was clarified that IFN $\gamma$  and EGF-induced STAT1 Ser727 phosphorylation are mechanistically independent and distinct, and regulate ECM1 expression in completely different ways: (1) Previous investigation has revealed that Tyr701 phosphorylation of STAT1 is necessary for IFN $\gamma$ -induced STAT1 Ser727 phosphorylation [57, 60], however under cellular stress conditions, Ser727 phosphorylation induced by p38 mitogen-activated protein kinase

(MAPK) is independent of Tyr701 phosphorylation, indicating mechanistically independent events with various biological consequences [58, 101]; (2) Similar to p38 MAPK, EGF only induces Ser727 phosphorylation in JB6 Cl 41 cells [59], which is consistent with my results showing a stronger Ser727 phosphorylation and no obvious Tyr701 phosphorylation after stimulation of MPHs with EGF (**Figure 13A**); (3) ChIP assay revealed that EGF treatment enhanced STAT1 binding to the *Ecm1* promoter in hepatocytes (**Figure 10B-C**), whereas IFN $\gamma$  treatment did not (**Figure 13B**). For evidence (3), I used different antibodies due to the following considerations: IFN $\gamma$ -induced Ser727 phosphorylation of STAT1 is derived from two components, (a) one is induced along with Tyr701 phosphorylation, and (b) the other is due to elevated total STAT1 expression, which then shuttles freely between the cytoplasm and nucleus and is phosphorylated by a constitutively active nuclear kinase [60, 61]. The antibody detecting p-STAT1 Y701 was used to confirm that the aforementioned p-STAT1 in (a) was not able to bind to the *Ecm1* promoter (**Figure 13B**). Intriguingly, however, antibody to p-STAT1 Ser727 revealed an increased binding of STAT1 to the *Ecm1* promoter in MPHs treated with IFN $\gamma$  (**Figure 15A**). This may be due to the fact that IFN $\gamma$  treatment significantly promoted the expression of total STAT1 (**Figure 15B**), in which STAT1 with only Ser727 phosphorylation was also enhanced during intracellular shuttling, resulting in increased p-STAT1 Ser727 binding to the *Ecm1* promoter. Since this is not the main mechanism by which IFN $\gamma$  regulates STAT1 signaling, the ultimate regulatory efficacy of IFN $\gamma$  on ECM1 expression should still be largely attributed to p-STAT1 Ser727 following the prerequisite Tyr701 phosphorylation as described in (a), implying that most STAT1 cannot bind to the *Ecm1* promoter upon IFN $\gamma$  stimulation (**Figure 13B**). Concerning the different impacts of IFN $\gamma$  and EGF on ECM1 expression in hepatocytes, from another perspective, we also need to realize the multipotent effects of STAT1 signaling, which may be regulated by EGF and involve essential physiological functions beyond IFN $\gamma$ .

#### 4.2 Excessive production of IFN $\gamma$ and liver injury

IFN $\gamma$ , mainly produced by activated T cells and natural killer cells, is an anti-viral, pro-inflammatory and anti-tumor cytokine, and has been reported to have anti-fibrotic properties on hepatic fibrosis with chronic HBV infection [102]. One trial showed that IFN $\gamma$  treatment for nine months improves fibrosis scores in patients, possibly through antagonizing TGF- $\beta$  signaling [102]. Later experiments revealed that the anti-TGF- $\beta$

effect is caused by the upregulation of Smad7 in activated HSCs via IFN $\gamma$ -induced STAT1 [103]. Other studies demonstrated that IFN $\gamma$  inhibits the proliferation and activation of HSCs in a STAT1-dependent manner, thereby inhibiting liver fibrosis [104, 105]. Nonetheless, a coin always has two sides. IFN $\gamma$  also induces liver damage, mainly through triggering hepatocytes apoptosis and hepatic inflammation. Growing evidence suggested that IFN $\gamma$  treatment *in vitro* inhibits hepatocyte proliferation [106] and liver regeneration, which in part also promotes the development of liver fibrosis. During Con A-induced hepatotoxicity, IFN $\gamma$  overproduction may result in T cell-dependent liver injuries, such as hepatocellular apoptosis and necrosis [107, 108]. Neutralization of IFN $\gamma$  prevents STAT1 activation and hepatic damage induced by Con A [109, 110]. In viral hepatitis, hepatic lesions can be attributed to T cell-dependent cytotoxicity against virus-infected hepatocytes, where IFN $\gamma$ , which is typically elevated in patients with chronic viral liver disease [111] plays a crucial role. When IFN $\gamma$  was administered to HBV transgenic mice that did not develop hepatitis, hepatic lesions with lymphocytes infiltration were observed [112]. Moreover, in a methionine and choline-deficient high-fat (MCDHF) diet mouse model, unlike CCl $_4$  or dimethylnitrosamine (DMN) injections, or a 3,5-diethoxycarbonyl-1,4-dihydrocollidine (DDC) diet, IFN $\gamma$  was even identified as a pro-fibrotic cytokine, and its deficiency suppressed the activation and infiltration of immune cells and the subsequent inflammatory response, further inhibiting the activation of HSCs, possibly leading to attenuation of liver fibrosis [113]. Such phenomenon is not a direct result of switching off IFN $\gamma$  on HSCs. The role of IFN $\gamma$  in hepatic damaged situations appears complex and controversial in light of these studies. In this research, I reported that one of the adverse effects of elevated hepatic IFN $\gamma$  levels in chronic liver diseases is the inhibition of ECM1 expression in hepatocytes, leading to the activation of L-TGF- $\beta$  and subsequent liver injuries. As hepatocytes are the main producers of ECM1, injured livers/hepatocytes can further influence the steady expression of ECM1, thus forming a vicious circle and resulting in the progression of chronic liver diseases.

#### 4.3 Regulation of EGFR by IFN $\gamma$

As previously described, ECM1 expression is maintained by EGF-EGFR signaling in liver homeostasis; hence, the crosstalk between IFN $\gamma$  and EGF-EGFR signaling prompted further investigation. It is still controversial yet regarding the modulatory role of IFN $\gamma$  on EGFR, some studies reported that IFN $\gamma$  transactivated EGFR [114,

115] and upregulated EGFR expression [116], however others described that IFN $\gamma$  inhibited EGFR phosphorylation [117] and its mRNA expression [118], possibly because different cell types have different responses in various contexts. Based on my findings, in primary hepatocytes, IFN $\gamma$  suppresses EGFR total protein expression and further prevents EGF-activated EGFR, thereby perturbing EGF-EGFR-maintained ECM1 expression and, to some extent, promoting HSCs activation and the development of hepatic fibrosis, or at least partially impairing the anti-fibrotic function of IFN $\gamma$ .

#### 4.4 Adverse consequences of excessive NRF2 activation

NRF2, a transcription factor with predictive binding sites on the *Ecm1* gene promoter, is activated by inflammatory mediators for example ROS, fatty acids, nitric oxide and prostaglandins [119, 120]. Studies have shown that activation of NRF2 provides a cytoprotective effect, reducing ROS and pro-inflammatory cytokines, thereby alleviating inflammation [119, 121]. Like in IFN $\gamma$ -polarized macrophages, NRF2 activity is increased, the antioxidant response is dependent on NRF2, and knockdown of *Nrf2* decreases hydrogen peroxide clearance [122]. However, excessive activation of NRF2 and constitutive nuclear accumulation also leads to detrimental effects. In a *Keap1*-null mouse model, no newborns survived after three weeks, possibly due to starvation caused by hyperkeratotic esophagus and cardia [123]. In addition, one group identified an association between NRF2 and hepatic steatosis, demonstrating that NRF2 in hepatocytes was responsible for the regulation of PPAR $\gamma$ , and specific deletion of NRF2 in hepatocytes reduced the expression of high-fat diet-induced PPAR $\gamma$  and lipid accumulation, thus impairing the progression of non-alcoholic fatty liver disease [124]. Moreover, pancreatic cancer patients with raised NRF2 levels have a shorter median survival time [125]. In my study, I found that NRF2 becomes activated by pro-inflammatory factor IFN $\gamma$  and negatively regulates *Ecm1* gene transcription through binding to the *Ecm1* gene promoter, leading to the disruption of homeostatic extracellular matrix and activation of L-TGF- $\beta$ .

#### 4.5 Outlook of the study

##### 4.5.1 HGF in ECM1 expression regulation

As shown in **Figure 5**, another growth factor, HGF, upregulates the expression of ECM1 in hepatocytes. Although the signaling pathways of two growth factors, EGF

and HGF, are comparable, their receptors are dissimilar: EGFR is the receptor for EGF, while c-Met is the receptor for HGF. In prior mechanistic investigations, it was discovered that IFN $\gamma$  inhibits EGFR and prevents EGF from maintaining homeostatic expression of ECM1 under normal physiological conditions. It is unknown whether IFN $\gamma$  has an inhibitory effect on c-Met, and this may be a novel area for future study. In addition, blocking STAT1 similarly inhibited the expression of ECM1 induced by HGF (**Figure 23**). As most studies on HGF downstream pathways have focused on STAT3 signaling, there are few reports of HGF-induced STAT1 activation, the inhibition of ECM1 may be due to interference with the formation of STAT1-STAT3 heterodimers, implying STAT3 rather than STAT1 is the main downstream target of HGF. In addition to STAT1, IFN $\gamma$  also induces STAT3 phosphorylation at Y705 (**Figure 24**), possibly resulting in heterodimer formation with STAT1 [126]. The distinct effects of HGF and IFN $\gamma$  on ECM1 expression regulation may be attributed to the different proportions of STAT1/STAT3 homodimers and STAT1-STAT3 heterodimers formed downstream, which could have diverse functions. Concerning how HGF/c-Met upregulates ECM1 expression, whether it is dependent on STAT1-STAT3 heterodimer formation, and how IFN $\gamma$  interrupts HGF/c-Met and STAT3 phosphorylation or heterodimer formation with STAT1, further investigation is required and will be the next step in ECM1 regulation studies.

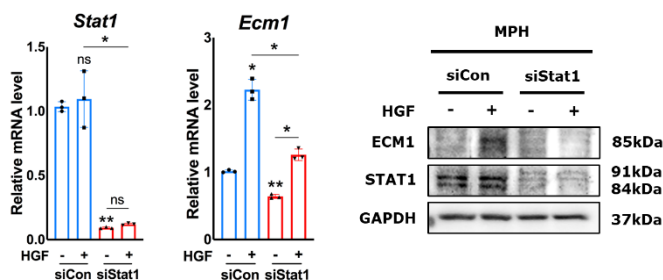


### Figure 23. HGF-upregulated ECM1 involves STAT1

qRT-PCR and Western blotting for ECM1 and STAT1 expression in HGF-treated MPHs with or without siStat1 knockdown. The results of qRT-PCR were normalized to *Ppia*. GAPDH was a loading control. *P*-values were calculated by unpaired Student's *t* test. Bars represent the mean  $\pm$  SD. \*, *P*<0.05; \*\*, *P*<0.01; \*\*\*, *P*<0.001.

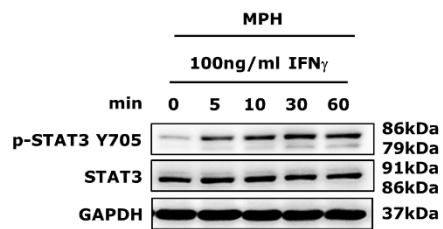


**Figure 24. Activation of STAT3 at Y705 in IFN $\gamma$ -treated MPHs**

Western blotting for the expression of p-STAT3 Y705 and STAT3 in MPHs treated with IFN $\gamma$  at different time points. GAPDH was a loading control.

#### 4.5.2 Downregulation of ECM1 expression in liver regeneration and HCC

In the partial hepatectomy (PHx) mouse model, *Ecm1* expression decreased during the initial phase of liver regeneration until day 4 (**Figure 25A**), then gradually recovered, but remained lower on day 21 compared to day 0 (sham). In parallel, TGF- $\beta$  signaling was enhanced and peaked on day 6. On day 21, the level of *Tgfb1* mRNA expression returned to the baseline (**Figure 25B**). These data suggest that ECM1 is downregulated during the early stage of liver regeneration, accompanied by increased TGF- $\beta$  signaling. In addition, as stated in the published article [16], hepatic ECM1 expression was significantly reduced in several mouse models of liver disease and in patients with HBV/alcoholic hepatitis-induced fibrosis/cirrhosis; therefore, analyzing the expression of ECM1 in liver cancer would be an intriguing direction for further study. **Figure 26A** demonstrated that hepatocellular carcinoma (HCC) cell lines, such as HuH7, HLF, Hep3B, HLE, and PLC/PRF/5 had lower levels of ECM1 expression than human primary hepatocytes (HPHs) and non-tumour (NT) areas of liver tissues from HCC patients. The same trend was also observed in tumour areas from HCC patients' livers compared with non-tumour areas (**Figure 26B**), indicating that ECM1 is regulated during HCC development and may be essential for maintaining homeostasis in the liver. In general, ECM1 plays a role in liver regenerative function and in liver cancer progression, and it would be fascinating to continue studying these features in the future.

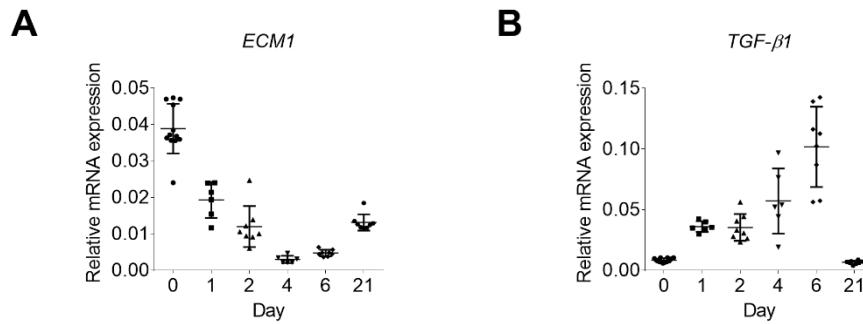


**Figure 25. ECM1 expression during liver regeneration**

(A) qRT-PCR showing the mRNA expression level of *Ecm1* gene in the mice subjected to PHx, mice liver tissues were collected on 0 (sham), 1, 2, 4, 6 and 21 days after the surgery. (B) qRT-PCR for the mRNA expression level of *Tgfb1* gene. The results were normalized to *Ppia*. *P*-values were calculated by unpaired Student's *t* test. Bars represent the mean  $\pm$  SD. \*,  $P < 0.05$ ; \*\*,  $P < 0.01$ ; \*\*\*,  $P < 0.001$ .

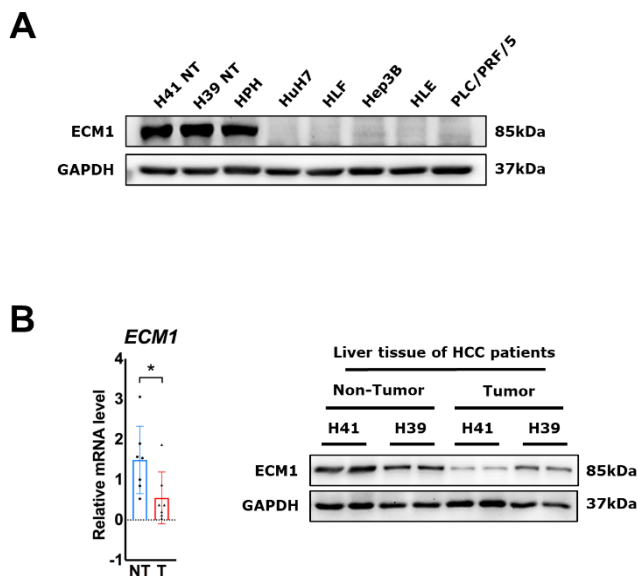


**Figure 26. ECM1 expression in HCC cell lines and HCC patients**

(A) Western blotting for the expression of ECM1 in HCC cell lines, HPHs, and non-tumour (NT) liver tissues from HCC patients. (B) qRT-PCR and Western blotting for the ECM1 expression in non-tumour (NT) and tumour (T) areas of HCC patients' livers. The results of qRT-PCR were normalized to *PPIA*. GAPDH was a loading control. *P*-values were calculated by unpaired Student's *t* test. Bars represent the mean  $\pm$  SD. \*,  $P < 0.05$ ; \*\*,  $P < 0.01$ ; \*\*\*,  $P < 0.001$ .

Taken together, the current study highlights that EGF and IFN $\gamma$  control the regulation of ECM1 expression under physiological and pathological liver conditions. In healthy liver, the EGF/EGFR/STAT1 signaling pathway maintains ECM1 expression; upon liver damage and injury, accumulated hepatic IFN $\gamma$  impedes homeostatic ECM1 expression through inhibiting EGFR expression and inducing NRF2 nuclear translocation, thereby failing to maintain the quiescence of L-TGF- $\beta$ . Regarding the clinical application of IFN $\gamma$  and NRF2 agonist, hepatotoxicity induced by IFN $\gamma$  and NRF2 over-accumulation should be taken into account. In this context, ECM1 has the potential to be developed as an anti-fibrotic agent, especially in combination with IFN $\gamma$  and NRF2 agonist, to safeguard the liver against the side effects of both administrations, which is promising for improving the prognosis of chronic liver diseases. It will be interesting to further investigate whether ECM1 peptides exert a more effective protective role in diseases such as liver fibrosis and cirrhosis.



## 5 SUMMARY

In healthy liver, L-TGF- $\beta$  is stored in the extracellular matrix and stabilized in an inactive form by ECM1. Upon damage, ECM1 production is downregulated, especially in hepatocytes, leading to spontaneous L-TGF- $\beta$  activation and fibrogenesis. I used *in silico* promoter analyses, performed *in vitro* studies in mouse/human hepatocytes and *in vivo* experiments with different mouse models, to mechanistically delineate maintenance versus downregulation of ECM1 expression under physiological and pathological conditions. I could identify the crosstalk of signaling pathways that maintain or inhibit ECM1 expression.

In my thesis, I found that:

(1) In healthy liver, EGF and HGF are mediators of ECM1 expression maintenance. Thereby, EGF signals via EGFR/p-STAT1 S727 to the *Ecm1* promoter. The HGF signal as well integrates at STAT1 signaling.

(2) Upon liver damage and injuries:

I. Inflammation-accumulated hepatic IFN $\gamma$  interferes with EGF signaling through downregulating EGFR.

II. In addition, IFN $\gamma$  induces STAT1 phosphorylation at Y701, which interferes with binding of p-STAT1 S727 to the *Ecm1* gene promoter.

I and II together result in a decreased ECM1 expression.

III. Further, IFN $\gamma$  promotes NRF2 nuclear translocation, which binds to the *Ecm1* gene promoter and negatively regulates its transcription, leading to inhibition of ECM1 expression.

Taken together, the EGF/EGFR/p-STAT1 S727 pathway that maintains ECM1 expression homeostasis in healthy hepatocytes is disrupted and inhibited by inflammation-accumulated IFN $\gamma$  and its effects in stressed hepatocytes with the consequence of L-TGF- $\beta$  activation and hepatic fibrosis.

In conclusion, my findings delineate the regulation of ECM1 expression in hepatocytes, which has potential for therapeutic manipulation of its expression with impact on TGF- $\beta$  availability to treat chronic liver diseases.

## 6 REFERENCES

- [1] Mathieu E, Meheus L, Raymackers J, Merregaert J. Characterization of the osteogenic stromal cell line MN7: identification of secreted MN7 proteins using two-dimensional polyacrylamide gel electrophoresis, western blotting, and microsequencing. *J Bone Miner Res* 1994;9:903-913.
- [2] Smits P, Poumay Y, Karperien M, Tylzanowski P, Wauters J, Huylebroeck D, et al. Differentiation-dependent alternative splicing and expression of the extracellular matrix protein 1 gene in human keratinocytes. *J Invest Dermatol* 2000;114:718-724.
- [3] Sercu S, Lambeir AM, Steenackers E, El Ghalbzouri A, Geentjens K, Sasaki T, et al. ECM1 interacts with fibulin-3 and the beta 3 chain of laminin 332 through its serum albumin subdomain-like 2 domain. *Matrix Biol* 2009;28:160-169.
- [4] Chan I. The role of extracellular matrix protein 1 in human skin. *Clin Exp Dermatol* 2004;29:52-56.
- [5] Deckers MM, Smits P, Karperien M, Ni J, Tylzanowski P, Feng P, et al. Recombinant human extracellular matrix protein 1 inhibits alkaline phosphatase activity and mineralization of mouse embryonic metatarsals in vitro. *Bone* 2001;28:14-20.
- [6] Han Z, Ni J, Smits P, Underhill CB, Xie B, Chen Y, et al. Extracellular matrix protein 1 (ECM1) has angiogenic properties and is expressed by breast tumor cells. *FASEB J* 2001;15:988-994.
- [7] Mongiat M, Fu J, Oldershaw R, Greenhalgh R, Gown AM, Iozzo RV. Perlecan protein core interacts with extracellular matrix protein 1 (ECM1), a glycoprotein involved in bone formation and angiogenesis. *J Biol Chem* 2003;278:17491-17499.
- [8] Fujimoto N, Terlizzi J, Brittingham R, Fertala A, McGrath JA, Uitto J. Extracellular matrix protein 1 interacts with the domain III of fibulin-1C and 1D variants through its central tandem repeat 2. *Biochem Biophys Res Commun* 2005;333:1327-1333.
- [9] Fujimoto N, Terlizzi J, Aho S, Brittingham R, Fertala A, Oyama N, et al. Extracellular matrix protein 1 inhibits the activity of matrix metalloproteinase 9 through high-affinity protein/protein interactions. *Exp Dermatol* 2006;15:300-307.
- [10] Oyama N, Chan I, Neill SM, Hamada T, South AP, Wessagowit V, et al. Autoantibodies to extracellular matrix protein 1 in lichen sclerosus. *Lancet* 2003;362:118-123.
- [11] Qing J, Maher VM, Tran H, Argraves WS, Dunstan RW, McCormick JJ. Suppression of anchorage-independent growth and matrigel invasion and delayed tumor formation by elevated expression of fibulin-1D in human fibrosarcoma-derived cell lines. *Oncogene* 1997;15:2159-2168.
- [12] Sercu S, Zhang L, Merregaert J. The extracellular matrix protein 1: its molecular interaction and implication in tumor progression. *Cancer Invest* 2008;26:375-384.

- [13] Wipff PJ, Hinz B. Integrins and the activation of latent transforming growth factor beta1 - an intimate relationship. *Eur J Cell Biol* 2008;87:601-615.
- [14] Su P, Chen S, Zheng YH, Zhou HY, Yan CH, Yu F, et al. Novel Function of Extracellular Matrix Protein 1 in Suppressing Th17 Cell Development in Experimental Autoimmune Encephalomyelitis. *J Immunol* 2016;197:1054-1064.
- [15] Wang L, Yu J, Ni J, Xu XM, Wang J, Ning H, et al. Extracellular matrix protein 1 (ECM1) is over-expressed in malignant epithelial tumors. *Cancer Lett* 2003;200:57-67.
- [16] Fan W, Liu T, Chen W, Hammad S, Longerich T, Hausser I, et al. ECM1 Prevents Activation of Transforming Growth Factor beta, Hepatic Stellate Cells, and Fibrogenesis in Mice. *Gastroenterology* 2019;157:1352-1367 e1313.
- [17] Le Gall SM, Auger R, Dreux C, Mauduit P. Regulated cell surface pro-EGF ectodomain shedding is a zinc metalloprotease-dependent process. *J Biol Chem* 2003;278:45255-45268.
- [18] Zeng F, Harris RC. Epidermal growth factor, from gene organization to bedside. *Semin Cell Dev Biol* 2014;28:2-11.
- [19] Harris RC, Chung E, Coffey RJ. EGF receptor ligands. *Exp Cell Res* 2003;284:2-13.
- [20] Schneider MR, Wolf E. The epidermal growth factor receptor ligands at a glance. *J Cell Physiol* 2009;218:460-466.
- [21] Massague J, Pandiella A. Membrane-anchored growth factors. *Annu Rev Biochem* 1993;62:515-541.
- [22] Savage CR, Jr., Hash JH, Cohen S. Epidermal growth factor. Location of disulfide bonds. *J Biol Chem* 1973;248:7669-7672.
- [23] Carpenter G. Receptors for epidermal growth factor and other polypeptide mitogens. *Annu Rev Biochem* 1987;56:881-914.
- [24] Zeineldin R, Hudson LG. Epithelial cell migration in response to epidermal growth factor. *Methods Mol Biol* 2006;327:147-158.
- [25] Dvorak B. Milk epidermal growth factor and gut protection. *J Pediatr* 2010;156:S31-35.
- [26] Read LC, Upton FM, Francis GL, Wallace JC, Dahlenberg GW, Ballard FJ. Changes in the growth-promoting activity of human milk during lactation. *Pediatr Res* 1984;18:133-139.
- [27] Carpenter G, Cohen S. Epidermal growth factor. *Annu Rev Biochem* 1979;48:193-216.
- [28] Fisher DA, Salido EC, Barajas L. Epidermal growth factor and the kidney. *Annu Rev Physiol* 1989;51:67-80.

- [29] Olsen PS, Poulsen SS, Kirkegaard P. Adrenergic effects on secretion of epidermal growth factor from Brunner's glands. *Gut* 1985;26:920-927.
- [30] Michalopoulos GK. Liver regeneration. *J Cell Physiol* 2007;213:286-300.
- [31] Earp HS, 3rd, Calvo BF, Sartor CI. The EGF receptor family--multiple roles in proliferation, differentiation, and neoplasia with an emphasis on HER4. *Trans Am Clin Climatol Assoc* 2003;114:315-333; discussion 333-314.
- [32] McGowan JA, Strain AJ, Bucher NL. DNA synthesis in primary cultures of adult rat hepatocytes in a defined medium: effects of epidermal growth factor, insulin, glucagon, and cyclic-AMP. *J Cell Physiol* 1981;108:353-363.
- [33] Bucher NL. Liver regeneration: an overview. *J Gastroenterol Hepatol* 1991;6:615-624.
- [34] Schreiber AB, Libermann TA, Lax I, Yarden Y, Schlessinger J. Biological role of epidermal growth factor-receptor clustering. Investigation with monoclonal anti-receptor antibodies. *J Biol Chem* 1983;258:846-853.
- [35] Ushiro H, Cohen S. Identification of phosphotyrosine as a product of epidermal growth factor-activated protein kinase in A-431 cell membranes. *J Biol Chem* 1980;255:8363-8365.
- [36] Kovacs E, Zorn JA, Huang Y, Barros T, Kuriyan J. A structural perspective on the regulation of the epidermal growth factor receptor. *Annu Rev Biochem* 2015;84:739-764.
- [37] Wang Z. ErbB Receptors and Cancer. *Methods Mol Biol* 2017;1652:3-35.
- [38] Shi F, Telesco SE, Liu Y, Radhakrishnan R, Lemmon MA. ErbB3/HER3 intracellular domain is competent to bind ATP and catalyze autophosphorylation. *Proc Natl Acad Sci U S A* 2010;107:7692-7697.
- [39] Yarden Y, Sliwkowski MX. Untangling the ErbB signalling network. *Nat Rev Mol Cell Biol* 2001;2:127-137.
- [40] Velu TJ, Beguinot L, Vass WC, Willingham MC, Merlino GT, Pastan I, et al. Epidermal-growth-factor-dependent transformation by a human EGF receptor proto-oncogene. *Science* 1987;238:1408-1410.
- [41] Arteaga CL, Engelman JA. ERBB receptors: from oncogene discovery to basic science to mechanism-based cancer therapeutics. *Cancer Cell* 2014;25:282-303.
- [42] Hynes NE, MacDonald G. ErbB receptors and signaling pathways in cancer. *Curr Opin Cell Biol* 2009;21:177-184.
- [43] Roskoski R, Jr. The ErbB/HER family of protein-tyrosine kinases and cancer. *Pharmacol Res* 2014;79:34-74.
- [44] Kim YT, Park SW, Kim JW. Correlation between expression of EGFR and the prognosis of patients with cervical carcinoma. *Gynecol Oncol* 2002;87:84-89.

- [45] Kopp R, Rothbauer E, Ruge M, Arnholdt H, Spranger J, Muders M, et al. Clinical implications of the EGF receptor/ligand system for tumor progression and survival in gastrointestinal carcinomas: evidence for new therapeutic options. *Recent Results Cancer Res* 2003;162:115-132.
- [46] Nicholson RI, Gee JM, Harper ME. EGFR and cancer prognosis. *Eur J Cancer* 2001;37 Suppl 4:S9-15.
- [47] Masuda H, Zhang D, Bartholomeusz C, Doihara H, Hortobagyi GN, Ueno NT. Role of epidermal growth factor receptor in breast cancer. *Breast Cancer Res Treat* 2012;136:331-345.
- [48] Lopez-Luque J, Bertran E, Crosas-Molist E, Maiques O, Malfettone A, Caja L, et al. Downregulation of Epidermal Growth Factor Receptor in hepatocellular carcinoma facilitates Transforming Growth Factor-beta-induced epithelial to amoeboid transition. *Cancer Lett* 2019;464:15-24.
- [49] Levy DE, Darnell JE, Jr. Stats: transcriptional control and biological impact. *Nat Rev Mol Cell Biol* 2002;3:651-662.
- [50] Wen Z, Zhong Z, Darnell JE, Jr. Maximal activation of transcription by Stat1 and Stat3 requires both tyrosine and serine phosphorylation. *Cell* 1995;82:241-250.
- [51] Zhang Y, Chen Y, Yun H, Liu Z, Su M, Lai R. STAT1beta enhances STAT1 function by protecting STAT1alpha from degradation in esophageal squamous cell carcinoma. *Cell Death Dis* 2017;8:e3077.
- [52] Zakharova N, Lymar ES, Yang E, Malik S, Zhang JJ, Roeder RG, et al. Distinct transcriptional activation functions of STAT1alpha and STAT1beta on DNA and chromatin templates. *J Biol Chem* 2003;278:43067-43073.
- [53] Semper C, Leitner NR, Lassnig C, Parrini M, Mahlakoiv T, Rammerstorfer M, et al. STAT1beta is not dominant negative and is capable of contributing to gamma interferon-dependent innate immunity. *Mol Cell Biol* 2014;34:2235-2248.
- [54] Bhattacharya S, Eckner R, Grossman S, Oldread E, Arany Z, D'Andrea A, et al. Cooperation of Stat2 and p300/CBP in signalling induced by interferon-alpha. *Nature* 1996;383:344-347.
- [55] Qureshi SA, Leung S, Kerr IM, Stark GR, Darnell JE, Jr. Function of Stat2 protein in transcriptional activation by alpha interferon. *Mol Cell Biol* 1996;16:288-293.
- [56] Quesnelle KM, Boehm AL, Grandis JR. STAT-mediated EGFR signaling in cancer. *J Cell Biochem* 2007;102:311-319.
- [57] Kovarik P, Mangold M, Ramsauer K, Heidari H, Steinborn R, Zotter A, et al. Specificity of signaling by STAT1 depends on SH2 and C-terminal domains that regulate Ser727 phosphorylation, differentially affecting specific target gene expression. *EMBO J* 2001;20:91-100.
- [58] Kovarik P, Stoiber D, Eysers PA, Menghini R, Neiningner A, Gaestel M, et al. Stress-induced phosphorylation of STAT1 at Ser727 requires p38 mitogen-activated

protein kinase whereas IFN-gamma uses a different signaling pathway. *Proc Natl Acad Sci U S A* 1999;96:13956-13961.

[59] Zhang Y, Cho YY, Petersen BL, Zhu F, Dong Z. Evidence of STAT1 phosphorylation modulated by MAPKs, MEK1 and MSK1. *Carcinogenesis* 2004;25:1165-1175.

[60] Sadzak I, Schiff M, Gattermeier I, Glinitzer R, Sauer I, Saalmuller A, et al. Recruitment of Stat1 to chromatin is required for interferon-induced serine phosphorylation of Stat1 transactivation domain. *Proc Natl Acad Sci U S A* 2008;105:8944-8949.

[61] Meyer T, Begitt A, Lodige I, van Rossum M, Vinkemeier U. Constitutive and IFN-gamma-induced nuclear import of STAT1 proceed through independent pathways. *EMBO J* 2002;21:344-354.

[62] Schroder K, Hertzog PJ, Ravasi T, Hume DA. Interferon-gamma: an overview of signals, mechanisms and functions. *J Leukoc Biol* 2004;75:163-189.

[63] Frucht DM, Fukao T, Bogdan C, Schindler H, O'Shea JJ, Koyasu S. IFN-gamma production by antigen-presenting cells: mechanisms emerge. *Trends Immunol* 2001;22:556-560.

[64] Carnaud C, Lee D, Donnars O, Park SH, Beavis A, Koezuka Y, et al. Cutting edge: Cross-talk between cells of the innate immune system: NKT cells rapidly activate NK cells. *J Immunol* 1999;163:4647-4650.

[65] Yoshimoto T, Takeda K, Tanaka T, Ohkusu K, Kashiwamura S, Okamura H, et al. IL-12 up-regulates IL-18 receptor expression on T cells, Th1 cells, and B cells: synergism with IL-18 for IFN-gamma production. *J Immunol* 1998;161:3400-3407.

[66] Munder M, Mallo M, Eichmann K, Modolell M. Direct stimulation of macrophages by IL-12 and IL-18 - a bridge built on solid ground. *Immunol Lett* 2001;75:159-160.

[67] Munder M, Mallo M, Eichmann K, Modolell M. Murine macrophages secrete interferon gamma upon combined stimulation with interleukin (IL)-12 and IL-18: A novel pathway of autocrine macrophage activation. *J Exp Med* 1998;187:2103-2108.

[68] Fukao T, Matsuda S, Koyasu S. Synergistic effects of IL-4 and IL-18 on IL-12-dependent IFN-gamma production by dendritic cells. *J Immunol* 2000;164:64-71.

[69] Pien GC, Satoskar AR, Takeda K, Akira S, Biron CA. Cutting edge: selective IL-18 requirements for induction of compartmental IFN-gamma responses during viral infection. *J Immunol* 2000;165:4787-4791.

[70] Salazar-Mather TP, Hamilton TA, Biron CA. A chemokine-to-cytokine-to-chemokine cascade critical in antiviral defense. *J Clin Invest* 2000;105:985-993.

[71] Schindler H, Lutz MB, Rollinghoff M, Bogdan C. The production of IFN-gamma by IL-12/IL-18-activated macrophages requires STAT4 signaling and is inhibited by IL-4. *J Immunol* 2001;166:3075-3082.

- [72] Boehm U, Klamp T, Groot M, Howard JC. Cellular responses to interferon-gamma. *Annu Rev Immunol* 1997;15:749-795.
- [73] Finkelman FD, Katona IM, Mosmann TR, Coffman RL. IFN-gamma regulates the isotypes of Ig secreted during in vivo humoral immune responses. *J Immunol* 1988;140:1022-1027.
- [74] Perussia B, Dayton ET, Fanning V, Thiagarajan P, Hoxie J, Trinchieri G. Immune interferon and leukocyte-conditioned medium induce normal and leukemic myeloid cells to differentiate along the monocytic pathway. *J Exp Med* 1983;158:2058-2080.
- [75] Lalor PF, Shields P, Grant A, Adams DH. Recruitment of lymphocytes to the human liver. *Immunol Cell Biol* 2002;80:52-64.
- [76] Lai HS, Lin WH, Hsu WM, Chen CN, Chang KJ, Lee PH. Variations in interferon gamma receptor gene expression during liver regeneration after partial hepatectomy in rats. *Am Surg* 2009;75:49-54.
- [77] Valente G, Ozmen L, Novelli F, Geuna M, Palestro G, Forni G, et al. Distribution of interferon-gamma receptor in human tissues. *Eur J Immunol* 1992;22:2403-2412.
- [78] Kano A, Watanabe Y, Takeda N, Aizawa S, Akaike T. Analysis of IFN-gamma-induced cell cycle arrest and cell death in hepatocytes. *J Biochem* 1997;121:677-683.
- [79] Shinagawa T, Yoshioka K, Kakumu S, Wakita T, Ishikawa T, Itoh Y, et al. Apoptosis in cultured rat hepatocytes: the effects of tumour necrosis factor alpha and interferon gamma. *J Pathol* 1991;165:247-253.
- [80] Farrar MA, Schreiber RD. The molecular cell biology of interferon-gamma and its receptor. *Annu Rev Immunol* 1993;11:571-611.
- [81] Bach EA, Aguet M, Schreiber RD. The IFN gamma receptor: a paradigm for cytokine receptor signaling. *Annu Rev Immunol* 1997;15:563-591.
- [82] Bernabei P, Coccia EM, Rigamonti L, Bosticardo M, Forni G, Pestka S, et al. Interferon-gamma receptor 2 expression as the deciding factor in human T, B, and myeloid cell proliferation or death. *J Leukoc Biol* 2001;70:950-960.
- [83] Young H, Hodge DL. *Encyclopedia of Hormones*; 2003.
- [84] Cook JR, Jung V, Schwartz B, Wang P, Pestka S. Structural analysis of the human interferon gamma receptor: a small segment of the intracellular domain is specifically required for class I major histocompatibility complex antigen induction and antiviral activity. *Proc Natl Acad Sci U S A* 1992;89:11317-11321.
- [85] Farrar MA, Campbell JD, Schreiber RD. Identification of a functionally important sequence in the C terminus of the interferon-gamma receptor. *Proc Natl Acad Sci U S A* 1992;89:11706-11710.

- [86] Heim MH, Kerr IM, Stark GR, Darnell JE, Jr. Contribution of STAT SH2 groups to specific interferon signaling by the Jak-STAT pathway. *Science* 1995;267:1347-1349.
- [87] Briscoe J, Rogers NC, Witthuhn BA, Watling D, Harpur AG, Wilks AF, et al. Kinase-negative mutants of JAK1 can sustain interferon-gamma-inducible gene expression but not an antiviral state. *EMBO J* 1996;15:799-809.
- [88] Plataniias LC. Mechanisms of type-I- and type-II-interferon-mediated signalling. *Nat Rev Immunol* 2005;5:375-386.
- [89] Ramana CV, Grammatikakis N, Chernov M, Nguyen H, Goh KC, Williams BR, et al. Regulation of c-myc expression by IFN-gamma through Stat1-dependent and -independent pathways. *EMBO J* 2000;19:263-272.
- [90] Deb A, Haque SJ, Mogensen T, Silverman RH, Williams BR. RNA-dependent protein kinase PKR is required for activation of NF-kappa B by IFN-gamma in a STAT1-independent pathway. *J Immunol* 2001;166:6170-6180.
- [91] Jaeschke H, Woolbright BL. Current strategies to minimize hepatic ischemia-reperfusion injury by targeting reactive oxygen species. *Transplant Rev (Orlando)* 2012;26:103-114.
- [92] Todd I, Hammond LJ, James RF, Feldmann M, Bottazzo GF. Epidermal growth factor and transforming growth factor-alpha suppress HLA class II induction in human thyroid epithelial cells. *Immunology* 1990;69:91-96.
- [93] McCullough CT, Tura BJ, Harrison DJ. Growth factor attenuation of IFN-gamma-mediated hepatocyte apoptosis requires p21waf-1. *Int J Exp Pathol* 2006;87:275-281.
- [94] Li Z, Zhang Y, Liu Z, Wu X, Zheng Y, Tao Z, et al. ECM1 controls T(H)2 cell egress from lymph nodes through re-expression of S1P(1). *Nat Immunol* 2011;12:178-185.
- [95] Godoy P, Hewitt NJ, Albrecht U, Andersen ME, Ansari N, Bhattacharya S, et al. Recent advances in 2D and 3D in vitro systems using primary hepatocytes, alternative hepatocyte sources and non-parenchymal liver cells and their use in investigating mechanisms of hepatotoxicity, cell signaling and ADME. *Arch Toxicol* 2013;87:1315-1530.
- [96] Lee SM, Schelcher C, Demmel M, Hauner M, Thasler WE. Isolation of human hepatocytes by a two-step collagenase perfusion procedure. *J Vis Exp* 2013.
- [97] Livak KJ, Schmittgen TD. Analysis of relative gene expression data using real-time quantitative PCR and the 2(-Delta Delta C(T)) Method. *Methods* 2001;25:402-408.
- [98] Nelson JD, Denisenko O, Bomsztyk K. Protocol for the fast chromatin immunoprecipitation (ChIP) method. *Nature protocols* 2006;1:179-185.



- [99] Miyawaki A, Iizuka Y, Sugino H, Watanabe Y. IL-11 prevents IFN-gamma-induced hepatocyte death through selective downregulation of IFN-gamma/STAT1 signaling and ROS scavenging. *PLoS One* 2019;14:e0211123.
- [100] Lee HJ, Oh YK, Rhee M, Lim JY, Hwang JY, Park YS, et al. The role of STAT1/IRF-1 on synergistic ROS production and loss of mitochondrial transmembrane potential during hepatic cell death induced by LPS/d-GalN. *J Mol Biol* 2007;369:967-984.
- [101] Uddin S, Lekmine F, Sharma N, Majchrzak B, Mayer I, Young PR, et al. The Rac1/p38 mitogen-activated protein kinase pathway is required for interferon alpha-dependent transcriptional activation but not serine phosphorylation of Stat proteins. *J Biol Chem* 2000;275:27634-27640.
- [102] Weng HL, Wang BE, Jia JD, Wu WF, Xian JZ, Mertens PR, et al. Effect of interferon-gamma on hepatic fibrosis in chronic hepatitis B virus infection: a randomized controlled study. *Clin Gastroenterol Hepatol* 2005;3:819-828.
- [103] Weng H, Mertens PR, Gressner AM, Dooley S. IFN-gamma abrogates profibrogenic TGF-beta signaling in liver by targeting expression of inhibitory and receptor Smads. *J Hepatol* 2007;46:295-303.
- [104] Jeong WI, Park O, Radaeva S, Gao B. STAT1 inhibits liver fibrosis in mice by inhibiting stellate cell proliferation and stimulating NK cell cytotoxicity. *Hepatology* 2006;44:1441-1451.
- [105] Rockey DC, Maher JJ, Jarnagin WR, Gabbiani G, Friedman SL. Inhibition of rat hepatic lipocyte activation in culture by interferon-gamma. *Hepatology* 1992;16:776-784.
- [106] Sun R, Park O, Horiguchi N, Kulkarni S, Jeong WI, Sun HY, et al. STAT1 contributes to dsRNA inhibition of liver regeneration after partial hepatectomy in mice. *Hepatology* 2006;44:955-966.
- [107] Kusters S, Gantner F, Kunstle G, Tiegs G. Interferon gamma plays a critical role in T cell-dependent liver injury in mice initiated by concanavalin A. *Gastroenterology* 1996;111:462-471.
- [108] Tagawa Y, Sekikawa K, Iwakura Y. Suppression of concanavalin A-induced hepatitis in IFN-gamma(-/-) mice, but not in TNF-alpha(-/-) mice: role for IFN-gamma in activating apoptosis of hepatocytes. *J Immunol* 1997;159:1418-1428.
- [109] Sun C, Fujisawa M, Ohara T, Liu Q, Cao C, Yang X, et al. Spred2 controls the severity of Concanavalin A-induced liver damage by limiting interferon-gamma production by CD4(+) and CD8(+) T cells. *J Adv Res* 2022;35:71-86.
- [110] Mizuhara H, Uno M, Seki N, Yamashita M, Yamaoka M, Ogawa T, et al. Critical involvement of interferon gamma in the pathogenesis of T-cell activation-associated hepatitis and regulatory mechanisms of interleukin-6 for the manifestations of hepatitis. *Hepatology* 1996;23:1608-1615.
- [111] Fukuda R, Ishimura N, Nguyen TX, Chowdhury A, Ishihara S, Kohge N, et al. The expression of IL-2, IL-4 and interferon-gamma (IFN-gamma) mRNA using liver

biopsies at different phases of acute exacerbation of chronic hepatitis B. *Clin Exp Immunol* 1995;100:446-451.

[112] Gilles PN, Guerrette DL, Ulevitch RJ, Schreiber RD, Chisari FV. HBsAg retention sensitizes the hepatocyte to injury by physiological concentrations of interferon-gamma. *Hepatology* 1992;16:655-663.

[113] Luo XY, Takahara T, Kawai K, Fujino M, Sugiyama T, Tsuneyama K, et al. IFN-gamma deficiency attenuates hepatic inflammation and fibrosis in a steatohepatitis model induced by a methionine- and choline-deficient high-fat diet. *Am J Physiol Gastrointest Liver Physiol* 2013;305:G891-899.

[114] Burova E, Vassilenko K, Dorosh V, Gonchar I, Nikolsky N. Interferon gamma-dependent transactivation of epidermal growth factor receptor. *FEBS Lett* 2007;581:1475-1480.

[115] Uribe JM, McCole DF, Barrett KE. Interferon-gamma activates EGF receptor and increases TGF-alpha in T84 cells: implications for chloride secretion. *Am J Physiol Gastrointest Liver Physiol* 2002;283:G923-931.

[116] Hamburger AW, Pinnamaneni GD. Increased epidermal growth factor receptor gene expression by gamma-interferon in a human breast carcinoma cell line. *Br J Cancer* 1991;64:64-68.

[117] Solis NV, Swidergall M, Bruno VM, Gaffen SL, Filler SG. The Aryl Hydrocarbon Receptor Governs Epithelial Cell Invasion during Oropharyngeal Candidiasis. *mBio* 2017;8.

[118] Midgley AC, Morris G, Phillips AO, Steadman R. 17beta-estradiol ameliorates age-associated loss of fibroblast function by attenuating IFN-gamma/STAT1-dependent miR-7 upregulation. *Aging Cell* 2016;15:531-541.

[119] Saha S, Buttari B, Panieri E, Profumo E, Saso L. An Overview of Nrf2 Signaling Pathway and Its Role in Inflammation. *Molecules* 2020;25.

[120] Wang L, He C. Nrf2-mediated anti-inflammatory polarization of macrophages as therapeutic targets for osteoarthritis. *Front Immunol* 2022;13:967193.

[121] Panda H, Wen H, Suzuki M, Yamamoto M. Multifaceted Roles of the KEAP1-NRF2 System in Cancer and Inflammatory Disease Milieu. *Antioxidants (Basel)* 2022;11.

[122] Staitieh BS, Egea EE, Fan X, Azih N, Neveu W, Guidot DM. Activation of Alveolar Macrophages with Interferon-gamma Promotes Antioxidant Defenses via the Nrf2-ARE Pathway. *J Clin Cell Immunol* 2015;6.

[123] Wakabayashi N, Itoh K, Wakabayashi J, Motohashi H, Noda S, Takahashi S, et al. Keap1-null mutation leads to postnatal lethality due to constitutive Nrf2 activation. *Nat Genet* 2003;35:238-245.

[124] Li L, Fu J, Liu D, Sun J, Hou Y, Chen C, et al. Hepatocyte-specific Nrf2 deficiency mitigates high-fat diet-induced hepatic steatosis: Involvement of reduced PPARgamma expression. *Redox Biol* 2020;30:101412.

- [125] Su H, Yang F, Fu R, Trinh B, Sun N, Liu J, et al. Collagenolysis-dependent DDR1 signalling dictates pancreatic cancer outcome. *Nature* 2022;610:366-372.
- [126] Sato T, Selleri C, Young NS, Maciejewski JP. Inhibition of interferon regulatory factor-1 expression results in predominance of cell growth stimulatory effects of interferon-gamma due to phosphorylation of Stat1 and Stat3. *Blood* 1997;90:4749-4758.

## 7 LISTS OF FIGURES AND TABLES

### 7.1 List of figures

Figure 1. EGFR signaling pathway

Figure 2. IFN $\gamma$ -JAK-STAT1 signaling pathway

Figure 3. Histology of liver and kidney from ECM1WT and ECM1KO mice

Figure 4. Increased portal vein pressure in ECM1KO mice

Figure 5. Growth factors EGF and HGF induce ECM1 expression in hepatocytes

Figure 6. EGF-EGFR keeps ECM1 expression in hepatocytes *in vitro*

Figure 7. EGF-EGFR keeps ECM1 expression in homeostatic liver *in vivo*

Figure 8. MEK-ERK pathway is not responsible for EGF-induced ECM1 expression in hepatocytes

Figure 9. EGF upregulates ECM1 expression through p-STAT1 S727

Figure 10. EGF-induced p-STAT1 S727 binds to and positively regulates *Ecm1* gene promoter

Figure 11. Selection of candidate factors inhibiting ECM1 expression under chronic liver disease conditions

Figure 12. IFN $\gamma$  abolishes EGF-EGFR-maintained ECM1 expression *in vitro*

Figure 13. IFN $\gamma$  blunts p-STAT1 S727 binding to *Ecm1* gene promoter via phosphorylation of STAT1 at Y701

Figure 14. IFN $\gamma$  abolishes EGF-EGFR-maintained ECM1 expression *in vivo*

Figure 15. Free shuttling of STAT1 total protein contributes to binding of *Ecm1* promoter

Figure 16. IFN $\gamma$  generates reactive oxygen species (ROS) and induces NRF2 in hepatocytes

Figure 17. IFN $\gamma$  administration activates NRF2 *in vivo*

Figure 18. NRF2 generated by H<sub>2</sub>O<sub>2</sub> reduces ECM1 expression

Figure 19. NRF2 agonist OPZ treatment inhibits ECM1 expression

Figure 20. NRF2 inhibits ECM1 expression by binding its gene promoter

Figure 21. EGF-maintained ECM1 is disrupted by H<sub>2</sub>O<sub>2</sub> or OPZ administration

Figure 22. Regulation of ECM1 expression in different contexts in the liver

Figure 23. HGF-upregulated ECM1 involves STAT1

Figure 24. Activation of STAT3 at Y705 in IFN $\gamma$ -treated MPHs

Figure 25. ECM1 expression during liver regeneration

Figure 26. ECM1 expression in HCC cell lines and HCC patients

## 7.2 List of tables

Table 1. Cells and culture medium

Table 2. Chemicals and reagents

Table 3.1 Antibodies for immunoblotting

Table 3.2 Antibodies for immunofluorescence

Table 3.3 Antibodies for ChIP assay

Table 4 Buffer

Table 5 Kits and assays

Table 6 Small interfering RNA

Table 7 Experimental consumables

Table 8 Experimental instruments

Table 9 Software

Table 10 Primers used for Genotyping

Table 11 Buffer for perfusion

Table 12 Primers used for qRT-PCR in the study

Table 13 ChIP-Primer used in the study

## 8 CURRICULUM VITAE

### PERSONAL INFORMATION

Name und Vorname: Li, Yujia  
Date of Birth: 17, 07, 1993  
Place of Birth: Huludao, Liaoning, China

### EDUCATION

01, 2020 – Present  
PhD student (Dr. sc. hum.)  
Department of Medicine II, University Medical Center Mannheim  
Medical Faculty Mannheim, Heidelberg University  
Mannheim, Germany  
Doctoral Thesis: EGF/STAT1-maintained ECM1 expression in hepatic homeostasis is disrupted by IFN $\gamma$ /NRF2 in chronic liver diseases

09, 2015 – 07, 2017  
Master of Science in Engineering  
Department of Food Science and Nutritional Engineering  
China Agricultural University  
Beijing, China  
Master's Thesis: Anti-prostate cancer activity and mechanism of Glycycoumarin and Isoangustone A

09, 2011 – 07, 2015  
Bachelor of Science in Engineering  
Department of Light Industry, Liaoning University  
Shenyang, China

### AWARDS

2015  
Second Class Academic Scholarship  
China Agricultural University

2015	Outstanding Graduate Liaoning Province
2012-2014	First-Class Academic Scholarship Liaoning University
2013	Excellent League Member of Shenyang Liaoning Province

## PUBLICATIONS

Li Y, Fan W, Link F, Wang S, Dooley S. Transforming growth factor  $\beta$  latency: A mechanism of cytokine storage and signalling regulation in liver homeostasis and disease. *JHEP Rep.* 2021 Nov 18;4(2):100397. doi: 10.1016/j.jhepr.2021.100397. PMID: 35059619; PMCID: PMC8760520.

Feng R, Kan K, Sticht C, Li Y, Wang S, Liu H, Shao C, Munker S, Niess H, Wang S, Meyer C, Liebe R, Ebert MP, Dooley S, Ding H, Weng H. A hierarchical regulatory network ensures stable albumin transcription under various pathophysiological conditions. *Hepatology.* 2022 Dec;76(6):1673-1689. doi: 10.1002/hep.32414. Epub 2022 Mar 7. PMID: 35257388.

Wang S, Feng R, Wang SS, Liu H, Shao C, Li Y, Link F, Munker S, Liebe R, Meyer C, Burgermeister E, Ebert M, Dooley S, Ding H, Weng H. FOXA2 prevents hyperbilirubinaemia in acute liver failure by maintaining apical MRP2 expression. *Gut.* 2022 Apr 20:gutjnl-2022-326987. doi: 10.1136/gutjnl-2022-326987. Epub ahead of print. PMID: 35444014.

Schnabl B, Arteel GE, Stickel F, Hengstler J, Vartak N, Ghallab A, Dooley S, Li Y, Schwabe RF. Liver specific, systemic and genetic contributors to alcohol-related liver disease progression. *Z Gastroenterol.* 2022 Jan;60(1):36-44. doi: 10.1055/a-1714-9330. Epub 2022 Jan 18. PMID: 35042252; PMCID: PMC8941985.

## CONFERENCE AND PUBLISHED ABSTRACTS

**GASL Annual Meeting 2023**, January 27-28, 2023. Bochum, Germany

Summary Presentation & Poster “EGF/STAT1-maintained ECM1 expression in hepatic homeostasis is disrupted by IFN $\gamma$ /NRF2 in chronic liver diseases”

**DGVS Viszeral Medizin 2022**, September 12-17, 2022. Hamburg, Germany

Oral Presentation “EGF-maintained ECM1 expression in hepatic homeostasis is disrupted by IFN $\gamma$  in liver fibrosis/cirrhosis”

**GASL Annual Meeting 2022**, January 28-29, 2022. Online. Germany

Presentation “Downregulation of ECM1 in hepatocytes as a damage response to liver injury”

**Sino-German scientific symposium 2021**, September 26-29, 2021. Homburg, Germany

Poster “ECM1 as gatekeeper for homeostasis in healthy liver”

**GASL Annual Meeting 2021**, January 29-30, 2021. Online. Germany

Poster “Low ECM1 expression temporally promotes proliferative, tumorigenic and inflammatory gene signatures in mouse liver”

**Falk Workshop 2020**, February 13–14, 2020. Mainz, Germany

Poster “Decreased ECM1 expression is consistent in HCC and correlates with overall survival”



## 9 ACKNOWLEDGEMENT

Time flies and I still remember the first time I met Prof. Dr. Steven Dooley and Dr. Hong-Lei Weng in Beijing, when I was struggling for my first job and very much looking forward to coming to Germany, but also feeling nervous and anxious. The journey here has really brought me a lot of joy and good memories. I once said to Steven: "I really learned a lot at AG Dooley", and I am sure I will be grateful for the rest of my life for choosing to study abroad.

Special acknowledgement to my respectable mentor, Prof. Dr. Steven Dooley, who gave me the topic for this thesis and the great opportunity to work here. Steven was always supportive and helpful in every aspect, not only in science but also in life. I am very grateful for his advice, comments, ways of thinking as well as his writing skills.

Particular thanks to my second supervisor, Dr. Sai Wang, who helped me understand many experiments and gave me important advice in practice. Throughout the course of my research work, she provided me with helpful assistance and valuable advice, without which the thesis would not be the same as it is now.

In addition, I am very grateful to all the members in the AG Dooley. It was a pleasure to work with all of them. I would like to take this opportunity to thank Dr. Hong-Lei Weng, who knew a lot and was glad to share the knowledge with me. Every time I went to him, he would not say no but would answer questions and discuss with me. Kerry Gould, a talented girl who helped me with almost everything at the animal house, although she left the group, I know she would be happy for me now. Dr. Seddik Hammad, who helped a lot with our animal applications and did a lot of communication work for the project. Thanks also to Dr. Anne Dropmann, Fritz, Chenhao, Fen, Alaa, Frederik and all the partners involved.

Thanks to my family and friends, I am sure we will see each other this year. 2023 must be a memorable year as my PhD is coming to an end and now, I feel relieved. I look forward to continuing my research at AG Dooley and enjoying my time with everyone!